EFFECTS OF COULOMB AND PAIRING INTERACTIONS BETWEEN NUCLEONS IN DETERMINING NUCLEAR STABILITY OF FINITE NUCLEI

BY

CHEROP KOMEN HEZEKIAH

A THESIS SUBMITTED IN PARTIAL FULFILLMENT OF THE REQUIREMENTS FOR THE AWARD OF THE DEGREE OF DOCTOR OF PHILOSOPHY IN PHYSICS, UNIVERSITY OF ELDORET, KENYA.

FEBRUARY, 2021

DECLARATION

Declaration by the Candidate

This thesis is my original work and has not been submitted for any academic award in any institution; and shall not be reproduced in part or full, or any format without prior written permission from the author and/or University of Eldoret.

Cherop Komen Hezekiah

_____   _____

SSCI/PHY/P/004/17   Date

Declaration by the Supervisors

This thesis has been submitted for examination with our approval as University Supervisors

_____   _____

Prof. Kapil M. Khanna   Date

University of Eldoret, Eldoret-Kenya

_____   _____

Dr. Kennedy M. Muguro   Date

University of Eldoret, Eldoret-Kenya

DEDICATION

I dedicate this thesis to my loving children Ivana, Imela and Ilyah.

ABSTRACT

From time to time, several nuclear models have been proposed by various research groups to explain the properties of finite nuclei and large nuclear systems in nuclear physics and astrophysics. However, no single model could explain the properties of all the nuclear systems due to the concept of many body interactions of particles, which cannot be solved by Schrödinger equation. The stability of the nuclei is one of the fundamental properties of the nuclear system that is related to the average binding energy of the nuclei. However, the binding energy calculations are not accurate since they are based on the rough estimates of the large number of nucleons that are in collective motion. Therefore, the energy terms in the binding energy equation have to be modified in order to describe accurately the interaction of the nucleons. In this research, the effects of Coulomb interaction and pairing interaction between nucleons in the binding energy equation have been carried out in order to determine the stability of finite nuclei. This was achieved by formulating a modified Coulomb potential based on the assumptions of charge distribution in a spherical nucleus. In addition, the pairing energies of finite nuclei were calculated using the principles of the shell model and the binding energies obtained from atomic mass evaluation tables. The results obtained in this study revealed that, the modified Coulomb energy model defines the limits of long-range Coulomb potential as well as generating the most stable isobars for a fixed mass number. The most stable atomic numbers (Z_{STABLE}) obtained from the derived models include, Z=126, Z=132, Z=134, Z=141, Z=148, Z=152, Z=162, Z=164 and Z=193. Furthermore, it was found that, the absolute values of pairing energies decrease with increase in the mass numbers with occurrence of undulating peaks and troughs in the pairing energy-mass number graphs. The modified Coulomb potential model is useful in calculating the finite range Coulomb potentials, describing the decay transformations of radioactive nuclei and predicting for the existence of the stable isobars among the super heavy elements that may reside in the island of stability. Similarly, the pairing energy calculations are important in describing the stability and nuclear abundance of all the nuclei isotopewise, using the peak-trough theory. Based on the results obtained from the Coulomb potential model and pairing energy model, a unifying model that can link up the two models can be developed, such that, the stability of the nuclei and the nuclear abundance can be described simultaneously.

TABLE OF CONTENTS

Content **Page**

LIST OF TABLES

LIST OF FIGURES

LIST OF ABBREVIATIONS

A	Mass number
a	The skin depth (0.5 femtometers)
AME	Atomic Mass Evaluation
BCS	Bardeen Cooper Schrieffer
BE(A,Z)	Binding energy
c	Velocity of light in vacuum
C_{dir}	Jänecke's correction term
C_t	Correction term
DGFRS	Dubna Gas Filled Recoil Separator
E_C	Coulomb energy
$E_C(Dir)$	Direct Coulomb energy
$E_C(Mod)$	Modified Coulomb energy
$E_C(SEMFE)$	Coulomb energy from semi-empirical mass formula
ε_0	Permittivity of free space
HFB	Hartree-Fock-Bogoliubov
IUPAC	International Union of Pure and Applied Chemistry
M_N	Mass of Neutron
M_P	Mass of Proton
N	Neutron (Neutron number)
NMDF	Nuclear Mass Defect Formula
$P_N(A,Z)$	Pairing energy
R	Effective radius of the nucleus for A=N+Z
R_0	Nuclear core radius for A=2Z
r_0	Universal radius parameter

RHB	Relativistic Hartree-Bogoliubov
RNB	Radioactive Nuclear Beams
SEMF	Semi Empirical Mass Formula
SF	Spontaneous Fission
SHE	Super Heavy Elements
SHF	Skyrme-Hartree-Fock
SHN	Super Heavy Nuclei
u	Atomic mass unit
Z	Atomic number (Proton Number)
$\rho\left(r\right)$	Nuclear charge density
ΔM	Mass defect

ACKNOWLEDGEMENT

I am very grateful to God almighty for His divine providence throughout my research. My special thanks go to my dedicated supervisors and great physicists Prof. Kapil Khanna and Dr. Kennedy Muguro for teaching me a lot in many body theory, nuclear theory and research ethics. Through their guidance, I saw the beauty of comprehending the abstractionism in Theoretical and nuclear Physics. I would like also to thank Prof. Joel Tonui for inspiring me to pursue Ph.D and the entire Physics department lecturers for their valuable guidance.

To my fellow researchers, Kenneth Sirma, Stanslous Obota, Wilkins Cheruiyot and Henry Chepkoiwo, I sincerely thank you for your team spirit and the motivation to start this worthy course. To my brother Alex Mwetich, I appreciate your overwhelming support that you bestowed me.

I am deeply grateful to my beloved wife Valarie whose ingenuity has made my academic journey brighter. I also thank my parents Mr. and Mrs. James Kibowen Cherop and my siblings for constantly following my research progress as well as inspiring me to pursue and attain my dreams.

CHAPTER ONE

INTRODUCTION

1.1 Background to the study

Ernest Rutherford discovered the fact that there exists a nucleus in each atom in 1911 (Rutherford, 1911). The experimental observations of Rutherford led to the following conclusions: Firstly, the nucleus behaves like a point charge with dimensions of the order of 10^{-11}cm or less. Secondly, the nucleus of an atom is excessively heavy in comparison to the electron mass, and finally the nucleus is positively charged and the charge on each nucleus is an integral multiple of the charge on the electron. Mathematically, the nuclear charge can be expressed as Ze, where Z is the atomic number of the atom and ℓ is the electronic charge. Since atoms are neutral systems, the charge on the nucleus must be positive and equal in magnitude to the charge on the electrons that surround the nucleus. Thus, the charge of the nucleus defines the number of electrons in the atom and most of the other properties of nuclear matter.

Furthermore, J.J Thomson became the first person to discover that the mass of a nucleus is an important quantity that it is not determined by the charge on the nucleus as proposed by Rutherford (Thompson and Thomson, 1913). He found out that there exist nuclei which have the same atomic number (charge) Z, but of different masses. Such kinds of nuclei were named isotopes. It was found that the mass of each isotope was roughly equal to an integral number of proton masses and the nearest integer is known as mass number, and it is denoted by A. It was further noted that, the mass number (A) is invariably twice or more than twice the proton number (Z). This contradicted the idea that the nucleus is composed of protons. In the meantime, J.

Chadwick discovered the neutral particle called neutron (Chadwick, 1932). This led Heisenberg to propose the hypothesis that the atomic nuclei are composed of neutrons and protons (Heisenberg, 1932). Thus, it can be stated emphatically that modern nuclear physics, as it is known today had its theoretical structure understood from the year 1932.

It is now sufficiently confirmed experimentally and theoretically that a nucleus is composed of neutrons (N) and protons (Z), and that its mass number is A=N+Z. A proton being positively charged has slightly less mass compared to the mass of the neutron that has no charge. The magnetic moment of the proton is positive, but that of the neutron is negative. Inside the nucleus, the protons and neutrons are referred to as nucleons since the nuclear forces between the neutrons and protons are charge independent. In addition, there exist different types of nuclei. Some nuclei have proton number constant (Z constant) but different mass number (A); such nuclei are called isotopes while the nuclei that have constant mass number but different atomic number are called isobars. Then there are nuclei with constant neutron number (N), but different A and Z. Such nuclei are called isotones. There is another set of nuclei, in which the proton number is equal to the neutron number $(Z = N)$ in two or more nuclei. Such nuclei are called isomers or mirror nuclei, for instance, $_{1}^{3}\text{H}$ and $_{2}^{3}\text{He}$ in which $_{1}^{3}\text{H}$ has two neutrons and $_{2}^{3}\text{He}$ has two protons.

The nuclei can also be categorized in terms of their nuclear masses. In the low mass nuclei, the atomic mass (A) is less or equal to 20; $(A \leq 20)$. Similarly, medium mass nuclei fall within the region described by $20 < A \leq 100$ and the heavy mass nuclei are those nuclei in which $A \geq 120)$. In terms of nucleons, we have symmetric nuclear matter in which the number of neutrons (N) is equal to the number of protons (Z),

asymmetric nuclear matter $(N \neq Z)$, neutron matter in which small percentage of protons and electrons exist and pure neutron matter which is found in the case of the neutron stars.

It is evident that, the number of protons in the nucleus of an atom is a crucial parameter since it is equal to the atomic number of the element, which is the determining factor in the periodic table of elements as described by Henry Moseley in 1913 (Scerri, 2013). As of today, the elements in the periodic table that have been confirmed experimentally span from Z=1 to Z=118. Some recent theoretical calculations show that the number of bound nuclei with atomic number between Z=2 and Z=120 is of the order of 7000 (Erler *et al.,* 2012; Agbemava *et al*., 2014). In addition, there are more than 3200 isotopes in the nuclear regime that have been discovered using different experimental techniques (Thoennessen, 2016; Thoennessen, 2017; Neufcourt *et al*., 2019). Among these isotopes, 286 have been in existence in their present form since the creation of the earth and they constitute the stable isotopes that form the valley of stability in the nuclear landscape.

The number of protons and neutrons that combine to form a bound atomic nucleus in the region of the periodic table whereby $Z \leq 92$ are known precisely. However, in the region described by $Z > 92$, which consists of the transuranic and transactinide elements (Super heavy elements), the exact number of protons and neutrons that form a bound atomic nucleus is not known. As one adds protons to the nuclei, one may move away from the region of stable isotopes and may transit into the region of short-lived radioactive nuclei and such nuclei may undergo nuclear decay to gain stability. At some point when a last nucleon (proton or neutron) is added to the nucleus, the binding energy per nucleon may become zero, and hence the nucleon simply drips off.

This stage is called drip line for neutron or proton and at this stage nuclear existence ends. In fact, the strong nuclear force cannot keep the last nucleon attached to the nucleus at this stage. Recently, extremely neutron-rich nuclei around $^{60}_{20}Ca$ were discovered (Tarasov *et al.,* 2018). In addition, masses of the nuclei $^{55-57}_{20}Ca$ have also been determined experimentally, and this can provide unique information as to how the binding energy changes by addition of a neutron (Michimasa *et al.*, 2018).

Currently, there is a large measure of data and information that is accessible on the atomic nuclei in the form of nuclear forces, nuclear models, nuclear binding energy, stability of nuclei, spontaneous nuclear fission (SF) etc. Nonetheless, we are still far away from a theoretical framework that can explain all the properties of nuclei, from low mass number (A) to very large mass number in the region of super heavy nuclei (SHN). Quite a number of nuclear models that include liquid drop model, Bethe-Weizsäcker mass formula, collective model, evaporation model, Fermi gas model, shell model, individual particle model, nuclear pairing model and superfluid model (Greiner and Maruhn, 1986; Rowe and Wood, 2010) have been proposed from time to time to explain the properties of nuclei in different regions of mass number. However, none of these nuclear models can explain all the properties of nuclei. In spite of the spectacular advances made in nuclear theory and experimental nuclear physics, it is still not exactly known as to how many protons and neutrons can constitute a bound atomic nucleus, especially in the region of periodic table when Z varies from Z=92 to say Z=120 or more.

It is well established that, the stability of nuclei is one of the most important properties that is related to the average binding energy of the nuclei. The nuclear binding energy and its magnitude plays an important role in the study of nuclear mass,

decay half-life, nuclear spontaneous fission (SF) and the stability of the nucleus. The limits of nuclear stability are determined by the interactions between nucleons. Moreover, the limits of nuclear stability are still not known especially in the case of super heavy nuclei (SHN) in the so called "island of stability". However, what is important is that the super heavy nuclei are at the limits of Coulomb stability (Oganessian, 2012).

Until today, the last of the super heavy elements to be produced artificially is Oganesson (Z=118) which was synthesized for the first time in the year 2002 and received official recognition in year 2016 (Oganessian and Utyonkov, 2015; Murthy, 2017). The discovery of this element has compelled physicists and chemists, to think of the possibility of having the eighth period and beyond in the periodic table of elements. However, this element (Oganesson) and other super heavy nuclei are radioactive with some having very short half-lives of about 10^{-14} seconds to 10^{-19} seconds and most of them ranging between milliseconds to seconds (Oganessian and Utyonkov, 2015 ; Murthy, 2017). On the contrary, other super heavy nuclei were predicted to have very long half-lives greater than the uranium half-lives of 10^{16} years (Oganessian, 2012). Such super heavy elements with very long half-lives are assumed to be very stable, thus, predicted to exist in the "island of stability" in the nuclear landscape while the unstable elements with short half-lives are likely to reside in the sea of instability. Interestingly, the physics of such unstable nuclei have gained enormous interest in the last two decades (Sakaguchi and Zenihiro, 2017). However, the limits of the stability of these nuclei are not defined and it is not yet clear whether this "island" of super heavy nuclei exists (Mackintosh *et al*., 2002).

Scientists are unrelenting in the search of these elements. For instance, in the last two decades, more than fifty super heavy isotopes and six new elements from Z=113 to Z=118 were synthesized in the laboratories by bombarding the doubly magic Calcium beams $\left({}^{48}_{20}Ca \right)$ onto actinide targets through the process of hot fusion (Oganessian and Rykaczewski, 2015). However, this technique had a major drawback; the decrease on both the survivability of the compound nucleus formed and production cross section of the super heavy elements (Oganessian and Utyonkov, 2015).

Despite these challenges, investigations are still on course to synthesize nuclei with $Z > 118$. However, the process of synthesizing the high-mass nuclei is extremely costly and very complex, thus, new technologies and theoretical models are required in order to actualize the synthesis of the SHN in region described by $Z > 118$. Up to date, no technique has been successful in synthesizing high Z and high mass nuclei. It has been suggested that, the impetus to these discoveries lies in the nuclear models, particularly, the shell model that was developed in the late 1940s (Kragh, 2017) and the binding energy which is dominated by the long-range Coulomb repulsive force in free - space.

The nuclear models have extensively described the properties of nuclei but due to the complexity of the nuclear systems, no single model can fully explain all the properties. The basic parameters that come into play in the formulation of such nuclear models are the nuclear masses and the binding energies of the nuclei. As the nuclear size increases among the nuclei, the ground state nuclear binding energies also increase due to the effect of increased shells that are occupied by paired nucleons. The nucleons in this interaction experience several forces that are dominated by the Coulomb repulsion between the proton pairs. Thus, the Coulomb

interaction contributes greatly to the stabilization of the super heavy nuclei that are likely to exist in the "island of stability" (Oganessian, 2012). Therefore, this study was carried out to formulate a modified Coulomb energy model for calculating accurately the stable values of atomic numbers, and to develop a pairing model for ascertaining the existence of the stable finite nuclei isotopewise.

1.2 Statement of problem

The most fundamental problem that is still not solved in nuclear theory is that, there is no single nuclear model that can predict all the properties of different nuclei. Even the exact nature of interactions inside the nucleus is still not known. This is because the properties of nuclei drastically change as Z and N and hence A changes.

Atomic calculations suggest that, the existence of nuclei on earth or on interstellar bodies may end at $Z \square 172$ (Fricke *et al*., 1971; Indelicato *et al*., 2011; Pyykkö, 2011). In addition, the shell model has predicted for the occurrence shell closures at Z=126 and N=184. However, the last known super heavy element to be produced artificially is Oganesson (Z=118). This implies that, the region between Z=118 to Z=172, is likely to accommodate the super heavy nuclei, with some of them residing in the "island of stability". However, the exact number of protons and neutrons that form a bound atomic nucleus in this region is not known.

Therefore, scientific efforts to unravel this mystery in nuclear theory have given rise to several nuclear models that include the famous semi-empirical mass formula, which describes the binding energy of the nucleus of an atom. However, the calculations of the binding energies are not accurate (Ghoshal, 2008) since they are based on the rough estimates of the large number of nucleons that are in collective

motion. Therefore, the energy terms in the binding energy equation have to be modified in order to describe accurately the interaction of the nucleons.

The binding energy of an atomic nucleus is composed of a number of different forms of energy. The most important ones are the Coulomb energy resulting from the Coulomb repulsion between the protons, and the pairing interaction energy which is associated with the pairs of nucleons in the shell structure. Several detailed calculations have been carried out in the past on the Coulomb's energy. However, these calculations are not exact (Ghoshal, 2008) because the Coulomb law is a long-range force whereas very small size protons are closely packed inside the nucleus whose radius is also very small in the order of 10^{-13}cm. Thus, the Coulomb potential inside the nucleus has to be modified to make it more effective inside the nucleus and allow for the calculation of the stable super heavy nuclei.

It has been found that, the super heavy elements are at the limits of Coulomb stability (Oganessian, 2012), however, Coulomb law is a long-range force. It is therefore important to formulate a relevant Coulomb potential model that can be used to calculate with precision the stable values of atomic numbers, among the isobaric nuclei, and to define the limits of the Coulomb stability.

Experiments on pairing interaction of nucleons have shown that the pairing energy depends on the mass number (Dean and Hjorth-Jensen, 2003; Ghoshal, 2008). However, the shell model does not predict the exact values of the mass numbers for the stability of the nuclei. Based on the shell model intimation, the pairing energy term in the binding energy equation has to be modified in order describe accurately the nucleon interactions of all the nuclei isotopewise and to develop a criterion for

ascertaining the existence of the stable nuclei on earth and other interstellar bodies such as the neutrons stars.

1.3 Justification

Several scientists across the world have carried out a whole myriad of investigations spread over decades on the stability of the nucleus of an atom. The results on these studies have provided solutions to several challenges facing mankind in various fields of science namely; nuclear medicine, nuclear energy, industrial applications, agriculture etc. However, there are some questions and gaps in nuclear theory that call for further investigations, both theoretically and experimentally. These include the microscopic composition and properties of celestial bodies such as the neutron stars, neutron matter, black holes and the recent discoveries of transuranic elements, which have proved to be more complex and prohibitively expensive to synthesize (Murthy, 2017). Other puzzles include the actual extent and the size of the periodic table, the limits of Coulomb stability of finite nuclei and the criterion for the distribution of the precious elements that are rare on earth, but predicted to be in plenty in neutrons stars and other interstellar bodies.

The solutions to the above questions and many other puzzles surrounding the nucleus of an atom lie within the structure of the nucleus of the atom itself and its binding energy. These facets can only be investigated in depth in theoretical nuclear physics, particle physics, astrophysics and condensed matter physics. Therefore, the study of the effects of Coulomb and pairing interactions between nucleons in this research provides solutions that are linked with the stability of finite nuclei by; enriching on the knowledge of the nucleus, defining the limits of Coulomb stability for the existence of SHN and predicting the island of stability.

1.4 Objectives of the study

1.4.1 General objective

The main objective of this research is to study the effects of Coulomb and pairing interactions between nucleons in the binding energy equation and investigate their contribution towards the stability of finite nuclei.

1.4.2 Specific objectives

The specific objectives of the study are:

i. To formulate a finite Coulomb potential energy model for nuclei with large atomic number (Z) and excess neutron number ($N > Z$).

ii. To calculate the values of stable atomic numbers (Z_{STABLE}) for the stability of isobars using the modified binding energy formula.

iii. To develop a criterion for ascertaining the existence of the most stable finite nuclei and the longest-lived radioactive nuclei, isotopewise.

CHAPTER TWO

LITERATURE REVIEW

2.1 Introduction

Various scientists and research groups have done several experimental and theoretical work on the nucleus of an atom in the past. The outcome of such studies has enriched the knowledge base in nuclear theory. Therefore, this chapter focuses on some of the important contributions in the nuclear theory, that are significant in describing some properties of spherical nuclei, as well as highlighting on their strengths and deficiencies. These areas include the atomic nucleus, the binding energy equation, the size of the nucleus and nuclear density, nuclear models, pairing interactions, super heavy nuclei and the island of stability.

2.2 Atomic nucleus

It is now well known that, the nucleus of an atom is a highly complex quantum system composed of protons and neutrons (Reid, 1984). Besides, a very strong short-range force holds the protons and neutrons together while the electrons orbit the nucleus in specified orbits having certain energy levels (Ghoshal, 2008). However, the exact nature of interaction of particles inside the nucleus remains to be unknown (Davies and Brown, 1993). Several scientific efforts both experimental and theoretical (Michimasa *et al*., 2018) are in place to unravel the mysteries in the nucleus of an atom. In order to understand the nuclear interaction of particles in the nucleus, it is essential to trace briefly the paths of the giants that were behind the discovery of the nucleus of an atom and its structure.

The genesis in the discovery of the nucleus of an atom emphatically dates back to 450BC, when a Greek philosopher named Democritus came up with the term "atom" meaning indivisible, to describe matter (Van Melsen, 2004). During that epoch, the Greeks believed that matter was made up of four basic elements namely earth, water, fire and air (Campbell, 2016). Several years later on 1808, John Dalton adopted Democritus theory (Rocke, 2005) and came up with a bold statement that elements such as Hydrogen, Oxygen, Phosphorus etc. were characterized by the weights of their atoms. In 1897, Joseph John Thomson performed the first experiment to investigate on the existence of an atom using the cathode ray tube (Hentschel, 2009). He found that, there was a negative charge that was 1000 times lighter than a hydrogen atom, which was deflected by the negative coil of the cathode ray tube. J.J. Thomson discovered that, the negative charge could conduct electricity in gases, and he named it an electron hence receiving the Nobel Prize in Physics in the year 1906 (Thomas, 2006).

In 1909, Ernest Rutherford looked at J.J. Thomson's model, which had been modified by Niels Bohr and Arnold Sommerfeld (Tilton, 1996) and bombarded fast moving alpha particles on a thin sheet of gold foil surrounded by circular detector screen. Rutherford observed the deflections of the alpha particles in the gold foil experiment with the assistance of his two co-workers, Hans Geiger and Ernest Marsden (Brynjolfsson and Wang, 2018). From his experiment, he made the following observations; firstly, most of the alpha particles did not deflect instead they tunneled through the foil, implying that, the atom is mostly made up of an empty space. Secondly, there existed a positive centre of the atom with a dense mass, which caused strong deflection of some alpha particles in all directions and he named it as the nucleus, which means a little nut in Latin. Lastly, Rutherford stated that, the electrons

orbit the nucleus in a wide orbit just like a mini solar system (Rutherford, 1911; Villeneuve, 2005; Webber and Davis 2012; Sivulka, 2017).

Unfortunately, Rutherford did not explain why the negatively charged particles were not attracted by the positive centre, instead, he postulated that there could be a particle with mass but no charge (neutral particle) and he called it a neutron, even though he imagined it as a paired proton and electron (Rutherford, 1920). Since there was no evidence for his imagination, Rutherford ended up missing the discovery of a neutron. In 1920, Rutherford postulated that the hydrogen nucleus is a new particle since it is a fundamental building block of all nuclei, and named it proton after Prout's hypothesis (Prout and Thomson, 1815).

Twelve years later in 1932, James Chadwick, the student of Ernest Rutherford, repeated Rutherford's experiment with an intention of searching for a neutral particle having the same mass as the proton (Chadwick, 1932). Chadwick's experiment was successful and he discovered the existence of neutrons, which was confirmed by Werner Heisenberg who showed that the neutron is a unique particle but not a proton-electron pairing as mentioned by Ernest Rutherford. Heisenberg (1932) proposed that the nucleus is composed of neutrons and protons.

It was the discovery of the neutrons that revolutionized the atomic and nuclear physics especially in the field of nuclear energy, nuclear medicine and nuclear weapons where neutrons or protons take part in nuclear reactions with other nuclei through fusion or fission process. The addition of neutrons to a given nuclei changes the properties of the nucleus of an atom thus interfering with its stability. For instance, hydrogen has two stable isotopes namely hydrogen $\left(_{1}^{1}\text{H}\right)$ and deuterium $\left(_{1}^{2}\text{H}\right)$. Deuterium is obtained by adding one neutron to hydrogen (single proton). On adding

a neutron to deuterium, we also obtain tritium $\left(_{1}^{3}\mathrm{H}\right)$, which is unstable. Similarly, on

adding proton to tritium, we get Helium $\left(_{2}^{3}\mathrm{He}\right)$. Subsequently, when a neutron is

added to $_{2}^{3}\mathrm{He}$ we get $_{2}^{4}\mathrm{He}$. This process explains vividly the creation of all the

elements in the nuclear landscape as recorded in the study of the big bang

nucleosynthesis (Dolgov, 2002).

The addition of protons or neutrons to the nucleus of an atom leads to a jump in the

binding energy of the nuclei (Del Bene *et al*., 1999). For instance, the experimental

measurement of the binding energies of $_{1}^{1}\mathrm{H}$, $_{1}^{2}\mathrm{H}$, $_{2}^{3}\mathrm{He}$ and $_{2}^{4}\mathrm{He}$ are 0.0000136MeV,

2.22MeV, 8.4820 MeV and 28.3 MeV respectively (Pritychenko *et al*., 2006). The

binding energies of the nuclei increase as the nucleus increases in size and this

occurrence determines the stability of the elements based on the ratio of the protons

and neutrons. The most stable element in the nuclear landscape is Nickel $\left(_{28}^{60}\mathrm{Ni}\right)$

which has even-even configuration of protons and neutrons (Z = 28 and N = 32) and it

is the most stable element known with binding energy of 526.864 MeV. From this

analogy, it is evident that the existence of nuclei on earth and other interstellar bodies,

such as the neutron stars, is determined by the stability of the nuclei. However, there

are a number of factors that may determine the limit of existence and stability of the

nuclei (Afanasjev *et al*., 2018). According to Weizsäcker mass formula, it was

predicted that nuclei with Z > 83 cannot exist since they have radioactive isotopes and

they undergo alpha decay (Mackintosh *et al*., 2002). Nonetheless, some nuclei with Z

greater than 92 (transuranic and transctinides) have been created artificially in the

laboratory using nuclear reactors and particle accelerators, and some of them are

stable against spontaneous fission.

The existence of stable nuclei is the most fundamental requirement in nuclear physics. For this reason, the existence of experimental nuclear physics will be threatened without the existence of stable nuclei. A stable nucleus has to be sufficiently bound, and this requires exact knowledge of the binding energy of the nucleus. The binding energy is defined as the amount of energy that has to be supplied to the nucleus of an atom containing protons (Z) and neutrons (N), to break their bonding in a manner that they are completely separated from each other (Brinkman, 1986 and Ghoshal, 2008). The magnitude of binding energy of a nucleus depends on the type of forces acting between the nucleons (neutrons and protons). The prominent forces that act between the nucleons are nuclear forces, pairing forces and Coulomb forces.

Some of the fundamental characteristics of an atomic nucleus are charge radius (Bohr and Mottelson, 1969), mass and density, composition, binding energy and or binding fraction, nuclear forces, Coulomb forces and pairing interactions. An appropriate pairing model and a suitable choice of pairing model parameters is important for obtaining realistic results that determine the properties of atomic nucleus.

2.3 The binding energy of the nucleus of an atom

During the formation of a nucleus of mass number A from Z protons and N neutrons, which are completely separated from each other (National Research Council, 1986; Ghoshal, 2008), a small amount of mass of the constituent nucleons is converted into energy (Rabinowitz, 2015). This energy is called the binding energy and it forms the basis of understanding the properties of atomic nucleus (Chemogos *et al*., 2019). The binding energies are calculated using the famous semi-empirical mass formula (SEMF) that was formulated by a German Physicist, C.F Von Weizsäcker in 1935 (Weizsäcker, 1935). The insights behind the formulation of this famous model

emanated from the concepts of the liquid drop model (LDM), that was first proposed by a Russian Physicist G. Gamow in 1928 (Mishra *et al*., 2016) and later improved by N. Bohr and J. Wheeler (Bohr and Wheeler, 1939).

According to Bethe-Weizsäcker semi-empirical mass formula, the binding energy equation is written as (Weizsäcker, 1935; Bethe and Batcher, 1936; Dai *et al*., 2017; Heyde, 2004);

$$BE(A,Z) = a_1 A - a_2 A^{\frac{2}{3}} - a_3 \frac{Z(Z-1)}{A^{\frac{1}{3}}} - a_4 \frac{(A-2Z)^2}{A} \pm \delta(A) \qquad (2.1)$$

where, A is the mass number, Z is the atomic number, a_1=15.99MeV represents the coefficient that is related to the volume term, a_2=18.34MeV represents the coefficient of the surface term, a_3=0.71MeV represents the coefficient that is associated with the Coulomb term, a_4=23.21MeV represents the coefficient of the asymmetry term and $\pm\delta(A)$ is the pairing energy correction term.

The existence of the stable nuclei in nuclear physics is the solid motivation for studying the properties of nuclei close to the drip line, through careful investigation on the nuclear binding energy. This is ascribed to the fact that, the magnitude of binding energy depends on the prominent forces that act between the nucleons. Any theoretical model that aims at unravelling this mystery in nuclear theory should be founded on the binding energy of the atomic nuclei.

The binding energy of the nuclei is of essence in describing the properties of the finite nuclei. Firstly, it gives information on stability of all the nuclei since the nuclei that have different number of protons and neutrons have different binding energies resulting into different decay probabilities (Oganessian, 2012). Secondly, the binding

energy may act as a tool that can predict the abundance of heavy elements that are rare on earth but present in neutron stars and other celestial bodies. This is due to the fact that, as the proton number increases, new shells get filled up creating fission barriers and thus the binding energy in the ground state increases resulting to greater stability for the nuclei. Consequently, the most stable nuclei become highly bound and chemically abundant. Lastly, the binding energy determines the synthesis of the super heavy elements through nuclear fission or fusion process of the nuclei (Williams, 2016). The production of the super heavy nuclei entails bombarding heavy atomic nuclei with protons in the process of nuclear fission while in nuclear fusion light nuclei are bound together under high-energy states.

In the heavy nuclei $(A \geq 120)$, the binding energy is significant in the process of cold fusion and hot fusion. In cold fusion, heavy targets such as lead or bismuth are bombarded with heavy ions of iron or nickel at energies above Coulomb barrier to form super heavy elements. In hot fusion, the actinide targets are bombarded with calcium beams to form highly excited compound nucleus (Oganessian and Utyonkov, 2015). Currently, the hot fusion is the most successful technique in artificial synthesis of the super heavy nuclei.

The study of the binding energy is very important and it has found several applications in industry. These include nuclear power, chemical manufacturing and nuclear medicine. It is predicted that, further studies on binding energy will provide more solutions in the synthesis of super heavy elements and production of reliable nuclear energy in the nuclear fusion processes (Williams, 2016).

The calculations of the binding energies are not accurate (Ghoshal, 2008) since they are based on the rough estimates of the large number of nucleons (protons and

neutrons) that are in collective motion. In view of this, the coefficients of the SEMF that are associated with their empirical terms have been subjected to several improvements over time while maintaining the structure of the binding energy equation (Bailey, 2011). These empirical terms include the volume energy, the surface energy, the Coulomb energy, the asymmetry energy and the pairing energy.

2.4 Coulomb potential of nuclei

The magnitude of the force between charged particles is described by the Coulomb's law which states that the force between two point charges is directly proportional to the magnitude of the charges (Q_1 and Q_2) and inversely proportional to the square of the distance between them (r^2) (Lowrie, 2007; Whittacker, 1910; Etkin, 2017). Therefore, the Coulomb's force can be written as;

$$F_C = \frac{1}{4\pi\varepsilon_0}\frac{Q_1 Q_2}{r^2} \tag{2.2}$$

where ε_0 is the permittivity of free space.

The Coulomb's energy (E_C) can also be written as;

$$E_C = \frac{1}{4\pi\varepsilon_0}\frac{Q_1 Q_2}{r} \tag{2.3}$$

Coulomb potential is one of the dominant terms in the determination of the binding energy equation of nuclei that is described in the famous Bethe-Weizsäcker semi-empirical formula (Dai *et al*., 2017). According to SEMF in Eq. (2.1) the Coulomb's energy is written as;

$$E_C\left(SEMFE\right) = -a_C Z\left(Z-1\right)A^{-\frac{1}{3}} \tag{2.4}$$

For large values of Z, the term Z(Z-1) in Eq. (2.4) is better represented as Z^2 (Ghoshal, 2008).

Several corrections on the Coulomb energies have been carried out in the past by modifying the Coulomb's law to yield the modified Coulomb energy equations. Jänecke, (1972) introduced the Fermi integral to obtain the quantum-mechanical direct Coulomb energy for spherical nuclei with diffuse surfaces. The calculations were then subjected to least-squares analysis and results similar to those of electron scattering and muon x-ray experiments were obtained (Jänecke, 1972; Collard *et al.*, 1967).

The direct Coulomb formula ($E_C(Dir)$) devised by Jänecke (Jänecke, 1972) is written as,

$$E_C(Dir) = \frac{3}{5} \frac{Z(Z-1)e^2}{R} C_{dir} \qquad (2.5)$$

where C_{dir} is the Jänecke's correction term which is written as,

$$C_{dir} = 1 + b_1 \left(\frac{a}{R}\right)^3 + b_2 \left(\frac{a}{R}\right)^4 \qquad (2.6)$$

where *a* is the skin depth, *R* is the radius of the nucleus and b_1 and b_2 are the coefficients obtained from integration of Fermi functions. The direct Coulomb energy ($E_C(Dir)$) was calculated using $r_0 \approx 1.135\,\text{fm}$ obtained from electron scattering experiment (Jänecke, 1972) and muon capture x-ray data (Collard *et al.*, 1967). The Jänecke's modified Coulomb energy, E_C (Dir), is based on the assumption that the Coulomb energy depends on distribution of charge near the nuclear surface, and it is characterized by the skin depth (*a* = 0.5 femtometers) and the nuclear radius. The nuclear radius is equivalent to the charge radius (R) which is given by;

$$R = r_0 A^{\frac{1}{3}} \left\{ 1 + \frac{5}{6}\pi^2 \left(\frac{a}{r_0 A^{\frac{1}{3}}}\right)^2 - \frac{7}{24}\pi^4 \left(\frac{a}{r_0 A^{\frac{1}{3}}}\right)^4 \right\} \qquad (2.7)$$

Coulomb energy correction on the Thomas-Fermi model in the case of metals was also investigated to describe the nature of Coulomb's potential. This modification was done by considering the interaction between electrons and their exchange correlation holes in metals (Naturali *et al*., 2013). Such interaction leads to the screening of the effective Coulomb force between the quasi-particles, which is corrected by introducing an exponential function in the Thomas-Fermi model.

Finslerian modification of the Maxwell's equation was also used to correct the Coulomb potential by a team of scientists from the Hebrew University of Jerusalem and University of Bremen (Itin *et al*., 2014). They found that the Finsler metric corrections yield the splitting of the energy levels that come on top of the fine structure and the hyperfine structure. Such energy levels, alongside their corresponding wave functions were also obtained by applying the factorization method to solve the Schrödinger equation with modified Coulomb potential (Antia *et al.*, 2015). Owing to the fact that the Coulomb's law can be written in both two and three-dimensional closed spaces (Jackson, 1999), paved way for the modification of Coulomb's law. Pedram carried out this modification and the results showed that, the total electrical charge in a closed space is zero and that the charge neutrality is experienced in both isotropic and homogeneous universe (Pedram, 2010).

The recent discovery of super heavy nuclei (SHN) relied on the Coulomb potential because the super heavy elements are found to exist at the limits of Coulomb stability (Oganessian, 2012). As the atomic numbers increase beyond the actinides, the Coulomb repulsion increases due to the effect of new shells with small energy gaps that are created (Bender *et al*., 2001). Consequently, the ground state binding energy increases hence increasing the stability of the super heavy elements that are

characterized by existence of very high neutron and proton numbers, and large densities of neutron and proton states.

Therefore, it is sufficiently evident that, the Coulomb energy plays a key role in understanding the mechanism of stability of transuranic elements and super heavy nuclei, the neutron excess of neutron rich nuclei, r-process, neutron stars phenomena and supernova (Gandolfi *et al*., 2014). In addition, several detailed calculations on the Coulomb energy that compare theory and experiments have been carried out in the past by several researchers (Jänecke, 1972). However, the calculations of the Coulomb potential are not accurate (Ghoshal, 2008) since the Coulomb potential in free space is a long-range potential, whereas the protons inside the nucleus are enclosed in a very small volume. In view of this fact, Coulomb energies must be subjected to modifications in order to understand the contributions of nuclear correlations, charge dependence, nuclear force, Coulomb perturbations (Nolen and Schiffer, 1969) and other new phenomena such as the limits of Coulomb stability among the super heavy elements (Oganneson, 2012).

Presumably, any new technique and model in theoretical and nuclear physics that may be designed to produce large quantities of stable super heavy nuclei should be centered on Coulomb potential models that can regulate the magnitude of fission barriers and the limits of Coulomb stability.

2.5 The radius of the nucleus, Size of the nucleus and Nuclear Density

Ernest Rutherford was the first one to carry out the investigation on the radius of the nucleus in 1909 while studying the structure of an atom (Wilson, 1983). From Rutherford's gold foil experiment using alpha particles emitted by a radioactive source, he found that the central charge that was interpreted to be the nuclear radius

for some few light elements such as hydrogen, magnesium and oxygen was estimated to be of the order of femtometers (Ghoshal, 2008). Experimental evidence have shown that, the nuclear charge and nuclear matter are uniformly distributed in the nucleus, and that the nuclear charge density and nuclear matter density are approximately constant (Ghoshal, 2008; Peter and Schuck, 1980).

Rutherford's estimates were not very accurate. However, new methods of determining the radius of nuclei have been developed. These techniques include x-ray spectroscopy, electron scattering and the use of laser beams (Mackintosh *et al.*, 2002) that take into consideration the sphericity, diffuseness and electric quadrupole moments of the nucleus, thanks to the advances in quantum realm. Similarly, accurate determination of the nuclear sizes of unstable nuclei, neutron halos and neutron skin depths have been investigated experimentally through the application of advanced technologies such as radioactive nuclear beams (RNB)(Ozawa *et al., 2001*).

The nuclear charge density $\rho(r)$ is one of the most important bulk properties of nuclei, which is important in determining the nuclear charge radius. It is determined by using the Born approximation techniques of quantum mechanics and the inverse Fourier transformations (Ghoshal, 2008). With the application of good fits on experimental nuclear data, the nuclear density distribution assumes the form;

$$\rho(r) = \rho_0 \left[1 + \exp\left(\frac{r-R}{a} \right) \right]^{-1} \tag{2.8}$$

Here, ρ_0 is the nuclear density at the centre $(r=0)$, r is the distance from the centre of the nucleus, R is the nuclear radius at half density and a is the skin depth of the nucleus. The exponential term is a mathematical function representing the phase

factor relative to the volume (Greiner and Maruhn, 1996; Ghoshal, 2008; Ozawa *et al.,* 2001).

The nuclear radius is considered as the radius of the nuclear matter (A) and the nuclear charge (Z), since nuclear charge parameter (Z) is linearly proportional to mass number (A) and charge density that is uniformly distributed in the nucleus. For a spherical shape of nucleus with radius (R) and nuclear volume (V) which is directly proportional to mass number, it has been proved mathematically that;

$$R = r_0 A^{\frac{1}{3}}$$ (2.9)

Here, the parameter r_0 is an empirical value called the nuclear radius parameter and it varies between $r_0 = 1.1\,\text{fm}$ for the light nuclei and $r_0 = 1.5\,\text{fm}$ for the heavy nuclei (Fan *et al.*, 1995 and Sakho, 2018). Therefore, the nuclear radius determines the strength of the long-range Coulomb potential energy, which is experienced at the nuclear surface in a charged sphere (Jänecke, 1972).

2.6 Super heavy nuclei

Super heavy nuclei represent a category of elements whose atomic number (Z) are beyond that of transuranic elements $(Z > 103)$. These elements are artificial, radioactive and they do not occur in large quantities but exist briefly under highly controlled conditions. Glenn Seaborg proposed the existence of transuranic elements in 1960s and they have been found to have half-lives ranging from hours to milliseconds (Murthy, 2017). Glenn Seaborg also predicted a possibility of an "island of stability" for the super heavy elements. It is not yet clear whether this island of super heavy nuclei exists (Mackintosh *et al.*, 2002). However, stable heavy nuclei

with increased life times of millions of years have been predicted to reside in the island of stability (Oganessian, 2012).

A considerable advancement in experimental techniques in the field of nuclear physics has been made in the last few decades following the production of several isotopes in some laboratories across the globe using radioactive beams (Changizi, 2017; Tarasov *et al.*, 2018). These advances have made it possible to explore the possibility of existence of heavy nuclei near the proton and neutron drip lines, the structure of exotic nuclei and the synthesis of super heavy nuclei (Oganessian and Utyonkov, 2015). The outcome of these rigorous theoretical and experimental investigations includes the creation of new elements and acquisition of pertinent information and data on half-lives of several nuclei. Such information is crucial in studying the long predicted "island of stability" (National Research Council, 2013).

The first super heavy element (transactinide) to be synthesized was Rutherfordium (Rf, Z=104), which was synthesized at Joint Institute for Nuclear Research, Dubna, Russia (Roberto *et al.*, 2015). The procedure involved bombarding Plutonium $\left(^{242}_{94}Pu\right)$ target with neon ions $\left(^{22}_{10}Ne\right)$ in a particle accelerator. The techniques that were used in 1990s in the production of other super heavy elements include cold fusion experiments whereby the heavy targets of elements such as lead and bismuth were bombarded with heavy ions of iron and nickel at energies slightly above the Coulomb barrier. However, in this technique, the capture cross-sections decrease steadily with increasing atomic numbers, hence making the technique impractical for elements above Z=112 (Zagrebaev *et al.*, 2003). The failure of cold fusion gave rise to the hot fusion in the early 2000s; a technique that entails bombardment of actinide targets

with $^{48}_{20}Ca$ beams to create a highly excited compound nucleus (Oganessian and Utyonkov, 2015).

The method of hot fusion technique led to the synthesis of six new super heavy elements whose atomic numbers range from Z=113 to Z=118. Until today, the last of the super heavy elements has Z=118, and several attempts are in place to produce the elements whose atomic numbers are Z=119 and Z=120 using projectiles whose atomic numbers are greater than 20 (Oganessian and Utyonkov, 2015; Oganessian and Rykaczewski, 2015). Furthermore, studies on transmission probabilities, compound nucleus formation probabilities, survival probabilities and cross-sections for projectiles that can be used in the synthesis of isotopes of Z=117 have also been carried out, and the results show that their synthesis largely depend on the reactions systems (Manjunatha and Sridhar, 2017).

Other super heavy nuclei that have been predicted to exist using sophisticated theoretical models include $^{292}120$, $^{340}122$, $^{360}130$, $^{432}134$, $^{392}134$, $^{364}138$, $^{416}164$ and $^{476}184$. The nuclide $^{292}120$ was predicted to have shell closures that were related to the central density depression at the central part of the spherical nucleus (Afanasjev *et al.,* 2018). This was achieved through the application of relativistic models and Skyrme interactions (Bender *et al.,* 1999; Afanasjev and Frauendorf, 2005). Studies on biconcave disks and toroidal shapes of some nuclei using Skyrme-Hartree-Fock (SHF) calculations revealed that the nuclide $^{364}138$ yields the lowest energy in the toroidal solutions (Staszczak and Wong, 2008). In addition, the Gogny-Hartree-Fock-Bogoliubov (HFB) calculations showed that, in the nuclei $^{416}164$ and $^{476}184$ their toroidal shapes represent the lowest in energy solutions at axial shape (Warda, 2007; Afanasjev *et al*., 2018). Similarly, the calculations obtained from triaxial Relativistic

Hartree-Bogoliubov (RHB) theory predicted the existence of the super heavy nuclei $^{360}130$, $^{432}134$, $^{340}122$ and $^{392}134$, which had more pronounced triaxial deformations that tend to reduce the stability of the nuclei against spontaneous fission (Afanasjev *et al*., 2018). Therefore, these super heavy nuclei were investigated in this study, in order to predict their most stable isobars.

2.7 Island of Stability of Super Heavy Elements

The island of stability is an allegorical term that was coined by William Myers and Wladyslaw Świątecki in 1960s and promoted by Glenn Seaborg (Kragh, 2017; Kragh 2018). This term came up as a result of calculations of half-lives for some nuclei on the island of spherical super heavy nuclei that yielded millions of years (Hoffmann *et al*., 2018). Therefore, the island of stability describes the region of nuclear landscape that is likely to accommodate the super heavy elements that have magic number of protons and neutrons. The super heavy elements (SHE) is a term that refers to the elements with Z=104 (Rutherfordium) and above. SHE can also be used interchangeably with super heavy nuclei (SHN) when one is referring to nuclei.

Therefore, super heavy elements (SHE) in the "island of stability" have been predicted to occur in the new closed shells at Z=114. Early predictions indicated that the next closed shell after Z=82 was Z=126, an analogous to the neutron magic number of N=126. Other calculations also suggested the existence of closures of subshells at Z=120 or Z=126 (Oganessian and Utyonkov, 2015). These predictions were in agreement with the earlier prediction of the magic numbers that were proved to have extremely high stability relative to their neighboring element as explained in the shell model.

Calculations based on the mass defects have been compared in the past with available experimental results and it was deduced that, the productions cross sections of the super heavy elements depends mainly on the position of the proton shell closures (Kuzmina *et al.*, 2012). Therefore, it is probable that the synthesis of the super heavy elements which are prohibitively costly to produce, and at the same time extremely difficult to identify even after being processed (Mackintosh *et al.*, 2002) might find their solution in accurate determination of the proton shell closures. This can be achieved through the modification of the Coulomb potential energy in the binding energy equation, the shell model calculations and the pairing interaction of the nucleons.

2.8 Nuclear models

Several nuclear models have been proposed to describe the structure of the nucleus but not in entirety. These models have brought enormous contributions in the study of the nucleus and they include the liquid drop model, Fermi gas model, the collective model, the shell model, the single particle model, individual particle model, superfluid model, Bethe-Weizsäcker mass formula, among others. Although the contributions of these models in describing the nature of nucleon-nucleon interaction are enormous, a theoretical model that can explain all the properties of nuclei entirely is yet to be developed. Notably, the study of these nuclear models and their modifications aided by the recent advances in nuclear theory may produce some useful models whose predictions can be confirmed experimentally.

Due to the challenges encountered in developing a satisfactory theory, several scientists have carried out investigations, spread over decades, on the nucleus of an atom with a view of understanding the complex nature of internucleon interaction that

exists in the nucleus. This includes the application of symmetry concepts to spin and iso-spin degrees of freedom (Heisenberg, 1932; Wigner, 1937) and the linking of the shell model with collective structure (Elliott, 1958) using SU (3) model (Harvey, 1968). The collective effects of SU (3) model in atomic nuclei are described as elementary modes (Bohr and Mottelson, 1998).

The recent discoveries about the properties of pure neutron matter and neutron stars emphatically point out the existence of many-body interactions, which can be studied using the many body theory and formulation of theoretical models that can accommodate such many body systems (Gandolfi *et al.*, 2015). Consequently, several theories have been proposed to describe the structure of the nucleus. However, none of the proposed theories and mathematical derivations have given a full understanding of the large number of the inter-nucleon interactions, since the Schrödinger equation cannot be accurately solved for such a many body system (Ghoshal, 2008). It is suggested that, the solution to this puzzle lies in the development of new models or in the modification of the existing nuclear models.

2.8.1 Liquid drop Model

The liquid drop model (LDM) was the first historical model to describe the nuclear properties of an atom (Barrett, 1999; Heyde, 2004). It was first proposed by a Russian Physicist G. Gamow in 1928 (Mishra *et al.,* 2016) and later improved by N. Bohr and J. Wheeler (Bohr and Wheeler, 1939). This model is unique in the sense that, it treats the nucleus as a liquid droplet of an incompressible fluid having huge amount of density, thus, it clearly explains the spherical shape of most nuclei as well as predicting roughly the binding energies of the nuclei. The binding energies are calculated using the famous Bethe-Weizsäcker mass formula, that was formulated by

a German Physicist, C.F Von Weizsäcker in 1935 (Weizsäcker, 1935) using the concepts of the liquid drop model. Even though the liquid drop model successfully describes the collective behavior of the nucleons, it is not successful in describing the low-lying excited states of the nucleus due to the collective motions of the large number of nucleons that are involved in nuclear interactions (Ghoshal, 2008).

2.8.2 Nuclear Shell Model

The shell model is credited for being the foundation of the nuclear structure theory (Wang *et al*., 2012). This model considers the nucleons in an atom to be moving in some potential in discrete shells called energy levels with some level schemes having extra potential. This concept was first discovered by W.M Elsasser in 1933 (Ghahramany *et al*., 2007). In 1948, M. G. Mayer showed that the nuclei that had 2, 8, 20, 28, 50 and 82 number of protons and 2, 8, 20, 28, 50, 82 and 126 number of neutrons had very high stability (Mayer, 1949). Again, O. Haxel, JHD Jensen and H. E. Suess independently showed this concept in 1949, and this became the genesis of the nuclear shell model (Haxel *et al*., 1949; Johnson, 2004). The numbers of protons and neutrons that exhibited extra stability among the nuclei were referred to as magic numbers and these numbers give rise to the most stable isotopes and isotones among the nuclei.

Notably, the occurrence of the so-called magic numbers; 2, 8, 20, 28, 50, 82 and 126 from experimental point of view has been one of the strongest motivation for the formulation of the nuclear shell model where the magic numbers correspond to the shell closures (Peter and Schuck, 1980). Apart from describing the magic numbers, the shell model describes well many features that include the spin-orbit interaction,

spin-parity and magnetic moments of nuclei, however, it has a limitation over the unknown form of potential resulting from the electric quadrupole moments.

In an attempt to explain the deformation of the nuclear core resulting from quadrupole moments in the shell model, Aage Bohr and Ben Mottelson in 1953 came up with a unified model called the collective model, which is a merger of the shell model and the liquid drop model (Rowe and Wood, 2010; Ghoshal, 2008). This model looks at the collective properties of nucleon as whole by considering the oscillations and the nuclear excitations of the liquid drop vibrating at high frequency. It introduces the concept of non-sphericity resulting from the rotation and vibration of the nucleus hence predicting additional rotational and vibrational energy levels (William, 2018).

2.8.3 Fermi Gas Model

The Fermi gas model is another model that is quite simple and provides invaluable insights into the nuclear structure by assuming the nucleus as a degenerate gas of protons and neutrons (Greiner and Maruhn, 1996). This model incorporates the concepts of quantum mechanics. Therefore, it enriches the predictions of the binding energy equation proposed in the liquid drop model by adding the asymmetry energy and the pairing energy term. The limiting factor in this model is that, it fails to predict the detailed properties of the low-lying states of nuclei observed in radioactive decay process (Shreepad, 2011).

2.8.4 Individual Particle Model

Individual particle model is also referred to as independent particle model. This model assumes that all the nucleons move independently in a common spherical potential. Independent particle model describes the nucleus in terms of non-interacting particles in mass-dependent orbits of spherical potential field. Its strength is that, it can be

used to calculate the wave function of a system (Ghoshal, 2008). However, the individual particle model is only applicable to those nuclei having a single nucleon outside the closed shells and it partially depends on the cogency of the shell model (Casten, 2000).

2.8.5 Super Fluid Model

The super fluid model is also known as the quasi-particle phonon nuclear model. This model explains the pairing interaction of even-even, odd-odd and even-odd or odd-even configuration in different shells (Dumitrescu and Horoi, 1990). The super fluid model is the only model that describes the existence of large energy gap in between the ground state and the excited states of the even-even nuclei (Malov and Solov'ev, 1980). Such energy gap also exists during the formation of the cooper pairs in superconductors and in the transformation of non-interacting quasi-particles into a new spectrum of single particle states (Ghoshal, 2008). This model is only limited to describing the pairing interaction of nucleons and quasi-particles.

2.8.6 Single Particle Model

The single particle model is special model that takes into account the internucleon interaction in a shell. It assumes that, the difference between the nucleon-nucleon interaction and the central potential or residual interactions does not cause perturbation of the single particle levels (Van Roosbroeck, 2002). The single particle model has several applications that include the calculation of nuclear magnetic moments. It also provides an elaborate explanation of the angular momentum of the nucleus through the application of Nordheim's rules (Talmi, 2005) and the parities of odd A nuclei. This model also provides an explanation for the existence of the islands of isomerism in excited states of some nuclei (Grzywacz *et al*., 1998). On the

contrary, the single particle model does not explain the occurrence of very large values of quadrupole moments in many nuclei (Ghoshal, 2008).

Despite the fact that there is sufficiently large amount of data and information that is obtainable from the applications of the nuclear models, a unified theoretical framework that can explain all the properties of nuclei especially the super heavy nuclei is yet to be developed. It is possible that, a breakthrough in these puzzles lies in the development of some advanced nuclear and theoretical models that can predict the nuclear structure of all the nuclei with minimal errors. This is only achievable through the application of computational techniques in many-body theory that may describe all the properties of the nucleus of an atom in a unified manner (Hjorth-Jensen *et al*., 2017).

2.9 The Closed shells of the Shell model

A closer review of all the nuclear models shows greater advances in understanding the structure of the nucleus (Mayer, 1949). Among these models, the shell model stands out to be a unique and sophisticated model. This is because it considers the nucleons as independent particles in a potential well, operating under the action of Pauli Exclusion Principle and the uncertainty principle (Peter and Schuck, 1980). In addition, the shell model is lauded for describing vividly the existence of highly stable nuclei that are doubly magic. These kind of nuclei include $^{4}_{2}He$, $^{40}_{20}Ca$, $^{208}_{82}Pb$ among others. Studies have also shown that, the naturally occurring isotopes and isotones of elements that contain magic number of protons or neutrons generally have greater relative abundance (Schwarzschild, 2010; Nakada and Sugiura, 2014). Similarly, such nuclei exist in large quantities compared to their neighbouring elements that do not have magic numbers. The strength of the shell model is that, it is open to refinements.

Therefore, many features of the nucleus in the ground state, the excited states and the closed shells of nuclei having magic number of protons and neutrons can be studied independently. This includes the properties of the super heavy nuclei that are predicted to reside in the island of stability.

2.10 Pairing Interactions between nucleons

The pairing effect of nucleons in atomic nuclei supplies the extra binding energy associated with pairs of nucleons having even-even, odd-even or even-odd and odd-odd nuclei, and the odd-even mass staggering of binding energies in nuclear spectroscopy (Changizi, 2017). Various formulae have been derived to study the pairing correlations of isotopes. One of such formulae is the famous Bethe-Weizsäcker semi-empirical mass formula written in Eq. (2.1). In this formula the pairing energy is written as $\pm\delta(A)$ and it is computed as (Peter and Schuck, 1980);

$$
\left.\begin{aligned}
\delta(A) &= +34A^{-\frac{3}{4}} \rightarrow \text{For even-even nuclei.} \\
\delta(A) &= 0 \rightarrow \text{For even-odd or odd-even nuclei.} \\
\delta(A) &= -34A^{-\frac{3}{4}} \rightarrow \text{For odd-odd nuclei.}
\end{aligned}\right\} \tag{2.10}
$$

The pairing interaction is one of the long-standing problems of nuclear structure, which was first investigated in even-odd staggering of binding energies (Ishkhanov *et al*., 2014) and it remains to be one of the long-studied topics in nuclei and nuclear matter (Dean and Hjorth-Jensen, 2003). Accordingly, particle pairing is an important interaction that is widely used in nuclear physics and other branches of physics (Draayer *et al.,* 2005). This is because it allows physicists to understand many important experimental facts such as the energy gap, the level density, odd-even effect, moment of inertia, low-lying 2^{+} states and nuclear deformations (Ring and Schuck, 2004).

The pairing interaction of nuclei contributes the pairing energy term in the binding energy equation, which is defined as the surplus binding energy of the nucleus that comes from the configuration of the nucleons according to Pauli-exclusion principle. This pairing effect leads to the nuclei having either odd A nuclei or even A nuclei. Experimental and theoretical studies have proved that, out of the 252 known stable nuclei, five (5) nuclides have odd-odd (Z-N) configuration while 48 nuclides have odd-even (Z-N) configuration. Similarly, 53 nuclides have even-odd configurations and 146 nuclides have even-even configuration. The later, are the most stable (Wikipedia Contributors, 2020). A comparison between the even A and the odd A nuclei shows that, odd A nuclei are more strongly bound than odd-odd nuclei but they are less strongly bound when compared with even-even nuclei. This is caused by the pairing of the nucleons of the same type with opposite spin in the shell structure. Therefore, the pairing energy term increases the binding energy of the nucleons in the sense that, it is maximum for even-even nuclei. The reason is that, all nucleons with opposite spin form a pair while the unpaired nucleons in odd A nuclei results in the weakening of the binding energies, thus, affecting the stability of the nuclei.

The low energy nuclear structure properties strongly depend on the nuclear pairing force. In the calculations of nuclear masses, the contributions of pairing effects are vital in the low-lying quasi-particle energies that depend on the low-energy microscopic structure of the nucleus. The Bardeen Cooper Schrieffer (BCS) pairing model (Bohr *et al*., 1958; Belyaev, 1959; Nilsson and Prior, 1961; Ogle *et al*., 1971) has been successfully used in the nuclear structure calculations while assuming the pairing force to be constant (Nilsson *et al*., 1969; Bolsterli *et al*., 1972; Möller and Nix, 1981a; Möller and Nix, 1981b).

The problem in the BCS model arises from the fact that, there exist large spacings between the single particle levels at the Fermi-surface. This is especially true at magic numbers for neutrons and protons in the shell model. The deformed actinide nuclei at neutron numbers N=142 and N=152 show large single-particle energy level spacing near the Fermi-surface. Thus, the level pairs included in the pairing calculation are generally chosen symmetrically around the Fermi surface. The level spacing depends on pairing, whereas the pairing gap depends on neutron excess, odd-odd, odd-even and even-even nuclei. Therefore, the pairing between nucleons in nuclei makes an important contribution to the determination of binding energy of nuclei.

It is evident that, extensive research has been carried out over a century on the study of atomic nucleus. Consequently, there is a large measure of information and data that is available in nuclear theory. However, there is no single nuclear model that can describe and predict all the properties of different nuclei. In addition, the exact nature of interactions inside the nucleus is still not known since the properties of nuclei drastically change as Z and N, and hence A changes. Therefore, there is need to develop a theoretical model that can explain the nuclear properties in entirety. It is surmised that, such models derive their functionalism in the binding energy of the nucleus. This research therefore, investigated the effects of Coulomb interaction and pairing interaction between nucleons in the binding energy equation in order to determine the stability of finite nuclei in the nuclear landscape.

CHAPTER THREE

METHODOLOGY

3.1 Introduction

This chapter describes the detailed account of the methods that were used in formulating the modified Coulomb energy model and the pairing energy equation. The techniques that were applied in deriving the nuclear models and data collection have been elaborated in this section of the thesis. In addition, the relevant sources of pertinent information and data on binding energies, Coulomb energies and pairing energies of nuclei have been pointed out in this chapter.

3.2 The formulation of modified Coulomb energy model

The formulation of the modified Coulomb energy model is anchored on the binding energy equation, which is famously referred to as Bethe-Weizsäcker semi-empirical mass formula (SEMF). The semi-empirical mass formula written in Eq. (2.1) is composed of five basic terms, which are of great importance in nuclear theory. This research work focused mainly on two unique terms in the semi-empirical mass formula, namely, the Coulomb potential and the pairing energy term. These terms were selected for investigation since they are directly connected with the interaction of the nucleons, and their roles are relatively more important as the nuclear sizes increase from the low mass nuclei to the high mass nuclei.

By considering a liquid droplet, in which the charge distribution in the nuclear interior is uniform, the Coulomb energy can be written as (Bjørnholm and Lynn, 1980),

$$E_C = \frac{3}{5} \frac{Z_1 Z_2 e^2}{4\pi\varepsilon_0 r} \tag{3.1}$$

where, e is the electron charge, Z_1 and Z_2 are the number of protons and r is the distance between the protons. The protons inside the nucleus are closely packed in a very small volume whose radius is of the order of 10^{-13} cm (Choppin *et al.*, 2002). Therefore, Coulomb potential must be modified by introducing a correction term in order to make the Coulomb energy more effective inside the nucleus.

Therefore, introducing a multiplier correction term (C_t) in Eq. (3.1) yields,

$$E_C = \frac{\lambda}{r} C_t \qquad (3.2)$$

$$\text{where } \lambda = \frac{3}{5} \frac{Z_1 Z_2 e^2}{4\pi\varepsilon_0}$$

The correction term (C_t) is a factor for expressing the Coulomb energy dependence on the nuclear shape parameters using uniform distribution of charge inside the nucleus, (Khugaev *et al.*, 2007) and it is determined by the effects of the proton-proton repulsion in the nuclear-core of an atom.

Since the Coulomb energy is a long-range potential, most of the potential energy should be confined within the volume of the nucleus and it may at best extend to the boundary of the nucleus. It is therefore surmised that an exponential function will suit this requirement since it is the only mathematical function that allows the reduction of some quantities to zero as the variable tends to infinity. Hence, it is proposed that the correction term for the modified Coulomb energy may be written as,

$$C_t = e^{-\alpha r^n} \qquad (3.3)$$

where α represents the modified Coulomb energy screening term, r is the charge radius and n is a positive integer greater than or equal to 1. The power n ensures that the function continuous and differentiable.

Substituting Eq. (3.3) in Eq. (3.2) yields,

$$E_C = \frac{\lambda}{r} e^{-\alpha r^n}$$

(3.4)

Since the variation of the Coulomb energy (E_C) at the nuclear boundary is equal to zero, the boundary condition is such that,

$$\left(\frac{\partial E_C}{\partial r} \right)_{r=R} = 0, \text{ for } 0 \leq r \leq R$$

(3.5)

The differentiation of Eq. (3.4) using the condition in Eq. (3.5) yields,

$$\alpha = -\frac{1}{nR^n}$$

(3.6)

Hence, Eq. (3.4) becomes,

$$E_C = \frac{\lambda}{r} e^{\frac{r^n}{nR^n}}$$

(3.7)

If the core of a nucleus of mass number A is assumed to be composed of neutron-proton pairs, and there are Z protons (N>Z), then the number of nucleons in the core is 2Z, and the core radius (R_0) is given by $R_0 = r_0 (2Z)^{\frac{1}{3}}$. Since r is the distance between any two protons inside the core, the maximum value of r will be $r = R_0$. Therefore, R_0 will replace r in Eq. (3.7), and in Eq. (3.2) to yield the modified Coulomb energy equation (Cherop *et al.*, 2019a) which is written as,

$$\left. \begin{array}{c} E_C(Mod) = \dfrac{\lambda}{R_0} e^{\frac{R_0^n}{nR^n}} \\[2mm] or \\[2mm] E_C(Mod) = \dfrac{3}{5} \dfrac{Z_1 Z_2 e^2}{4\pi\varepsilon_0 R_0} e^{\frac{R_0^n}{nR^n}} \end{array} \right\}$$

(3.8)

The correction term (C_t) from Eq. (3.8) is written as,

$$C_t = e^{\frac{R_0{}^n}{nR^n}} \tag{3.9}$$

Therefore, the derived modified Coulomb energy model (finite Coulomb energy model) in Eq. (3.8) was used to calculate the Coulomb energies of some selected finite nuclei whose neutron number is greater than the proton number. The effects of the correction term in Eq. (3.9) was studied in order to investigate the role of Coulomb energy in the binding energy equation for the finite nuclei and to calculate the values of stable atomic numbers that are responsible for the stability of the isobars.

3.3 The application of the modified Coulomb energy equation

The modified Coulomb energy model was substituted in the binding energy equation to obtain the modified binding energy equation. The modified binding energy equation was studied to determine its contribution in the calculations for the stability of isobaric nuclei and the limits of Coulomb stability.

3.3.1 Derivations of Z_{STABLE} formula for finite nuclei using the modified Coulomb potential term

By substituting the modified Coulomb energy term in Eq. (2.1), the resultant equation takes the form;

$$BE(A,Z) = a_1 A - a_2 A^{\frac{2}{3}} - \frac{3}{5}\frac{Z^2 e^2}{4\pi\varepsilon_0 R_0}e^{\frac{R_0{}^n}{nR^n}} - a_4\frac{(A-2Z)^2}{A} \pm \delta(A) \tag{3.10}$$

To find the value of Z for which a nucleus for a given A is stable, Eq. (3.10) is differentiated with respect to Z and its derivative is equated to zero, to get the value of

Z for a stable nucleus that may be denoted by $Z_{STABLE\text{-}SEMF}$. The differentiation is done keeping A constant. Thus, for isobars,

$$\left(\frac{\partial BE}{\partial Z}\right)_{A=\text{Costant}} = -\frac{3}{5}(2Z)\frac{e^2}{4\pi\varepsilon_0 R_0}e^{\frac{R_0{}^n}{nR^n}} - a_4\frac{(A-2Z)}{A}(-4) = 0 \qquad (3.11)$$

Replacing Z with $Z_{STABLE\text{-}SEMF}$ in Eq. (3.11) yields,

$$-\frac{3}{5}(2)(Z_{STABLE\text{-}SEMF})\frac{e^2}{4\pi\varepsilon_0 R_0}e^{\frac{R_0{}^n}{nR^n}} + 4a_4 - \frac{8a_4}{A}(Z_{STABLE\text{-}SEMF}) = 0 \qquad (3.12)$$

The nuclear radius R_0 in Eq. (3.12) can be replaced with $R_0 = r_0(2Z)^{\frac{1}{3}}$, and upon making $Z_{STABLE\text{-}SEMF}$ the subject of the formula, the resulting equation can be written as,

$$Z_{STABLE\text{-}SEMF} = \frac{2a_4 A}{4a_4 + \frac{3}{5}\frac{e^2}{4\pi\varepsilon_0 r_0}A^{\frac{2}{3}}e^{\frac{R_0{}^n}{nR^n}}} \qquad (3.13)$$

Taking the nuclear radius parameter $r_0 = 1.22\,\text{fm}$ and substituting the numerical value

of the term $\dfrac{3}{5}\dfrac{e^2}{4\pi\varepsilon_0 r_0}$ in Eq. (3.13), yields Eq. (3.14);

$$Z_{STABLE\text{-}SEMF} = \frac{2a_4 A}{4a_4 + a_3 A^{\frac{2}{3}}e^{\frac{R_0{}^n}{nR^n}}} \qquad (3.14)$$

$$\text{where } a_3 = \frac{3}{5}\frac{e^2}{4\pi\varepsilon_0(1.22\,fm)} = 0.709 MeV$$

In Eq. (3.14), as $n \to \infty$, the term $e^{\frac{R_0{}^n}{nR^n}}$ goes to unity. Hence, Eq. (3.14) becomes

$$Z_{STABLE\text{-}SEMF} = \frac{2a_4 A}{4a_4 + a_3 A^{\frac{2}{3}}} \qquad (3.15)$$

The binding energy of the nucleus can also be written in terms of the mass defect (Choppin *et al.*, 2002; Rabinowitz, 2015) as shown in Eq. (3.16);

$$BE(A,Z) = \left\{ ZM_p + NM_n - M(A,Z) \right\} c^2 \qquad (3.16)$$

where, N is the neutron number, $M(A,Z)$ is the mass of an atom of mass number A and atomic number Z, $M_p = 1.00727650u$ is the proton rest mass, $M_n = 1.0086650u$ is the neutron rest mass and c is the velocity of light in vacuum. Eq. (3.16) can also be written as;

$$\left\{ M(A,Z) \right\} c^2 = (ZM_p + (A-Z)M_n)c^2 - BE(A,Z) \qquad (3.17)$$

where $BE(A,Z)$ is the semi-empirical mass formula written in Eq.(3.10). On substituting for the binding energy from Eq. (3.10) in Eq. (3.17) the resulting equation takes the form;

$$\left\{ M(A,Z) \right\} c^2 = \left\{ ZM_p + (A-Z)M_n \right\} c^2 - a_1 A + a_2 A^{\frac{2}{3}} + \frac{3}{5} \frac{Z^2 e^2}{4\pi\varepsilon_0 R_0} e^{\frac{R_0^n}{nR^n}} + a_4 \frac{(A-2Z)^2}{A} \pm \delta(A)$$

$$(3.18)$$

To find the value of Z for which the nucleus for a given A is stable, the value of $M(A,Z)$ in Eq. (3.18) is differentiated with respect to Z and the resulting expression is equated to zero to get,

$$\left(\frac{\partial M(A,Z)}{\partial Z} \right)_{A=\text{Costant}} = \left\{ M_p - M_n \right\} c^2 + \frac{3}{5}(2Z)\frac{e^2}{4\pi\varepsilon_0 R_0} e^{\frac{R_0^n}{nR^n}} + a_4 \frac{(A-2Z)}{A}(-4) = 0$$

$$(3.19)$$

The atomic number (Z) in Eq. (3.19) can now be replaced with $Z_{\text{STABLE-NMDF}}$, where NMDF stands for Nuclear Mass Defect Formula. This will yield,

$$\left(M_p - M_n\right)c^2 + \frac{3}{5}(2)\left(Z_{\text{STABLE-NMDF}}\right)\frac{e^2}{4\pi\varepsilon_0 R_0}e^{\frac{R_0{}^n}{nR^n}} - 4a_4 + \frac{8a_4}{A}\left(Z_{\text{STABLE-NMDF}}\right) = 0$$

(3.20)

Similarly, the nuclear radius R_0 can be replaced with $R_0 = r_0(2Z)^{\frac{1}{3}}$ and re-written in

terms of $Z_{\text{STABLE-NMDF}}$ to yield;

$$Z_{\text{STABLE-NMDF}} = \frac{2a_4 A - \frac{1}{2}Ac^2(M_p - M_n)}{4a_4 + \frac{3}{5}\frac{e^2}{4\pi\varepsilon_0 r_0}A^{\frac{2}{3}}e^{\frac{R_0{}^n}{nR^n}}}$$

(3.21)

Substituting for the values of M_P, M_n , c and replacing the numerical value of the

term $\frac{3}{5}\frac{e^2}{4\pi\varepsilon_0 r_0}$ with a_3 in Eq. (3.21) yields,

$$Z_{\text{STABLE-NMDF}} = \frac{2a_4 A + 0.646695A}{4a_4 + a_3 A^{\frac{2}{3}}e^{\frac{R_0{}^n}{nR^n}}}$$

(3.22)

The term $0.646695A$ in Eq. (3.22) comes from the mass formula. This term is due to

the difference in the mass of protons and neutrons whereby $M_P < M_n$.

In Eq. (3.22), as $n \rightarrow \infty$, the term $e^{\frac{R_0{}^n}{nR^n}}$ goes to unity. Hence, Eq. (3.22) becomes,

$$Z_{\text{STABLE-NMDF}} = \frac{2a_4 A + 0.646695A}{4a_4 + a_3 A^{\frac{2}{3}}}$$

(3.23)

Therefore, Eq. (3.14) and (3.22) were applied in the calculations of the most stable

values of Z in isobaric nuclei.

3.4 The modification of the pairing energy model

As the protons and neutrons pair up in the nuclear shell structure, the pairing energy

affects the binding energy in the sense that, the binding energy is maximum for even-

even nuclei and minimum for odd-odd nuclei as described in the Bethe-Weizsäcker mass formula (Dai *et al*., 2017). However, Bethe-Weizsäcker mass formula does not allow for the accurate calculations of the pairing energies isotope wise.

Calculations have shown that the pairing energy formula in Eq.(2.10) does not give sufficiently accurate and uniform results in the calculations of pairing energies for the pairs of isotopes, especially in the region where N>Z. This is attributed to the fact that, the proton-neutron pairing correlations are suppressed when more neutrons are added to the isotopes (Négréa, 2013). Furthermore, in the nuclear structure calculations, the pairing force has been assumed constant (Nilsson *et al*., 1969; Bolsterli *et al*., 1972; Möller and Nix, 1981a; Möller and Nix, 1981b). Therefore, to calculate the pairing energies, isotope wise, the pairing energy equation derived by Wang *et al*. (2017) is modified using the binding energies of the nuclei.

According to Wang *et al*. (2017), the pairing energy for pairs of neutrons can be calculated using the formula in Eq. (3.24),

$$P_n(A,Z) = \frac{1}{4}(-1)^{A-Z+1}\left[-M(A+1,Z)+3M(A,Z)-3M(A-1,Z)+M(A-2,Z)\right]$$

(3.24)

where $P_n(A,Z)$ is the neutron pairing energy, A is the mass number of the element, Z is the atomic number, and the right hand side gives the combination of the involved masses. The mass excess, free of the bound nucleus can be written as ΔM, defined as the difference between the total mass of nucleons and the combined mass of the nucleus (Ghoshal, 2008) such that,

$$\Delta M = ZM_P + NM_N - M(A,Z)$$

(3.25)

where N is the neutron number, M_P is the proton mass, M_N is the neutron mass and A is the mass number of a nucleus.

The mass excess of any element can also be expressed as a function of binding energy (Rabinowitz, 2015). Therefore, Eq. (3.24) can be modified such that the binding energy (BE(A, Z)) is used instead of the mass (M) to calculate the pairing energies of nuclei isotope wise (Cherop *et. al.,* 2019b). Thus, Eq. (3.24) can be written as,

$$P_N(A,Z) = \frac{1}{4}(-1)^{A-Z+1}\left[-B(A+1,Z)+3B(A,Z)-3B(A-1,Z)+B(A-2,Z)\right]$$

$$(3.26)$$

To calculate $P_N(A,Z)$, the values of binding energy, were taken from atomic mass evaluation tables, AME2016 (Wang *et al*., 2017) and they were be used to calculate the pairing energies of various isotopes.

Experiments on pairing interaction of nucleons have shown that, pairing energy depends on the mass number (A) (Dean and Hjorth-Jensen, 2003; Ghoshal, 2008). Therefore, the pairing energies of O-O (odd-odd), O-E (odd-even), E-E (even-even) and E-O (even-odd) nuclei, in the shell structure, were computed using the modified pairing energy equation, Eq. (3.26). The calculations of the pairing energies that were obtained were plotted against the mass numbers (A) and the nature of their graphs were analyzed in order to predict the stability and abundance of the elements isotope wise. In addition, the tables of natural abundance (Rosman and Taylor, 1999) were used as a constraint to the results; to check on the natural abundance of the elements, to draw some comparisons and to ascertain the validity of the model. This was carried out in order to investigate the role of the shell model in determining the pairing

interaction of some finite nuclei, isotope wise, as well as establishing a criterion for their existence on earth, collapsed neutron star merger and the "island of stability".

3.5 Selection of Universal radius parameters

The universal radius parameter is also referred to as the nuclear radius parameter. It is an empirical value that is useful in the calculation of radius of a spherical nucleus of an atom. Several experimental and theoretical techniques have been applied in determining the universal radius parameter (r_0). Calculations reveal that, this parameter varies between $r_0 \approx 1.1\,\text{fm}$ and $r_0 \approx 1.5\,\text{fm}$ depending on the nuclear size (Fan *et al*., 1995; Sakho, 2018). In this thesis, the nuclear radii parameter chosen were; $r_0 = 1.22\,\text{fm}$, a value that was applied in the derivation of the Coulomb constant, $a_3 = 0.71\text{MeV}$ (Dai *et al*., 2017), and $r_0 = 1.135\,\text{fm}$ that was obtained from electron scattering experiment and muon capture x-ray data (Collard *et al*., 1967).

For the hyperheavy nuclei, the value of nuclear radius parameter that was selected for calculation was $r_0 = 1.5\,\text{fm}$ since their nuclear masses are extremely large. The values of the nuclear radii parameters were used separately to calculate the nuclear effective radius (R) and the nuclear core radius (*R₀*), which were then substituted in the derived model to calculate the modified Coulomb energy. The values of the Coulomb energies obtained were compared with other modified Coulomb energy values (E_C (Dir) and E_C (SEMFE)) in order to study their variations and trends.

CHAPTER FOUR

RESULTS AND DISCUSSION

4.1 Introduction

This chapter presents the results and discussions of the findings that were obtained from this study. The calculations obtained from the theoretical models that were formulated in Chapter three were analysed and interpreted accordingly. The results are presented in form of graphs, figures and tables and a detailed discussion of the findings is provided.

4.2 The results of the correction terms for finite nuclei

The model of the correction term derived in Eq. (3.9) gives us the exponential terms of the ratio of the powers of the nuclear core radius (R_0) to the powers of the effective nuclear radius (R). The values of R_0 and R were calculated using the formula $R_0 = r_0 (2Z)^{\frac{1}{3}}$ and $R = r_0 (A)^{\frac{1}{3}}$ respectively. These terms were used in the calculation of the correction terms of some selected nuclei which include $^{238}_{92}\text{U}$ using the nuclear radius parameter $r_0 = 1.22\,\text{fm}$.

The results from the calculations (Table 4.1) show that, the exponential correction terms decrease with an increase in the values of n in R^n and $R_0{}^n$ because the positive integer $n \geq 1$ confines the proton charge in the nucleus. Similarly, as the powers of their radii increase from $n = 1$ to $n > 21$, the powers of the effective nuclear radius (R) and powers of the nuclear core radius (R_0) become infinitely small. Consequently,

the ratio of $\dfrac{R_0{}^n}{nR^n}$ tends to the value zero and the exponential correction term goes to

unity as shown in the Table 4.1. Mathematically, this can be expressed as,

$$\lim_{n\to\infty}\left(\frac{R_0{}^n}{nR^n}\right)=0. \tag{4.1}$$

Table 4.1: Correction term for $^{238}_{92}U$ calculated using Eq. (3.9) and the nuclear radius parameter $r_0 = 1.22\,\text{fm}$

n	$R_o{}^n$	R^n	$e^{\frac{R_O^n}{nR^n}}$
1	6.94E-15	7.56E-15	2.50377
2	4.81E-29	5.72E-29	1.64872
3	3.34E-43	4.32E-43	1.39561
4	2.32E-57	3.27E-57	1.28403
5	1.61E-71	2.47E-71	1.22140
6	1.12E-85	1.87E-85	1.18136
7	7.7E-100	1.4E-99	1.15356
8	5.4E-114	1.1E-113	1.13315
9	3.7E-128	8.1E-128	1.11752
10	2.6E-142	6.1E-142	1.10517
11	1.8E-156	4.6E-156	1.09517
12	1.2E-170	3.5E-170	1.08690
13	8.6E-185	2.6E-184	1.07996
14	6E-199	2E-198	1.07404
15	4.2E-213	1.5E-212	1.06894
16	2.9E-227	1.1E-226	1.06449
17	2E-241	8.6E-241	1.06059
18	1.4E-255	6.5E-255	1.05712
19	9.7E-270	4.9E-269	1.05404
20	6.7E-284	3.7E-283	1.05127
21	4.6E-298	2.8E-297	1.04877
n>21	$R_o{}^n < 4.6E-298$	$R^n < 2.8E-297$	1.00000

Similar calculations were also done using $r_0 = 1.135\,\text{fm}$ and different values of nuclear radii were obtained, however, the same values of correction term were obtained as shown in Appendix I. This shows that the correction term is independent of the nuclear radius parameter that varies between $r_0 = 1.1\,\text{fm}$ for light nuclei and $r_0 = 1.5\,\text{fm}$ for the heavy nuclei.

The correction terms for other selected finite nuclei that range from the light nuclei to the super heavy nuclei were calculated using Eq. (3.9). The finite nuclei selected include Phosphorus (Z=15), Chromium (Z=24), Manganese (Z=25), Gellinium (Z=32), Zirconium (Z=40), Neodymium (Z=60), Nihonium (Z=113), Oganesson (Z=118) and three other hyperheavy nuclei which were given some arbitrary names; K*, L* and M*. These finite nuclei were selected randomly from the periodic table of elements while the hyperheavy nuclei, K*, L* and M* with atomic numbers $Z \simeq 138$, $Z \simeq 156$ and $Z \simeq 174$, respectively, are elements that were predicted to be stable against spontaneous fission (Afanasjev $et.$ $al.$, 2018). The results of the calculations are shown in Table 4.2 and Appendix II. So far, it has not been possible experimentally to produce nuclei with $Z > 118$; new experiments with very different targets and projectiles may have to be used to produce nuclei with Z=138, Z=156 and Z=174, although the calculation done in this thesis predict them as stable nuclei against spontaneous fission (SF).

Table 4.2: Correction terms of finite nuclei with Z=15, Z=24, Z=25, Z=32, Z=40 and Z=60, calculated using Eq. (3.9) and the nuclear radius parameter $r_0 = 1.22 \, \text{fm}$

n	CORRECTION TERMS					
	Z=15 (A=32)	Z=24 (A=55)	Z=25 (A=62)	Z=32 (A=72)	Z=40 (A=100)	Z=60 (A=162)
1	2.6610	2.6314	2.5365	2.6156	2.5303	2.4714
2	1.6143	1.5969	1.5422	1.5876	1.5386	1.5058
3	1.3668	1.3524	1.3084	1.3449	1.3056	1.2800
4	1.2578	1.2449	1.2064	1.2382	1.2040	1.1824
5	1.1967	1.1848	1.1500	1.1786	1.1478	1.1289
6	1.1577	1.1465	1.1145	1.1408	1.1126	1.0957
7	1.1307	1.1200	1.0903	1.1146	1.0886	1.0735
8	1.1110	1.1007	1.0730	1.0956	1.0714	1.0577
9	1.0959	1.0860	1.0600	1.0812	1.0585	1.0462
10	1.0840	1.0745	1.0500	1.0699	1.0487	1.0374
11	1.0744	1.0653	1.0422	1.0608	1.0409	1.0307
12	1.0665	1.0577	1.0359	1.0534	1.0347	1.0254
13	1.0599	1.0513	1.0307	1.0473	1.0297	1.0212
14	1.0543	1.0460	1.0265	1.0421	1.0255	1.0178
15	1.0495	1.0415	1.0230	1.0377	1.0221	1.0150
16	1.0453	1.0375	1.0200	1.0339	1.0192	1.0127
17	1.0416	1.0341	1.0175	1.0306	1.0168	1.0108
18	1.0384	1.0311	1.0154	1.0278	1.0147	1.0092
19	1.0356	1.0285	1.0136	1.0253	1.0129	1.0079
20	1.033	1.0262	1.012	1.0231	1.0114	1.0068
21	1.0308	1.0241	1.0106	1.0211	1.0100	1.0058
n>21	1.0000	1.0000	1.0000	1.0000	1.0000	1.0000

It is found that the correction terms decrease in all the elements as n increases from $n = 1$ to $n > 21$. As n goes beyond $n > 21$, the correction term (C_t) goes to unity. This implies that, no correction to the Coulomb law is required at large distances. In

fact, the correction term is meaningful only at small distances, which are of the order of the size of the nucleus since all the protons in the nucleus are confined to the core region of the nucleus.

4.3 The Modified Coulomb energies for the selected finite nuclei

The values of the correction terms in Table 4.1, Table 4.2 and Appendix II were substituted in modified Coulomb energy equation (Eq. (3.8)) to calculate the Coulomb energies. The results that were obtained are shown in Table 4.3 and in Appendices III and IV.

Table 4.3: Coulomb energies of finite nuclei with Z=15, Z=24, Z=25, Z=32, Z=40 and Z=60, calculated using Eq. 3.8 and the nuclear radius parameter of $r_0 = 1.22$ fm

n	Coulomb Energies (MeV)					
	Z=15	Z=24	Z=25	Z=32	Z=40	Z=60
1	127	283	292	459	648	1254
2	77	172	178	278	394	764
3	65	145	151	236	334	650
4	60	134	139	217	308	600
5	57	127	132	207	294	573
6	55	123	128	200	285	556
7	54	120	126	196	279	545
8	53	118	124	192	274	537
9	52	116	122	190	271	531
10	52	115	121	188	269	527
11	51	114	120	186	267	523
12	51	114	119	185	265	520
13	51	113	119	184	264	518
14	50	112	118	183	263	517
15	50	112	118	182	262	515
16	50	111	117	181	261	514
17	50	111	117	181	260	513
18	50	111	117	180	260	512
19	49	110	117	180	259	512
20	49	110	117	179	259	511
21	49	110	116	179	259	511
n>21	48	107	115	175	256	508

It was noted that, the Coulomb energies of the light nuclei were less than the heavy nuclei and decrease as the powers of their radii increase. This is attributed to the number of protons, which are less in the light nuclei but increase with increase in the mass number (A). When $n > 21$, the Coulomb potential decreases gradually due to the effects of the correction term. The Coulomb potential at short distances is unsteady since all the protons are confined in the nuclear core. At long distances, the Coulomb potential is accurate since Coulomb law is a long-range force. Therefore, introducing an exponential correction term confines the long range Coulomb law such that a finite range Coulomb energy is achieved, thus, defining the range of the Coulomb force inside the nucleus.

4.4 Comparison of Coulomb energies calculated from E_C(SEMFE), E_C(Dir) and E_C(Mod)

The Coulomb energies were calculated using the Coulomb energy equation in the Semi empirical mass formula (E_C(SEMFE)) written in Eq. (2.4), Jänecke's modified Coulomb energy (E_C(Dir)) shown in Eq. (2.5) and E_C(Mod) derived in Eq. (3.8). The values that were obtained are tabulated in Table 4.4.

Table 4.4: Comparison of Coulomb energies of some nuclei calculated using E_C(Dir),

E_C(SEMFE) and E_C(Mod) with nuclear radius parameter $r_0 = 1.22\,\text{fm}$

ELEMENTS	A	Z_1	Z_2	E_C(SEMFE) (MeV)	E_C(Dir) (MeV)	E_C(Mod) (MeV)
P	32	15	14	46.96	41.99	47.80
Cr	55	24	23	103.06	95.02	107.42
Mn	62	25	24	107.63	99.79	115.18
Ge	72	32	31	169.30	157.97	175.39
Zr	100	40	39	238.63	225.36	256.05
Nd	162	60	59	461.06	441.53	507.58
U	238	92	91	959.17	926.33	1041.01
Nh	282	113	112	1370.27	1327.50	1469.45
Og	294	118	117	1474.16	1429.18	1580.01
K*	368	138	137	1873.16	1822.51	2053.65
L*	466	156	155	2214.38	2161.53	2521.35
M*	584	174	173	2556.91	2502.63	3026.66

The results of Coulomb energies in Table 4.4 show that, the Coulomb energies calculated using the three methods increase steadily from the light nuclei to the hyperheavy nuclei. This is mainly due to the increase in the mass number (A) among the elements. As the mass number increases, the radius of the nucleus increases and the proton-proton repulsion in the core of the nucleus also increases leading to greater magnitude of Coulomb energy. Similarly, a comparison between E_C(SEMFE) , E_C(Dir) and E_C(Mod) showed that, E_C(Mod) is slightly higher than both E_C(Dir) and E_C(SEMFE) . The reason for this is that, the exponential correction term in the modified Coulomb energy formula (E_C(Mod)) confines all the nuclear charge in the nucleus, hence, more of the Coulomb's energy gets accounted for within the nucleus.

The calculations of Coulomb energies using Eq. (2.4), Eq. (2.5) and Eq. (3.8) were also done using the nuclear radius parameter $r_0 = 1.135\,\text{fm}$. The purpose was to study

the effects of the universal radius parameter on the Coulomb energies. The results obtained are shown in Table 4.5.

Table 4.5: Comparison of Coulomb energies of some nuclei calculated using E_C(Dir), E_C(SEMFE) and E_C(Mod) with nuclear radius parameter $r_0 = 1.135$ fm

ELEMENTS	A	Z_1	Z_2	E_C(SEMFE) (MeV)	E_C(Dir) (MeV)	E_C(Mod) (MeV)
P	32	15	14	50.27	44.41	51.38
Cr	55	24	23	110.31	100.88	115.46
Mn	62	25	24	115.21	106.03	123.81
Ge	72	32	31	181.22	168.00	188.53
Zr	100	40	39	255.43	240.12	275.22
Nd	162	60	59	493.53	471.47	545.62
U	238	92	91	1026.72	990.53	1118.96
Nh	282	113	112	1466.76	1420.25	1579.50
Og	294	118	117	1577.97	1529.21	1698.34
K*	368	138	137	2005.08	1951.25	2207.44
L*	466	156	155	2370.33	2315.49	2710.19
M*	584	174	173	2736.98	2682.11	3253.50

A comparison of the Coulomb energy results in Table 4.4 and Table 4.5 shows that the Coulomb energies obtained from the use of the nuclear radius parameter $r_0 = 1.135$ fm are greater than the results obtained from the use of $r_0 = 1.22$ fm. In addition, E_C(Mod) is greater than both E_C(Dir) and E_C(SEMFE). This suggests that, even though the nuclear radius parameter is a constant term, its interaction with the nuclear masses incidentally increases the nuclear radius, which is inversely proportional to the Coulomb's energy. Consequently, the nuclear radius parameter, $r_0 = 1.135$ fm gives out greater values of Coulomb energy than $r_0 = 1.22$ fm in all the nuclei, especially, the super heavy nuclei as shown in Appendix V. It is therefore evident that, the Coulomb energy depends on the nuclear radius parameter that varies between $r_0 = 1.1$ fm for light nuclei and $r_0 = 1.5$ fm for the heavy nuclei (Fan *et al*., 1995 and Sakho, 2018).

4.5 The Coulomb energies per nucleon

The Coulomb energies per nucleon for some fifteen randomly selected elements, whose masses increase with increase in Z but $Z \leq 92$ were computed using Eq. (2.4), Eq. (2.5) and Eq. (3.8). These elements include Li, B, C, O, F, P, Ca, Cr, Kr, Zr, In, Ba, Gd, Po and U. Their calculations for Coulomb energies per nucleon are shown in Appendix VI part (a) while their graphical representation is shown in Figure 4.1.
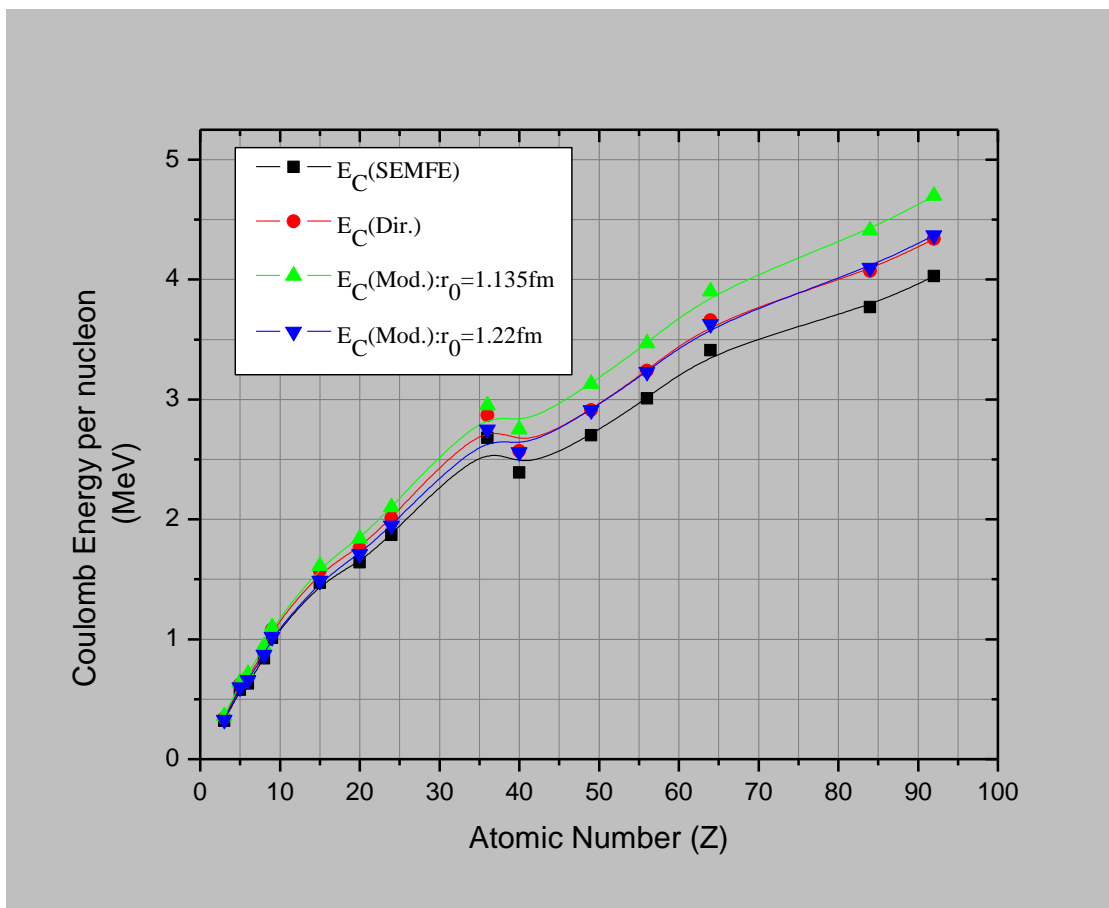
Figure 4.1: Graphical representation of the Coulomb Energies per nucleon of some Elements with $Z \leq 92$ obtained using Eq. (2.4), Eq. (2.5) and Eq. (3.8).

The graph of Coulomb energy per nucleon in Figure 4.1 shows that, the Coulomb energies per nucleon increase gradually as the atomic numbers (Z) increase. This is because of the proton-proton repulsion that brings about the multiplying effect of the Coulomb's energy, causing it to spread throughout the entire volume of the nucleus as

the nuclear size of the elements increases. A sharp increase in Coulomb energy per nucleon is observed in the element Krypton, and this is attributed to its inert nature; thus, it is more bound and stable than the neighbouring elements.

It has been noted that, there is a sharp decrease in the stability of transuranic elements as the proton number increases beyond $Z > 92$ (Oganessian, 2012). Therefore, to investigate the effects of Coulomb potential in the stability of the nuclei in this region $(Z > 92)$, the derived models in Eq. (2.4), Eq. (2.5) and Eq. (3.8) were used to calculate the Coulomb potentials per nucleon of the super heavy elements that were discovered recently using the method of hot fusion. These elements include Nihonium, Flerovium, Moscovium, Livermorium, Tennessine and Oganesson (Murthy, 2017). Since these elements are radioactive with very short half-lives, very little experimental information is known about their existence. Therefore, the Coulomb energies per nucleon of the isotopes of these elements were calculated using the available data in AME2016 (Wang *et al*., 2017). In order to study the contributions of excess neutrons in super heavy nuclei, some neutrons (100 neutrons) were added to the super heavy elements whose mass number is A to obtain A*, where A* is the mass of the isotopes with neutron excess. The results of these calculations are shown in Table 4.6.

Table 4.6: Coulomb energies per nucleon of both super heavy isotopes with Excess neutrons ranging between Z=113 to Z=118 calculated using Eq. (3.8)

ELEMENTS	A	E_C(Mod) (r_0=1.135fm)	E_C(Mod) (r_0=1.22fm)	A*	E_C(Mod) (r_0=1.135fm)	E_C(Mod) (r_0=1.22fm)
Nihonium Z=113	282	5.601	5.211	382	4.135	3.847
	283	5.581	5.193	383	4.124	3.837
	284	5.561	5.174	384	4.113	3.827
	285	5.542	5.156	385	4.102	3.817
	286	5.522	5.138	386	4.092	3.807
Flerovium Z=114	285	5.624	5.233	385	4.164	3.874
	286	5.605	5.214	386	4.153	3.864
	287	5.585	5.196	387	4.142	3.854
	288	5.566	5.178	388	4.131	3.844
	289	5.547	5.160	389	4.121	3.834
Moscovium Z=115	287	5.668	5.273	387	4.203	3.910
	288	5.648	5.254	388	4.192	3.900
	289	5.628	5.236	389	4.182	3.890
	290	5.609	5.218	390	4.171	3.880
Livermorium Z=116	291	5.672	5.277	391	4.221	3.927
	292	5.652	5.259	392	4.210	3.917
	293	5.633	5.241	393	4.200	3.907
Tennessine Z=117	293	5.714	5.316	393	4.260	3.963
	294	5.695	5.298	394	4.250	3.953
Oganesson Z=118	294	5.777	5.374	394	4.311	4.010

The results in Table 4.6 show that the Coulomb energy per nucleon among the super heavy nuclei decreases as the mass numbers increase among the isotopes. It was also noted that, the Coulomb potential among the isotopes of each super heavy element decreases with increase in the mass number. As neutrons are added to form nuclei having mass numbers with neutron excess (A*), the Coulomb energy decreases further with the minimum values recorded in the model, E_c(Mod), calculated using the nuclear radius parameter $r_0 = 1.22\,\text{fm}$. The reason for the decrease in Coulomb energies lies in the fact that, the excess neutrons lower the Coulomb potential by repressing the proton-proton repulsion.

4.5.1 The Coulomb energies per nucleon for elements with $Z \leq 174^*$

With the quest of peering into the "island of stability", the Coulomb energy per nucleon for the elements in Table 4.5 that include hyperheavy elements were also calculated. The graphical illustrations are shown in Figure 4.2 and the tabulated results are shown in Appendix VI part (b).
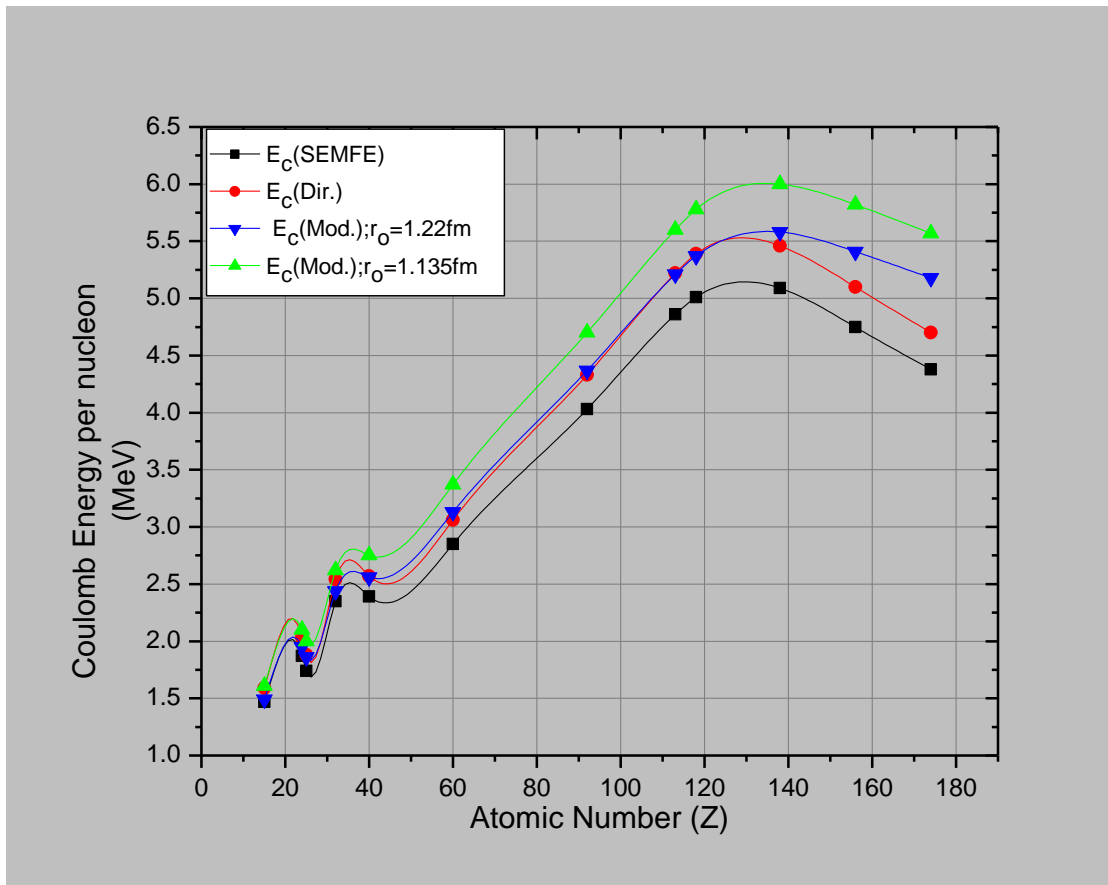
Figure 4.2: Graphical representation of the Coulomb Energies per nucleon of some Elements with $Z \leq 174^*$ obtained using Eq. (2.4), Eq. (2.5) and Eq. (3.8).

The results obtained in Figure 4.2 show some gradual increase in the Coulomb energy per nucleon among the light mass nuclei, intermediate mass nuclei and the super heavy and hyperheavy nuclei. However, unusual behavior was noted in the hyperheavy nuclei, that is, the Coulomb potentials stabilized and then dropped uniformly in all the models. This region lies in the range $120 \leq Z \leq 160$ which points

out to the region where the "island of stability" is likely to exist. Incidentally, the region described by the models is wider. Therefore, calculations that are more detailed are required in order to identify more precisely the most stable nuclei for some values of Z (Z_{STABLE}), particularly in the isobaric super heavy nuclei.

4.6 Calculation of Z_{STABLE} values for the stability of isobars

Isobars are nuclei of different elements having the same value of the mass number (A) but different values of protons (Z). The calculation of the most stable values of Z was based on the mathematical evaluation of Eq. (3.10) to yield Eq. (3.14) and Eq. (3.22). The derived models were applied in determining the most stable values of Z for a given mass number, having either even mass number or odd mass number. For the even mass numbers, the following values were selected; A=10, A=72, A=172, A= 368, A= 466 and A=584. For the odd mass numbers, the nuclei selected were A= 27, A=113 and A=277. It was found that, the two methods ($Z_{STABLE-NMDF}$ and $Z_{STABLE-SEMF}$) of determining the most stable values of Z gave similar results in the light nuclei and intermediate mass nuclei. However, different values of Z_{STABLE} were obtained when the two methods were applied in the calculation of the most stable isobars in the super heavy nuclei and the hyperheavy nuclei. The results obtained the for even A nuclei are shown in Table 4.7 and in Appendix VII.

Table 4.7: Calculations for Z_{STABLE} values for A=10 using Eq. (3.14) and Eq. (3.22)

A=10						
n	$R_0{}^n$	R^n	$\dfrac{R_0^n}{e^{nR^n}}$	$Z_{STABLE\text{-}SEMF}$	$Z_{STABLE\text{-}NMDF}$	ELEMENT
1	2.44E-15	2.62841E-15	2.530249	5	5	
2	5.95E-30	6.90854E-30	1.538622	5	5	
3	1.45E-44	1.81585E-44	1.305605	5	5	
4	3.54E-59	4.77279E-59	1.204017	5	5	
5	8.65E-74	1.25449E-73	1.147842	5	5	
6	2.11E-88	3.2973E-88	1.112563	5	5	
7	5.1E-103	8.6667E-103	1.088581	5	5	
8	1.3E-117	2.278E-117	1.071374	5	5	
9	3.1E-132	5.9874E-132	1.058538	5	5	
10	7.5E-147	1.5737E-146	1.048678	5	5	
11	1.8E-161	4.1364E-161	1.040927	5	5	
12	4.5E-176	1.0872E-175	1.034723	5	5	
13	1.1E-190	2.8577E-190	1.029681	5	5	BORON
14	2.7E-205	7.5111E-205	1.025534	5	5	
15	6.5E-220	1.9742E-219	1.022086	5	5	
16	1.6E-234	5.1891E-234	1.019194	5	5	
17	3.9E-249	1.3639E-248	1.01675	5	5	
18	9.4E-264	3.5849E-263	1.01467	5	5	
19	2.3E-278	9.4226E-278	1.01289	5	5	
20	5.6E-293	2.4766E-292	1.011359	5	5	
21	1.4E-307	6.5096E-307	1.010036	5	5	
n>21	$R_0{}^n$ < 1.4E-307	R^n < 6.509E-307	1.000000	5	5	

In the nuclei having even mass numbers A=10 and A=72, the two methods used gave the same results for the stable Z values. The values of Z_{STABLE} obtained from the calculations are Boron and Germanium, respectively. In the super heavy and hyperheavy nuclei, different values of Z_{STABLE} were obtained from each method. The variation in the results of Z_{STABLE} is caused by the effect of the masses of protons and neutrons whose influence is significant only in the heavy nuclei. It is also found that, similar trend of values for Z_{STABLE} in odd A nuclei is obtained. The results for odd A nuclei are shown in Table 4.8 and Appendix VIII.

Table 4.8: Calculations for Z_{STABLE} values for A= 113 using Eq. (3.14) and Eq. (3.22)

A=113							
N	$\mathbf{R_o^n}$	$\mathbf{R^n}$	$\dfrac{R_0^n}{e^{nR^n}}$	$\mathbf{Z_{STABLE\text{-}SEMF}}$	**ELEMENTS**	$\mathbf{Z_{STABLE\text{-}NMDF}}$	**ELEMENTS**
1	5.66E-15	5.9E-15	2.611904	39	YTTRIUM	39	YTTRIUM
2	3.21E-29	3.48E-29	1.585463	44	RUTHENIUM	45	RHODIUM
3	1.82E-43	2.05E-43	1.343107	46	PALLADIUM	46	PALLADIUM
4	1.03E-57	1.21E-57	1.236651	46		47	SILVER
5	5.82E-72	7.14E-72	1.177204	47		47	
6	3.3E-86	4.21E-86	1.139426	47		48	
7	1.9E-100	2.5E-100	1.113393	47	SILVER	48	
8	1.1E-114	1.5E-114	1.09443	47		48	
9	6E-129	8.6E-129	1.080048	47		48	
10	3.4E-143	5.1E-143	1.068802	47		48	
11	1.9E-157	3E-157	1.059794	48		48	
12	1.1E-171	1.8E-171	1.052439	48		48	
13	6.2E-186	1E-185	1.046336	48		48	CADMIUM
14	3.5E-200	6.2E-200	1.041207	48		48	
15	2E-214	3.6E-214	1.036847	48		48	
16	1.1E-228	2.1E-228	1.033104	48		48	
17	6.3E-243	1.3E-242	1.029866	48		48	
18	3.6E-257	7.5E-257	1.027044	48	CADMIUM	48	
19	2E-271	4.4E-271	1.024568	48		48	
20	1.1E-285	2.6E-285	1.022384	48		48	
21	6.5E-300	1.5E-299	1.020447	48		48	
$n>21$	$\mathbf{R_o^n <}$ 6.5E-300	$\mathbf{R^n <}$ 1.5E-299	1	48		49	INDIUM

It is found that, as the values of n increase from $n = 1$ to $n > 21$, different values of stable Z (Z_{STABLE}) are obtained. The most stable value of Z is obtained when $n > 21$. As n increases, the calculated values of Z_{STABLE} also increase by gaining protons. Considering the odd mass nuclei (A=113) in Table 4.8, it was found that the series for obtaining Z_{STABLE} are $Z=39 \rightarrow 44 \rightarrow 46 \rightarrow 47 \rightarrow 48$ for $Z_{STABLE\text{-}SEMF}$, and $Z=39 \rightarrow 45 \rightarrow 46 \rightarrow 47 \rightarrow 48 \rightarrow 49$ for $Z_{STABLE\text{-}NMDF}$. This series indicates that, as the nuclei stabilize, they undergo some beta and gamma decay transformations. Prior to

this, high energy nuclear reactions were predicted to occur during the initial stages of the nuclear transformation, for instance, the change occurring from $Z = 39 \rightarrow 44$ and $Z = 39 \rightarrow 45$.

The calculated values of stable atomic numbers (Z_{STABLE}) for the hyperheavy nuclei were compared with the values of K*, L* and M* that were predicted to be stable against spontaneous fission (Afanasjev *et. al.*, 2018). The stable values of Z for the masses A=368, A=466 and A=584 were predicted to be $Z \approx 138$, $Z \approx 156$ and $Z \approx 174$ respectively. These values of Z are approximate, thus, the accurate values of Z for the given masses were calculated using the derived models in Eq. (3.14) and Eq. (3.22) to yield the accurate results shown in Table 4.9.

Table 4.9: Comparisons between the Z_{STABLE} for Hyperheavy nuclei obtained from Eq. (3.14) and Eq. (3.22) with $Z_{STABLE\text{-Afanasjev }et al.}$

A	$Z_{STABLE\text{-Afanasjev }et al.}$	$Z_{STABLE\text{-SEMF}}$	Dev.	$Z_{STABLE\text{-NMDF}}$	Dev.
368	~138	132	-6	134	-4
466	~156	160	+4	162	+6
584	~174	190.	+16	193	+19

A comparison between the stable values of $Z_{STABLE\text{-SEMF}}$ and $Z_{STABLE\text{-NMDF}}$ shows wide deviations (Dev.) from the approximate values of $Z_{STABLE\text{-Afanasjev }et al.}$ The reason for these deviations was attributed to the irregularity in the neutron-proton ratio and the additional term 0.646695A which increases with increase in the nuclear size. Consequently, the binding energy and the probability decays of the super heavy and

hyperheavy nuclei will decrease with increase in the nuclear size. Similarly, the deviations in the values of stable atomic numbers between $Z_{STABLE-SEMF}$ and $Z_{STABLE-NMDF}$ arose from the contributions in the difference of protons and neutron masses, which are involved only in the calculation of $Z_{STABLE-NMDF}$ as illustrated in Eq. (3.22). With reference to the results of Eq. (3.22), it was noted that the effect of the mass difference between the protons and neutrons was minimal in the light nuclei whereas in heavy nuclei, the mass difference increases with increase in A, thus, affecting the calculated values of Z_{STABLE}. Therefore, the values of $Z_{STABLE-NMDF}$ are more accurate than $Z_{STABLE-SEMF}$.

The calculations for Z_{STABLE} values of the super heavy nuclei that were predicted using SHF, HFB and RHB models as discussed in section 2.6 of the literature review were calculated using Eq. (3.22). These nuclei include $^{292}120$, $^{340}122$, $^{360}130$, $^{432}134$, $^{392}134$, $^{364}138$, $^{416}164$ and $^{476}184$. The results of these calculations are shown in Appendix IX. The results revealed that, the application of Eq. (3.22) predicted the existence of some stable or long-lived nuclei among the super heavy isobars. These nuclei include $^{292}111$ which falls under the category of Roentgenium isotopes. Other stable isobars predicted by the model include $^{340}126$, $^{360}132$, $^{364}133$, $^{392}141$, $^{416}148$, $^{432}152$ and $^{476}164$. It is probable that, the nuclei $^{340}126$ and $^{432}152$ having magic and semi-magic proton numbers respectively, resides in the island of stability.

The stability of isobaric nuclei can also be studied using the mass parabolas (Ghoshal, 2008; Chemogos *et al*., 2019). In this research, the values of stable atomic numbers (Z_{STABLE}) that are shown in Tables 4.7, 4.8 and Appendices VII and VIII were compared with the graphs of the mass parabolas shown in appendix X, XI and XII. These mass parabolas were plotted using the values of the mass excess for isobaric

nuclei obtained from the atomic mass evaluation tables AME2016 (Wang *et al*., 2017).

It was found that, the mass parabolas shows accurately the most stable elements among the isobars in light nuclei with A=72 and in the intermediate mass nuclei in which A=113. However, as the mass number increases towards the super heavy nuclei, the mass parabolas change their trend to yield exponential curves as shown in Appendix XII. It was noted that, no single value of Z_{STABLE} could be obtained from the graphs of the mass parabolas among the super heavy elements, since the turning points of the curves cannot be traced with ease. The reason for the change in the nature of the graphs of the heavy nuclei is that, the super heavy nuclei are unstable and radioactive, thus, they undergo beta plus decay (β^{+}) in order to gain stability. As a result, the graphs of the mass excess against the atomic numbers among the super heavy nuclei does not give rise to meaningful parabolas which can predict the stable elements among the isobaric nuclei. Therefore, this anomaly in the trend of the mass parabolas can be solved by applying the Coulomb energy correction term derived in Eq. (3.9).

The correction terms operates on the Coulomb energy such that, as n increases from $n = 1$ to $n > 21$ as shown in Appendix I, the correction term goes to unity. As a result, different values of stable isobars are generated as shown in Appendices VIII and IX. The reason is that, the nuclei undergo beta minus (β^{-}) transformation step by step with Z=1 unit higher, until the most stable isobar is reached when $n > 21$.

4.7 Defining the limits of Coulomb stability

The modified Coulomb potential equation derived in Eq. (3.8) can be applied in defining the limits of Coulomb stability. Eq. (3.8) can be re-written in the form;

$$E_C (Mod) = \beta e^{\frac{R_0{}^n}{nR^n}} \tag{4.2}$$

where $\beta = \dfrac{3}{5} \dfrac{Z_1 Z_2 e^2}{4\pi\varepsilon_0 R_0}$ and $C_t = e^{\frac{R_0{}^n}{nR^n}}$ is the correction term.

Therefore, when $n = 1$, the $\lim\limits_{n=1}\left(\dfrac{R_0{}^n}{nR^n}\right) = \dfrac{R_0}{R}$, and the correction term (C_t) becomes,

$$C_t = e^{\frac{R_0}{R}} = 2.718^{\frac{R_0}{R}} \tag{4.3}$$

Similarly, when $n \to \infty$, the $\lim\limits_{n\to\infty}\left(\dfrac{R_0{}^n}{nR^n}\right) = 0$, and the correction term takes the form,

$$C_t = e^0 = 1 \tag{4.4}$$

The significance of above conditions is that, as $n \to \infty$, the correction term (C_t) goes to unity. This implies that, no correction to the Coulomb law is required at large distance. In fact, Coulomb law is a long-range force, thus, the Coulomb energies are very accurate at large distances. At very small distance, which is of the order of the size of the nucleus, the correction term is meaningful since all the protons in the nucleus are confined to the core region of the nucleus. Therefore, the range of Coulomb energy inside the nucleus varies in a range defined by;

$$2.718^{\frac{R_0}{R}}\beta \le E_c (Mod) \le \beta \tag{4.5}$$

The range described in Eq. (4.5) provides the limit of Coulomb stability. This range describes the magnitude of the Coulomb barrier that prevents the fission of the nucleus. It also describes the boundary within which the maximum and minimum number of protons or neutrons can lead to shell stabilization.

4.8 The calculations of the pairing energies

The Calculations of pairing energies of O-O (odd-odd) and O-E (odd-even), E-E (even-even) and E-O (even-odd) isotopes were calculated using Eq. (3.26) and their results are shown in Table 4.10 and Table 4.11.

Table 4.10: The table of calculated Pairing Energies (P_N) for $_{15}$P and $_{25}$Mn using Eq. (3.26).

PHOSPHORUS (P)			MANGANESE (Mn)		
(A)	*Odd-Odd* *(Z-N)*	*P_N* *(keV)*	*(A)*	*Odd-Odd* *(Z-N)*	*P_N* *(keV)*
26	15-11	-77.85	46	25-21	-42.58
28	15-13	-80.25	48	25-23	-26.07
30	15-15	-66.72	50	25-25	-20.32
32	15-17	-52.86	52	25-27	-22.95
34	15-19	-44.75	54	25-29	-20.83
36	15-21	-58.62	56	25-31	-19.70
38	15-23	-37.75	58	25-33	-15.70
40	15-25	-28.48	60	25-35	-15.15
42	15-27	-31.50	62	25-37	-14.55
44	15-29	-17.75	64	25-39	-16.31
46	15-31	-16.00	66	25-41	-12.06
			68	25-43	-12.30
			70	25-45	-11.25
(A)	*Odd-Even* *(Z-N)*	*P_N* *(keV)*	*(A)*	*Odd-Even* *(Z-N)*	*P_N* *(keV)*
27	15-12	-75.18	47	25-22	-31.93
29	15-14	-85.29	49	25-24	-24.96
31	15-16	-42.52	51	25-26	-18.21
33	15-18	-45.51	53	25-28	-21.84
35	15-20	-50.03	55	25-30	-19.25
37	15-22	-44.51	57	25-32	-15.88
39	15-24	-34.98	59	25-34	-15.35
41	15-26	-27.60	61	25-36	-13.68
43	15-28	-26.40	63	25-38	-15.32
45	15-30	-16.00	65	25-40	-15.77
			67	25-42	-10.32
			69	25-44	-11.75
			71	25-46	-11.25

Table 4.11: The table of calculated Pairing Energies (P_N) for _40Zr and _60Nd using Eq. (3.26)

ZIRCONIUM (Zr)			NEODYMIUM (Nd)		
(A)	*Even-Even (Z-N)*	P_N *(keV)*	*(A)*	*Even-Even (Z-N)*	P_N *(keV)*
80	40-40	-21.15	126	60-66	-9.750
82	40-42	-21.36	128	60-68	-10.00
84	40-44	-20.88	130	60-70	-10.81
86	40-46	-18.85	132	60-72	-9.960
88	40-48	-16.96	134	60-74	-9.670
90	40-50	-20.64	136	60-76	-9.258
92	40-52	-9.110	138	60-78	-8.150
94	40-54	-8.657	140	60-80	-8.173
96	40-56	-9.556	142	60-82	-9.733
98	40-58	-7.270	144	60-84	-6.536
100	40-60	-11.06	146	60-86	-7.009
102	40-62	-9.410	148	60-88	-7.343
104	40-64	-9.290	150	60-90	-7.328
106	40-66	-5.850	152	60-92	-6.552
108	40-68	-7.500	154	60-94	-5.416
110	40-70	-9.000	156	60-96	-6.335
			158	60-98	-5.305
			160	60-100	-6.000
(A)	*Even-Odd (Z-N)*	P_N *(keV)*	*(A)*	*Even-Odd (Z-N)*	P_N *(keV)*
79	40-39	-15.00	127	60-67	-9.750
81	40-41	-23.87	129	60-69	-10.38
83	40-43	-21.62	131	60-71	-10.86
85	40-45	-20.16	133	60-73	-9.768
87	40-47	-18.30	135	60-75	-9.620
89	40-49	-16.08	137	60-77	-8.528
91	40-51	-17.32	139	60-79	-8.466
93	40-53	-9.165	141	60-81	-7.368
95	40-55	-8.333	143	60-83	-9.508
97	40-57	-8.126	145	60-85	-6.702
99	40-59	-11.24	147	60-87	-7.364
101	40-61	-8.968	149	60-89	-7.795
103	40-63	-9.468	151	60-91	-6.621
105	40-65	-8.318	153	60-93	-5.478
107	40-67	-5.335	155	60-95	-6.080
109	40-69	-9.250	157	60-97	-6.030
111	40-71	-8.250	159	60-99	-5.510
			161	60-101	-6.000

The pairing energy calculations showed that the mass number (A) increases with decrease in the absolute values of the pairing energies (P_N). However, some unusual rises in the values of pairing energies (P_N) are obtained for some isotopes. For instance, the Phosphorus isotopes have unusual rises at A=28 and A=35 in the odd-even isotopes while in the odd-odd isotopes, unusual rises in the curve are found at A=28, A=36 and A=42 as shown in Figure 4.3 and Figure 4.4. The odd-even Phosphorus isotopes predict the most stable isotopes than the odd-odd isotopes due to the extra-unpaired nucleons.
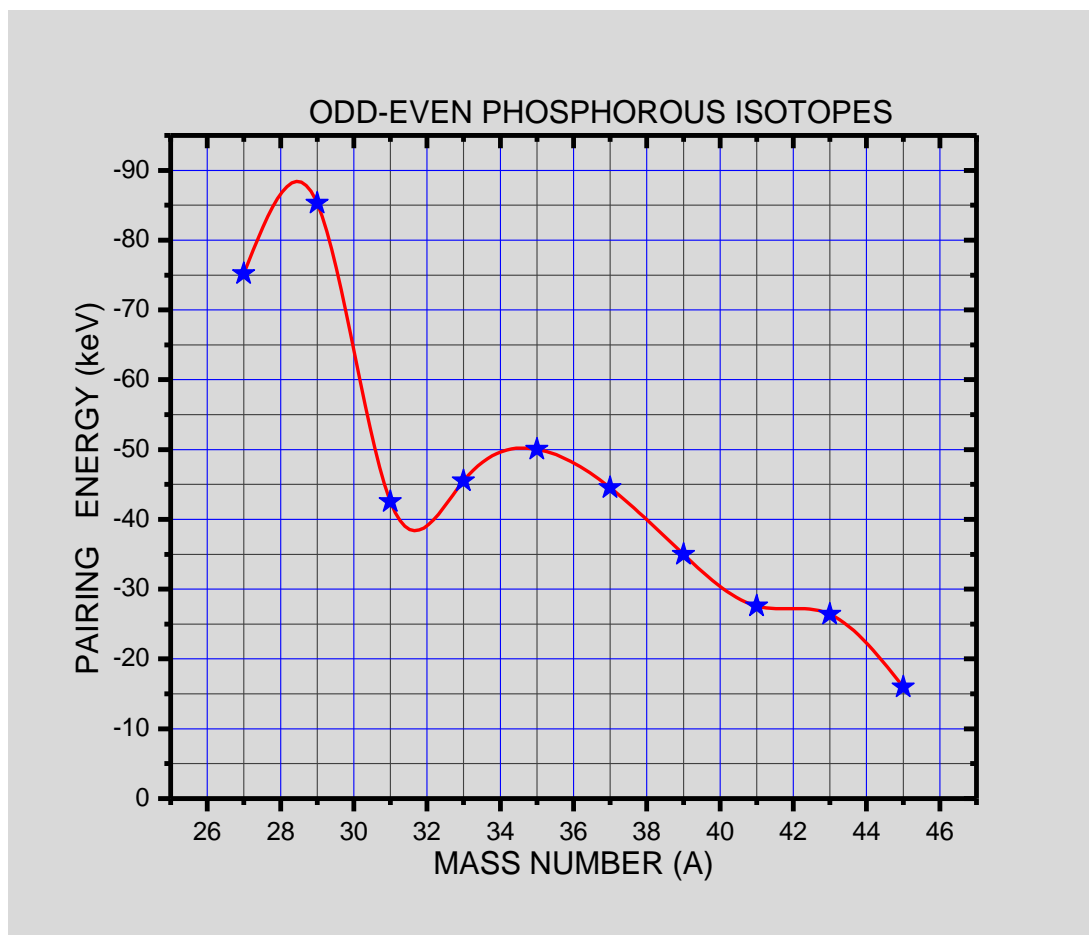
Figure 4.3: The graphical illustration of Odd-Even Phosphorus isotopes using the calculations in Table 4.10
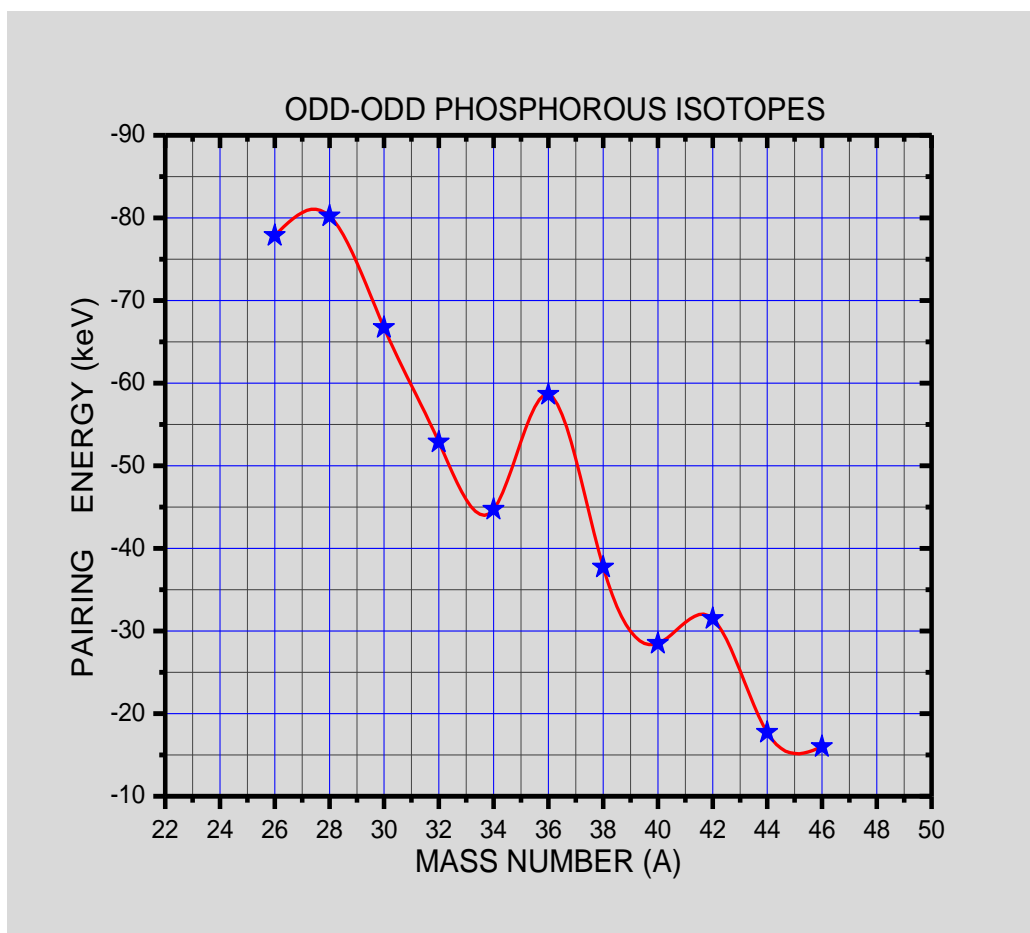
Figure 4.4: The graphical illustration of Odd-Odd Phosphorus isotopes using the calculations in Table 4.10

The unusual rises and minimum points in the curves of Phosphorus isotopes can be regarded as peaks and troughs, respectively. In the odd-even Phosphorus, there is an occurrence of two peaks while in odd-odd Phosphorus three peaks are obtained. It is noted that, in the odd-even phosphorus isotopes, the peak at A=29 corresponds to neutron sub-shell (N=14), while the peak at A=35 corresponds to a neutron magic number (N=20). Thus, it can be deduced that, the occurrence of peaks represents the regions of shell or sub shell closures where the isotopes are more stable.

Phosphorus is a monoisotopic element having 24 isotopes ranging from Phosphorus-24 to Phosphorus- 47. Among these isotopes, only one isotope that is ^{31}P, is 100%

abundant and stable (Wang *et al.*, 2017; Mohammadi and Bakhshabadi, 2015). The other isotopes are radioactive with the longest-lived isotope being ^{33}P. The stable and long-lived Phosphorus isotopes reside in the first trough of the graph in Figure 4.3, and this trough can be treated as the "valley of stability" for the Phosphorus isotopes.

In $_{25}$Mn isotopes, minor peaks were found at A=52 and A=64 and a single trough was noted at A=50 in the odd-odd manganese isotopes as illustrated in Figure 4.5.
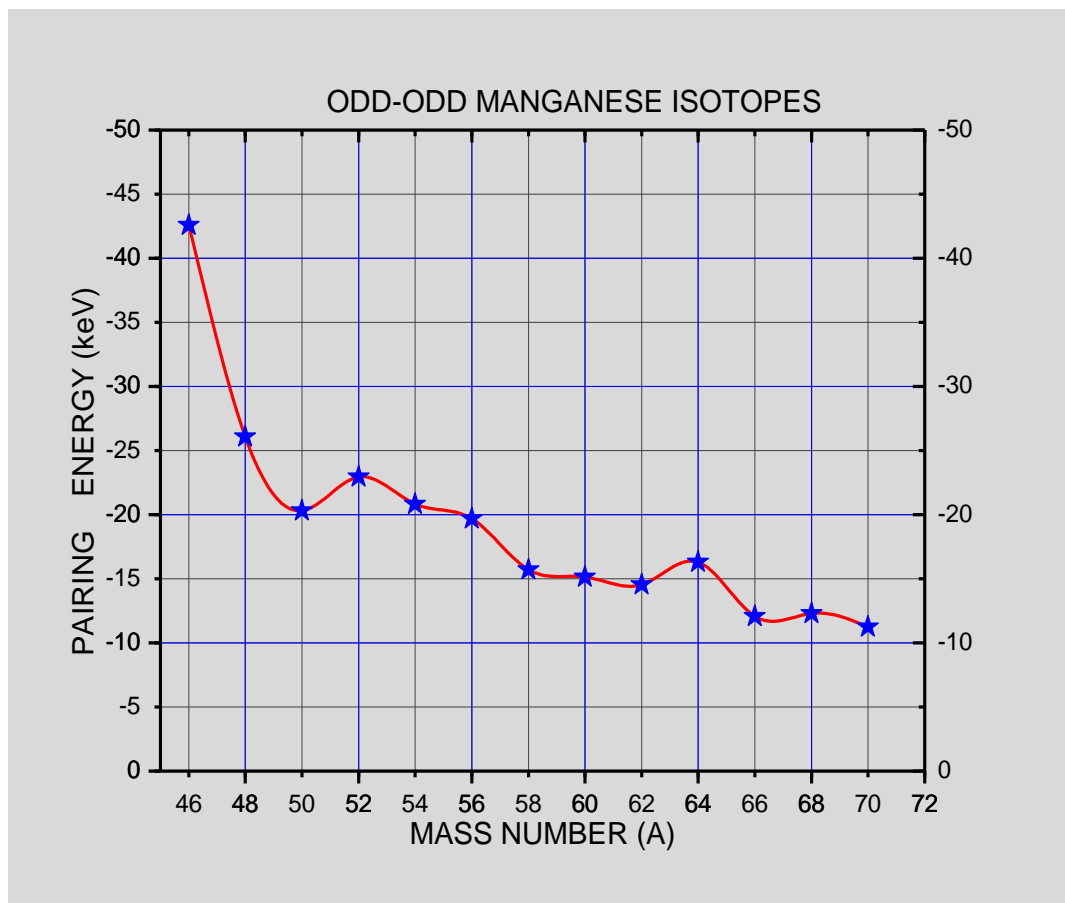
Figure 4.5: The graphical illustration of Odd-Odd Manganese isotopes using the calculations in Table 4.10

By applying the concept of distribution of nucleons among the energy levels in a potential well, it is evident that the odd-even Manganese isotopes are more stable than the odd-odd isotopes. The reason is that, the unpaired nucleons in the odd-odd isotope configuration weaken the binding energy. Therefore, in the odd-odd Manganese isotopes, the occurrence of a single trough at A=50 emanates from the pairing of 25

protons and 25 neutrons in the shell structure. This leaves only one unpaired proton and one unpaired neutron at the fermi surface. Consequently, this isotope depicts greater stability than the immediate neighbouring isotopes.

In odd-even Manganese isotopes, the peaks are slightly higher and they were found at A=53, A=64 and A=70. Similarly, three troughs were identified at A=51, A=61 and A=67 as shown in Figure 4.6.
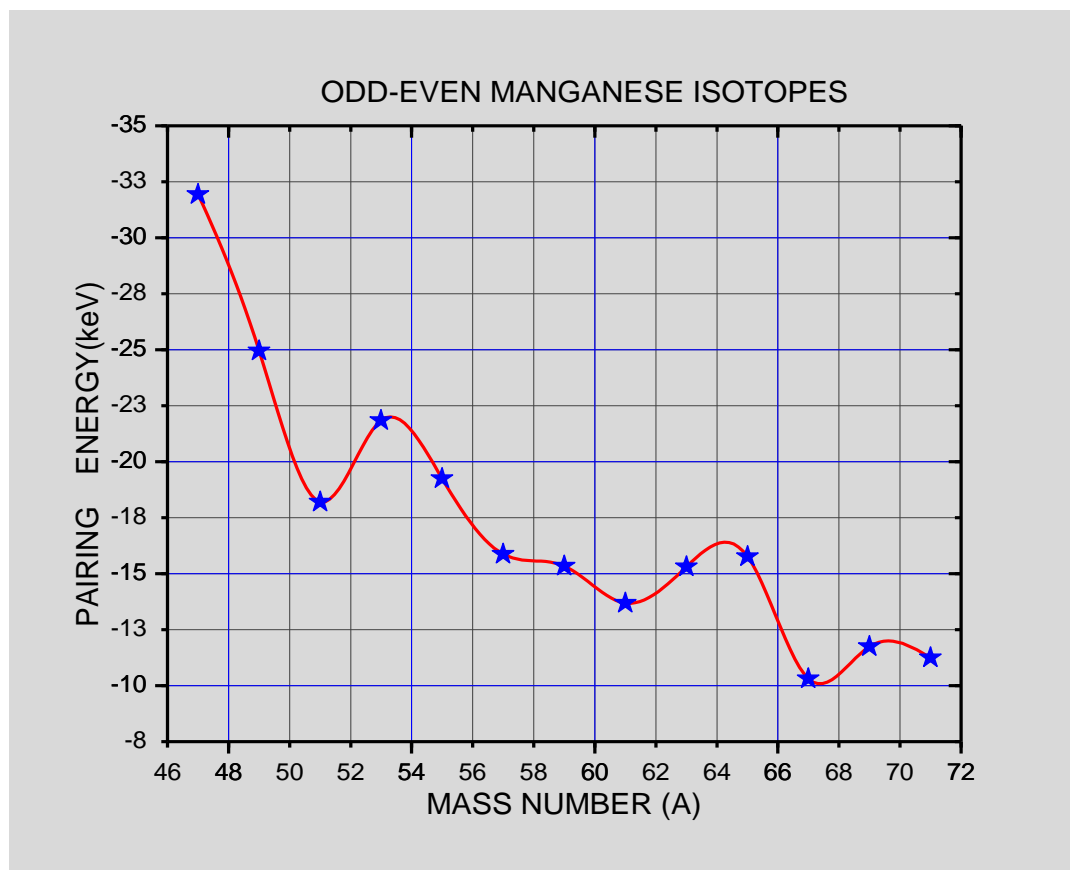
Figure 4.6: The graphical illustration of Odd-Even Manganese isotopes using the calculations in Table 4.10

The first peak noted at A= 53 in Figure 4.6 represents the existence of the most stable isotope. This isotope has a neutron magic number (N=28), hence, it is more stable than the neighbouring isotopes with half-live of 3.7 million years (Zinner, 2002). However, Manganese is a monoisotopic element having 29 isotopes ranging from Manganese-44

to Manganese-72 (Wang *et al*., 2017). Among these isotopes, only one isotope is stable and 100% abundant, that is ^{55}Mn, (Gross, 2017). This implies that, the other Manganese isotopes are radioactive but the isotopes found in troughs and on the peaks are long-lived isotopes.

The pairing energy calculations of Zirconium and Neodymium isotopes revealed an increase in the occurrence of peaks and troughs. This is attributed to the fact that, Zirconium and Neodymium elements form part of intermediate mass nuclei having an increased number of nucleons compared to Manganese and Phosphorus isotopes. In the case of Zirconium, the even-even isotopes are strongly bound than the even-odd isotopes since all the nucleons form pairs in the shell structure, thus, the most stable Zirconium isotope is found in the graph of the even-even isotopes. The four peaks obtained in the graph of the even-even isotopes were located at A=82, A=90, A=95 and A=100 as shown in Figure 4.7.
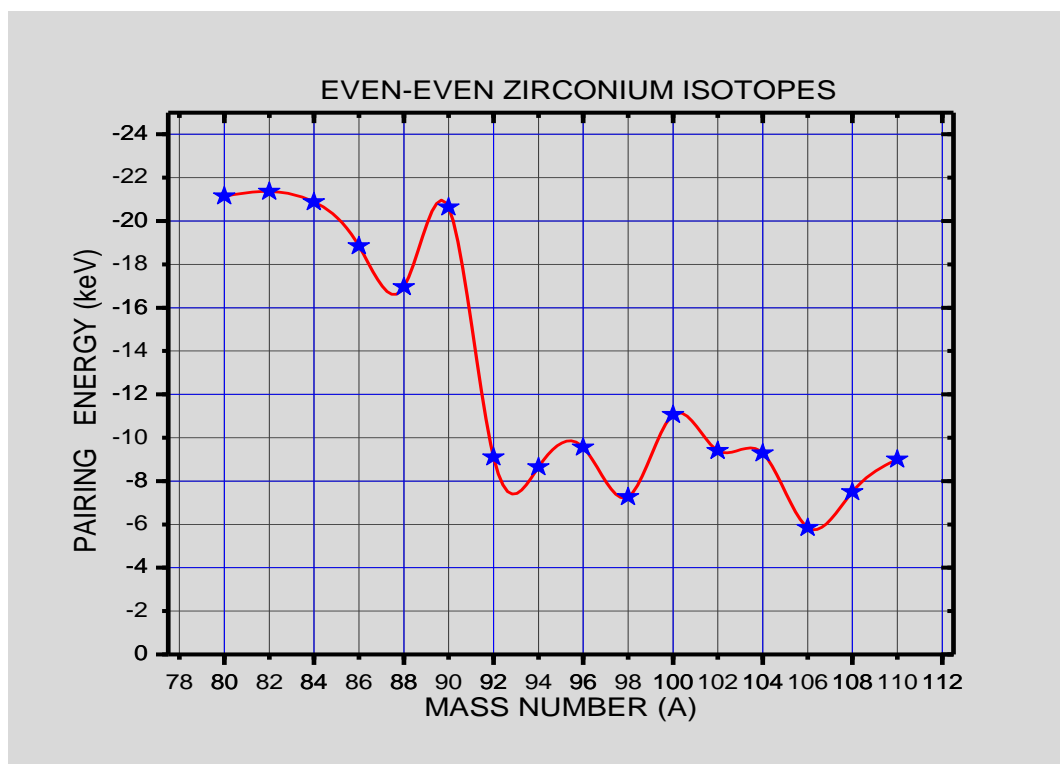
Figure 4.7: The graphical illustration of Even-Even Zirconium isotopes using the calculations in Table 4.11

The most stable and abundant isotope of Zirconium has a mass number of A=90 as shown in the first peak of Figure 4.7. It was noted that at A=90, this peak has a neutron magic number of N=50, thus it has some extra binding energy, which contributes to greater stability of the isotope. Similarly, the occurrence of troughs are noted at A=88, A=93, A=98 and A=106. These troughs represent the regions where minor sub shells are located in the shell structures of the energy level scheme.

The even-odd graph of Zirconium isotopes are shown in Figure 4.8. The occurrence of peaks are noted at A=81, A=91, A=99, A=110 and minor troughs are noted at A=89, A=94, A=96 and A=107. It was found that, the troughs and peaks for the even-odd Zirconium isotopes lie within the neighborhoods of the even-even Zirconium isotopes, hence, they experience some extra stability.

Figure 4.8: The graphical illustration of Even-Odd Zirconium isotopes using the calculations in Table 4.11

The graphs of even-even Neodymium isotopes shown in Figure 4.9 illustrates the occurrence of four peaks at A=130, A=142, A=148 and A=156. Out of the four peaks, a sharp and a more pronounced peak is located at A=142 which also corresponds to the isotope bearing the neutron magic number N=82. This peak represents the most stable and abundant Neodymium isotope. Similarly, an enlarged crest between A=146 and A=150 (A=146, A=148, A=150) is noted in Figure 4.9. The occurrence of this crest corresponds to the region containing relatively stable and more abundant isotopes. Similarly, occurrence of troughs are also noted at A=139, A=145, A=154 and A=158, representing Neodymium isotopes that are likely to be abundant or stable.
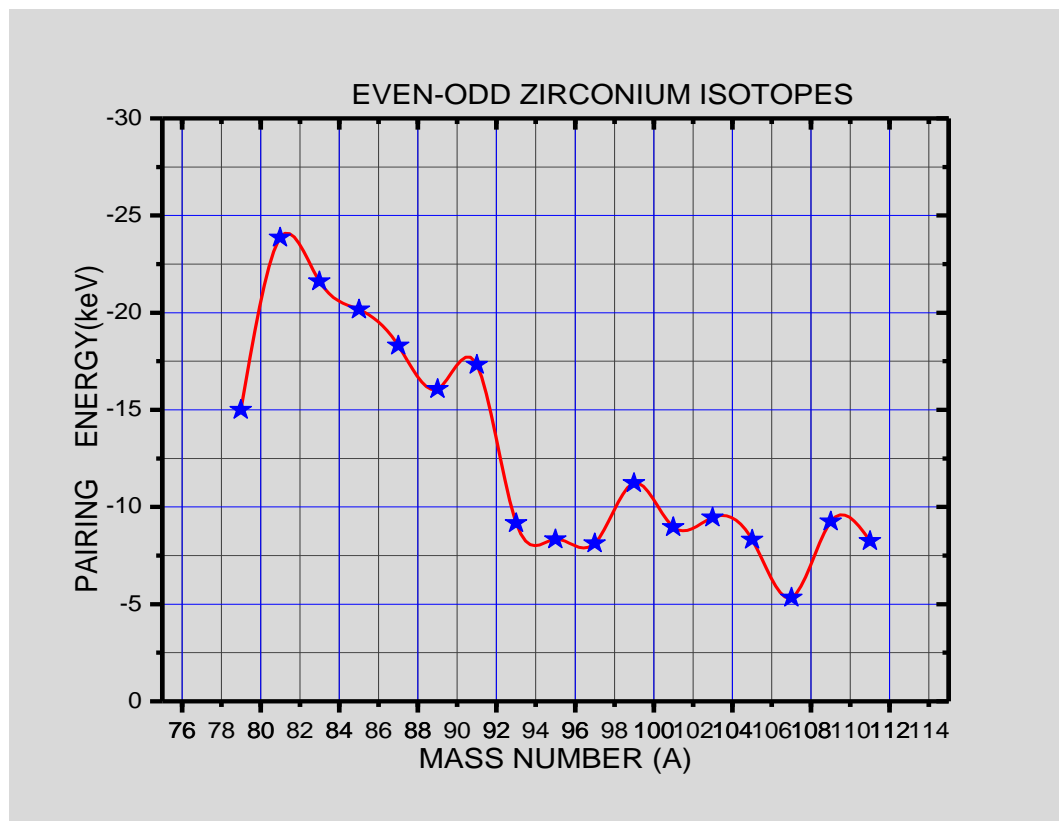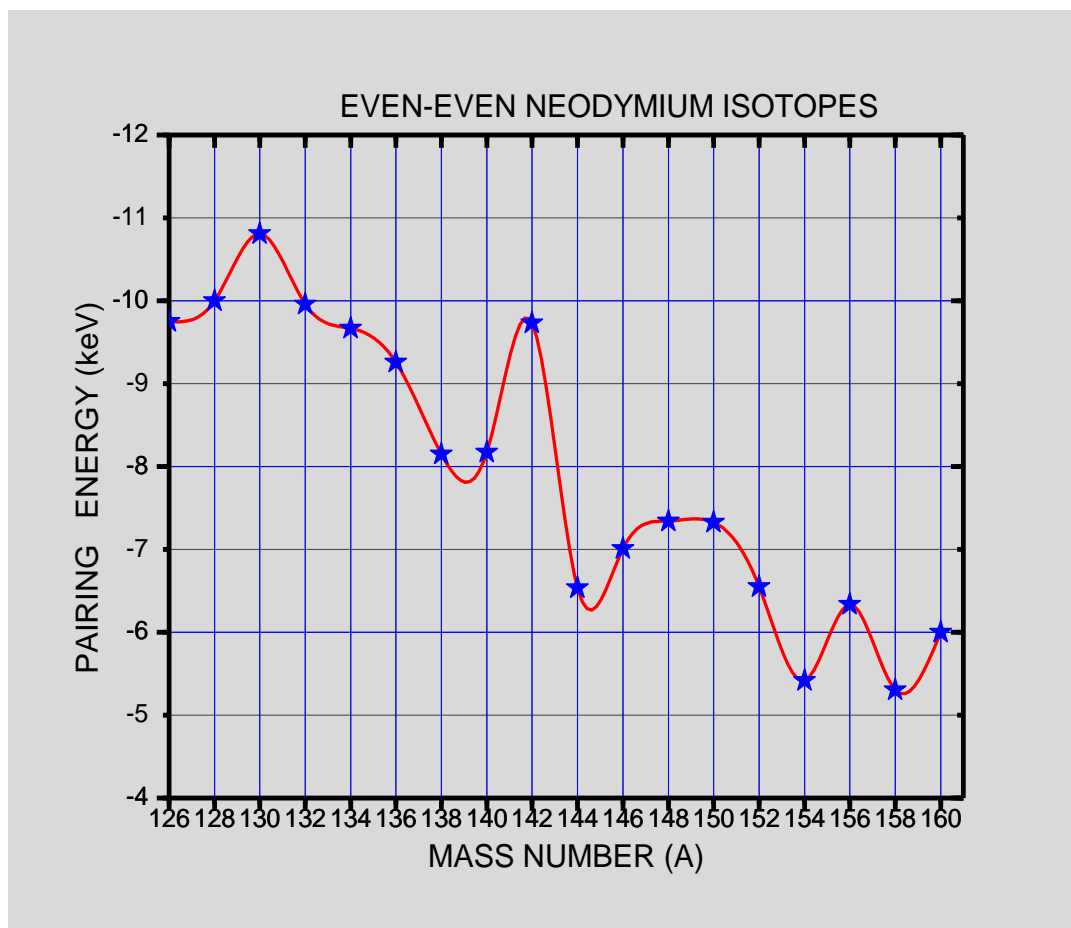

Figure 4.9: The graphical illustration of Even-Even Neodymium isotopes using the calculations in Table 4.11

In the graph of even-odd Neodymium isotopes shown in Figure 4.10, peaks are noted at A=131, A=143, A=149, and A=156. These peaks represent the isotopes

experiencing greater magnitudes of pairing energies resulting from the neutron pairs. However, they are less stable than the even-even Neodymium isotopes. It is also found that, there is a stepwise decrease in the absolute values of the pairing energies between A=132 to A=140. This region describes the location where there is a possibility of an occurrence of unstable isotopes. The occurrence of troughs are also noted at A=141, A=146, A=153 and A=159. Similarly, these Neodymium isotopes are also considered the stable and abundant.
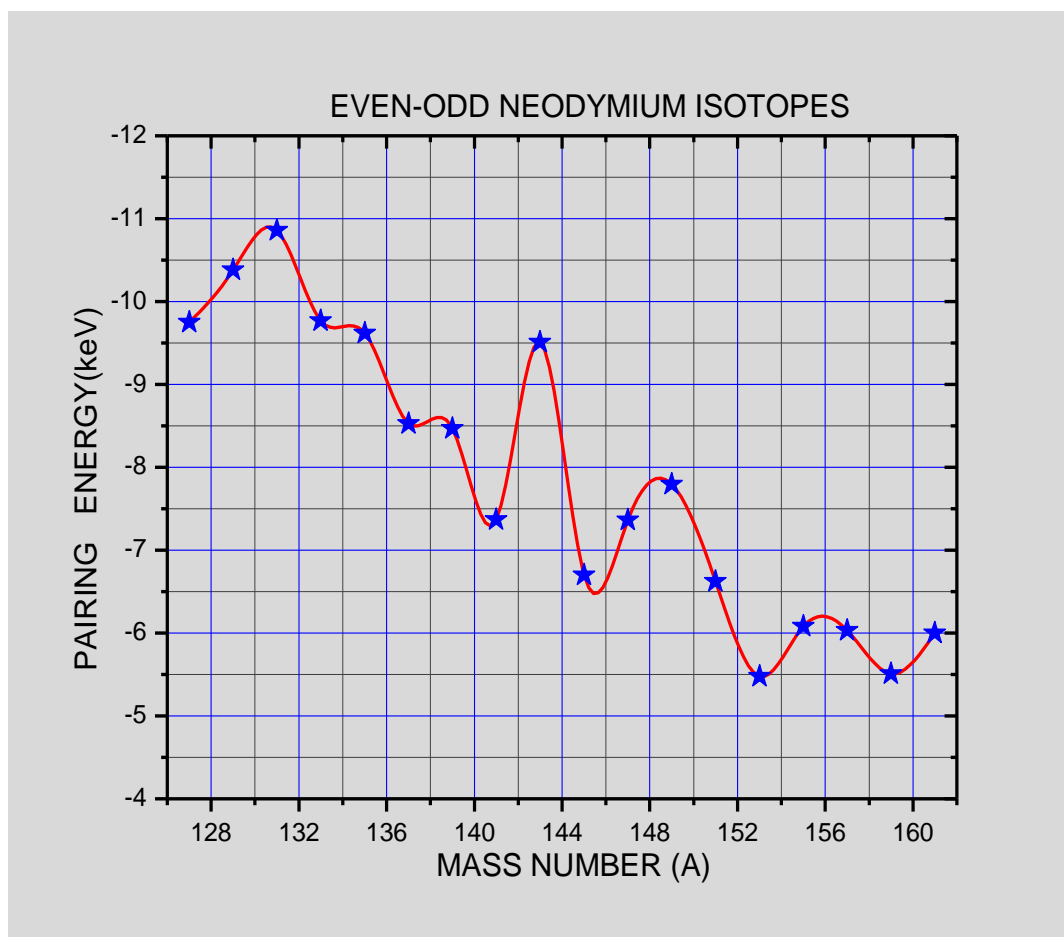
Figure 4.10: The graphical illustration of Even-odd Neodymium isotopes using the calculations in Table 4.11

Generally, the pairing energy graphs in Figure 4.3 to Figure 4.10 illustrate the curves of decreasing pairing energies with increase in the mass numbers. The occurrence of peaks (periodic humps) and troughs represent the regions where there is an existence of shell closures, stable isotopes or the longest-lived radioactive isotopes and the

regions where the most abundant isotopes of the elements are located. The graphs of $_{15}$P and $_{25}$Mn shown in Figure 4.3 to Figure 4.6, fall under the category of light nuclei and intermediate-mass nuclei. These nuclei have 2-3 periodic humps and troughs indicating regions of greater stability. Similarly, the graphs in Figure 4.7 to Figure 4.10 of $_{40}$Zr and $_{60}$Nd isotopes have four periodic humps and troughs indicating a very high likelihood of existence of stable isotopes. As the absolute values of the pairing energies decrease in magnitude, the nature of the curves also decrease randomly indicating that, the isotopes become unstable with increase in mass number. This implies that, the pairing interaction between nucleons in the high-mass nuclei is least felt compared to the light and intermediate mass nuclei. However, other forms of interactions such as electron-phonon pairing are likely to be common in the high-mass nuclei and such problem can be solved by application of the Bardeen-Cooper-Schrieffer (BCS) model.

4.9 The isotopic abundance of elements

The creation and existence of elements in nature as recorded in the nuclear landscape is described by the big bang theory (Dolgov, 2002). Studies on the isotopic abundance and stability of the naturally occurring elements and the exotic nuclei are still in progress, and their applications in diverse scientific fields are enormous (Brand and Coplen, 2012). Therefore, there is need to investigate the properties of these isotopes in order to enrich the existing knowledge on their stability and abundance. The pairing energy-mass number graphs in Figure 4.3 to Figure 4.10, showed the occurrence of periodic humps and troughs representing the existence of the most stable isotopes, the most abundant isotopes and the presence of the shell closures among the isotopes. The results of the isotopic natural abundance of Neodymium and Zirconium (Rosman and Taylor, 1999) were compared with the results obtained from the pairing energy-mass number graphs shown in Table 4.12.

TABLE 4.12: The table of natural abundance of $_{40}$Zr and $_{60}$Nd, adapted from Rosman and Taylor, (1999)

Known Isotopes	Abundance In %	Isotopes with peaks or troughs obtained from Fig. 4.7 to Fig 4.10	Isotopes with peaks or troughs and the most abundant in nature
^{90}Zr	51.45	**Peaks** ^{81}Zr, ^{82}Zr, ^{90}Zr, ^{91}Zr, ^{95}Zr, ^{99}Zr, ^{100}Zr, ^{110}Zr **Troughs** ^{88}Zr, ^{89}Zr, ^{92}Zr, ^{93}Zr, ^{94}Zr, ^{96}Zr, ^{106}Zr, ^{107}Zr	^{90}Zr ^{91}Zr ^{92}Zr ^{94}Zr ^{96}Zr
^{91}Zr	11.22		
^{92}Zr	17.15		
^{94}Zr	17.38		
^{96}Zr	2.8		
^{142}Nd	27.2	**Peaks** ^{130}Nd, ^{131}Nd, ^{142}Nd, ^{143}Nd, ^{146}Nd, ^{148}Nd, ^{149}Nd, ^{150}Nd, ^{156}Nd **Troughs** ^{139}Nd, ^{141}Nd, ^{144}Nd ^{145}Nd, ^{146}Nd, ^{153}Nd, ^{154}Nd, ^{158}Nd, ^{159}Nd	^{142}Nd ^{143}Nd ^{145}Nd ^{146}Nd, ^{148}Nd ^{150}Nd
^{143}Nd	12.2		
^{144}Nd	23.8		
^{145}Nd	8.3		
^{146}Nd	17.2		
^{148}Nd	5.7		
^{150}Nd	5.6		

From the comparison of the results in Table 4.12, it was found that eight isotopes had peaks and eight isotopes had troughs in the even-even and even-odd Zirconium isotopes respectively. Out of these isotopes, two naturally occurring and abundant isotopes were identified from the peaks, these are ^{90}Zr and ^{91}Zr and three isotopes namely ^{92}Zr, ^{94}Zr and ^{96}Zr were identified from the troughs. In the same manner, it was found that nine isotopes had peaks and nine isotopes had troughs in the even-even and even-odd Neodymium isotopes respectively. From these isotopes, five naturally occurring and abundant isotopes were identified from the peaks, namely, ^{142}Nd, ^{143}Nd, ^{146}Nd, ^{148}Nd and ^{150}Nd, and three naturally occurring and abundant isotopes were

identified from the troughs; these are ^{144}Nd, ^{145}Nd and ^{146}Nd. From this comparison, it was noted that all Neodymium isotopes that are naturally occurring and abundant were located either on the peaks or in the troughs of the pairing energy-mass number graphs.

Therefore, isotopes that are stable and abundant in nature or long-lived radioisotopes were found either in the troughs or on the peaks of the pairing energy-mass number graphs. In addition, some stable and radioactive isotopes were found within the vicinity of the troughs and the peaks (crests) of the pairing energy-mass number graphs. This shows that, a relationship between stability and abundance of nuclei exists

4.10 The calculations of the pairing energies for the super heavy elements

The pairing interaction of super heavy nuclei was investigated by considering four super heavy nuclei whose isotopes were discovered experimentally. These super heavy nuclei were selected randomly based on the fact that, their nucleons form pairs in configuration of even-even, even-odd, odd-odd and odd-even. These nuclei include Darmstadtium (Z=110), Roentgenium (Z=111), Copernicium (Z=112) and Nihonium (Z=113). Their values of the calculated pairing energies that were obtained using Eq. (3.26) are shown in Table 4.13.

Table 4.13: The table of calculated Pairing Energies (P$_N$) for $_{110}$Ds, $_{111}$Rg, $_{112}$Cn and $_{113}$Nh isotopes using Eq. (3.26)

DARMSTADTIUM (Z=110)			ROENTGENIUM (Z=111)		
A	Even-Even (Z-N)	P$_N$ (keV)	A	Odd-Odd (Z-N)	P$_N$ (keV)
270	110-160	-2.72	274	111-163	-3.00
272	110-162	-3.44	276	111-165	-2.50
274	110-164	-2.75	278	111-167	-1.50
276	110-166	-2.25	280	111-169	-1.00
278	110-168	-2.25	282	111-171	-2.00
280	110-170	-2.50			
A	Even-Odd (Z-N)	P$_N$ (keV)	A	Odd-Even (Z-N)	P$_N$ (keV)
269	110-159	-2.83	275	111-164	-2.25
271	110-161	-3.54	277	111-166	-2.25
273	110-163	-3.75	279	111-168	-1.00
275	110-165	-2.25	281	111-170	-1.50
277	110-167	-2.25			
279	110-169	-2.50			
CORPENICIUM (Z=112)			NIHONIUM (Z=113)		
A	Even-Even (Z-N)	P$_N$ (keV)	A	Odd-Odd (Z-N)	P$_N$ (keV)
278	112-166	-2.50	280	113-167	-2.75
280	112-168	-2.25	282	113-169	-2.25
282	112-170	-2.75	284	113-171	-2.00
284	112-172	-3.25	286	113-173	-2.25
A	Even-Odd (Z-N)	P$_N$ (keV)	A	Odd-Even (Z-N)	P$_N$ (keV)
279	112-167	-2.25	281	113-168	-2.50
281	112-169	-2.50	283	113-170	-2.00
283	112-171	-2.75	285	113-172	-2.25

It was found that the absolute values of the calculated pairing energies among the super heavy elements using the available data on AME2016 (Wang *et al*., 2017) were very small in magnitude compared to the light and intermediate mass nuclei. This

implies that, the pairing interaction of nucleons among the super heavy elements is limited due to the instability of the nuclei.

The results of the pairing energies obtained in Table 4.13 were plotted against the mass numbers of the nuclei. The results for even-even Darmstadtium isotopes are illustrated in Figure 4.11
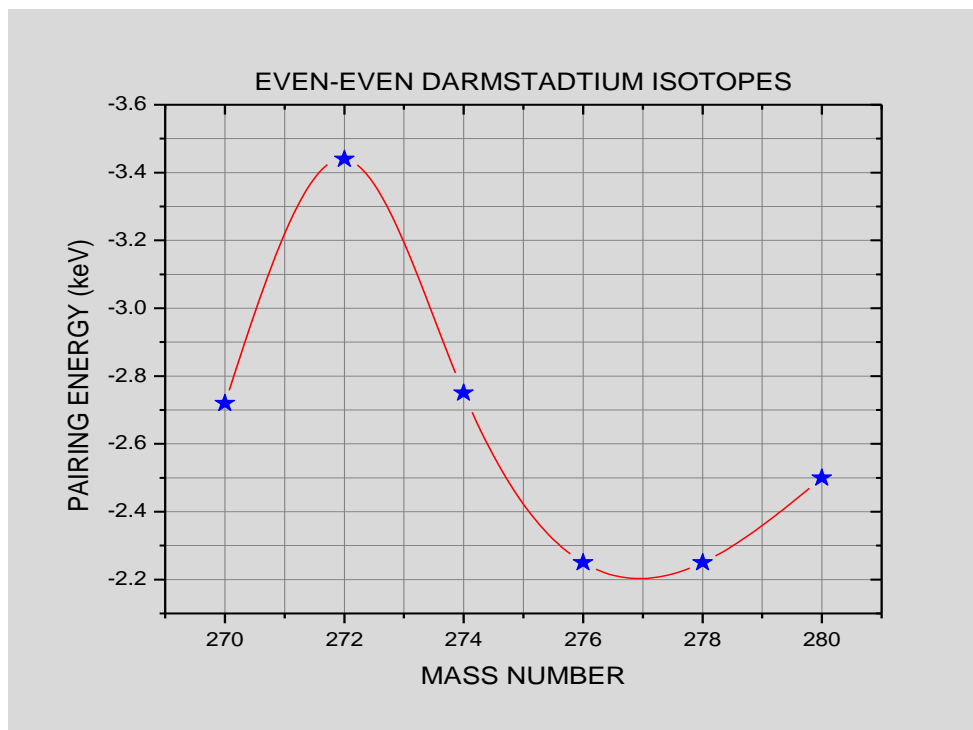
Figure 4.11: The graphical illustration of Even-Even Darmstadtium isotopes using the calculations in Table 4.13

It was noted that in the even-even Darmstadtium isotopes, the occurrence of a peak was noted at A=272 while a trough was noted at A=277. However, the isotope ^{272}Ds has not yet been discovered and experimental studies have shown that, ^{277}Ds has half-live of about 0.006 seconds (Oganessian and Utyonkov, 2015).

The graphical illustration for the even-odd Darmstadtium isotopes is shown in Figure 4.12. It was found that, a similar peak was noted at A=272 just like in the case of the even-even Darmstadtium isotopes, while a trough was noted at A= 276. The existence

of the two isotopes is not yet known, however, their nucleon-nucleon configuration predicts some greater magnitude of stability.

Figure 4.12: The graphical illustration of Even-Odd Darmstadtium isotopes using the calculations in Table 4.13

The graphical illustration odd-odd Roentgenium isotope is shown in Figure 4.13 while the odd-even Roentgenium isotope is shown in Figure 4.14. It was found that, an occurrence of a single trough is noted at A=280 in odd-odd Roentgenium isotopes and another trough in the odd-even Roentgenium isotopes is observed at A=279 and a peak is noted at A=276. The occurrence of the troughs represents the regions associated with stable isotopes and this is in agreement with experimental measurements that have revealed the half-lives of ^{279}Rg and ^{280}Rg as 90^{+170}_{-40} ms and $4.6^{+0.8}_{-0.7}$ ms respectively (Oganessian and Utyonkov, 2015). However, the isotope ^{276}Rg has not yet been discovered.
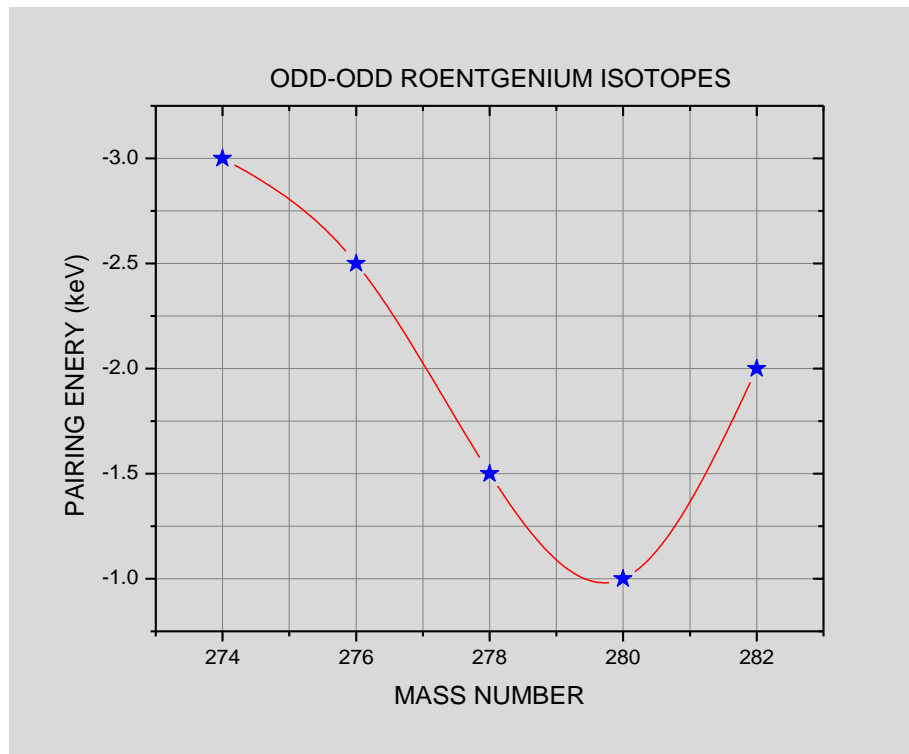
Figure 4.13: The graphical illustration of Odd-Odd Roentgenium isotopes using the calculations in Table 4.13
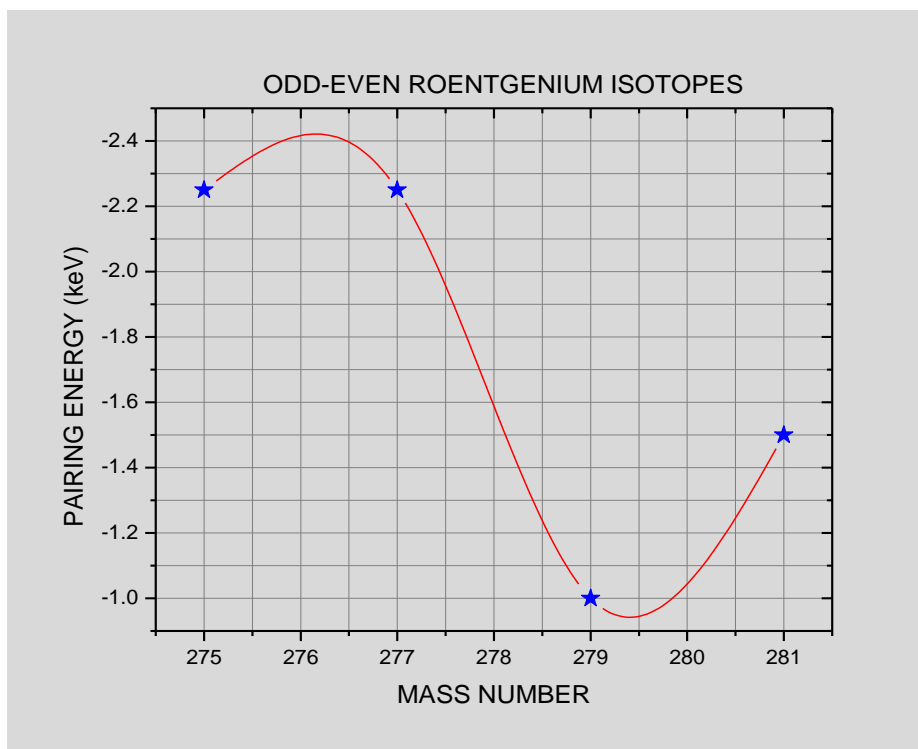
Figure 4.14: The graphical illustration of Odd-Even Roentgenium isotopes using the calculations in Table 4.13

Among the even-even Copernicium isotopes, a single trough was noted at A=280 as illustrated in Figure 4.15. The isotope ^{280}Cn is predicted to be the longest-lived isotope, however, this isotope is not yet known. It is probable that, an extrapolation of the curve beyond A=284 may yield the known longest-lived isotope, which is ^{285}Cn, however, this is limited by unavailability of experimental data on the binding energies of such isotopes.
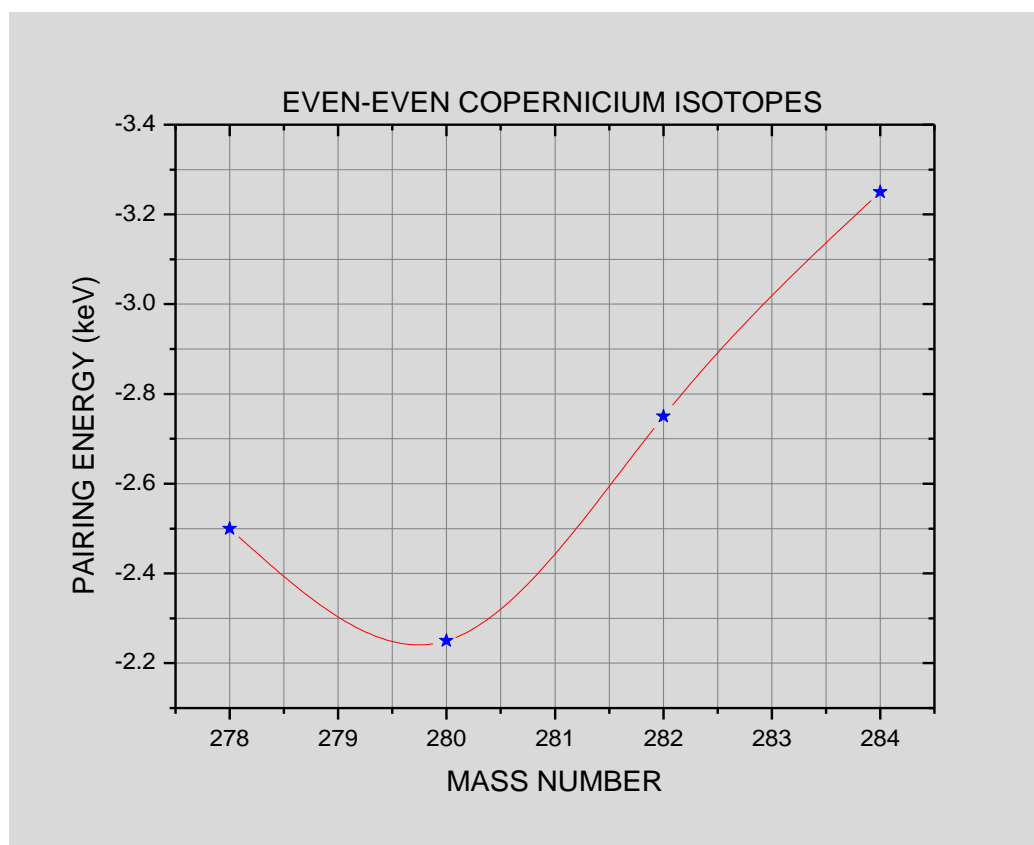
Figure 4.15: The graphical illustration of Even-Even Copernicium isotopes using the calculations in Table 4.13

The graphical illustration of the even-odd Copernicium isotopes is shown in Figure 4.16. A straight line was obtained in the Pairing energy-mass number graphs. The occurrence of the straight line indicates nonexistence of a stable isotopes of Copernicium element in the region between A=279 to A=283. However, experimental studies has revealed that the half-live of Copernicium isotopes in this region (A=281 to A=283) vary between 0.0009 seconds to 4.2 seconds (Oganessian and Utyonkov,

2015). Some calculations on Copernicium isotopes have also predicted existence ^{291}Cn and ^{293}Cn as the longest living isotopes in the island of stability having half-lives of about 100 years (Karpov *et al.*, 2012)
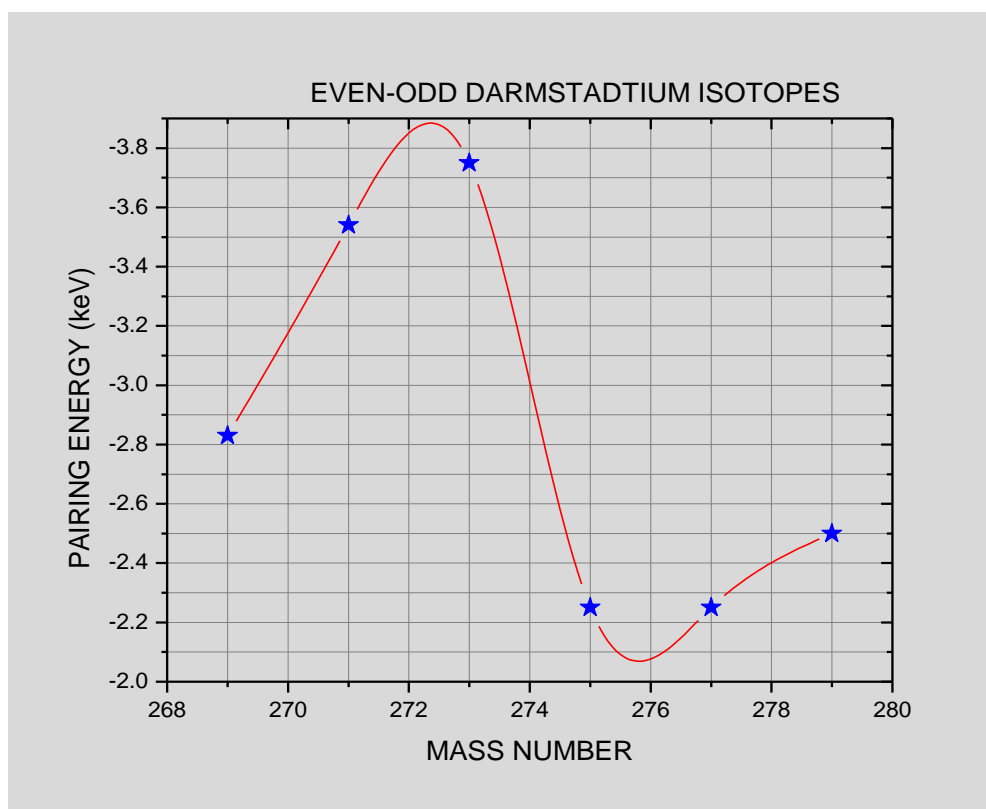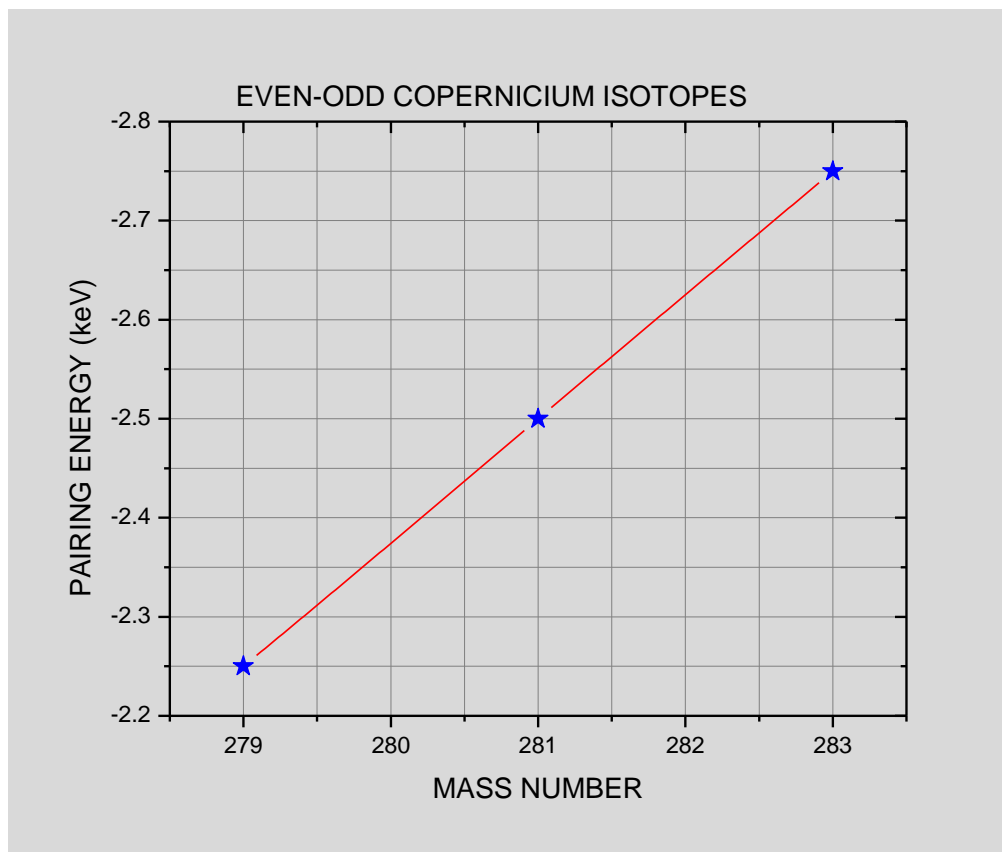

Figure 4.16: The graphical illustration of Even-Odd Copernicium isotopes using the calculations in Table 4.13

The graphical illustration of odd-even and odd-odd Nihonium isotopes is shown in Figure 4.17 and Figure 4.18. It was found that, the occurrence of troughs were noted at A=283 and A=284 in odd-even and odd-odd Nihonium isotopes respectively. The occurrence of these troughs revealed the regions where the longest-lived radioactive isotopes are likely to exist and they include ^{283}Nh and ^{284}Nh. Experimental measurements suggest that, ^{283}Nh and ^{284}Nh isotopes have half-lives of about 0.075 seconds and 0.94 seconds respectively (Hoffman *et al.*, 2004; En'yo, 2019). The longest-lived isotope, from experimental measurement is ^{286}Nh with half-life of about

9.5 seconds followed by ^{285}Nh with half-live of 4.2 seconds (Oganessian and Utyonkov, 2015).
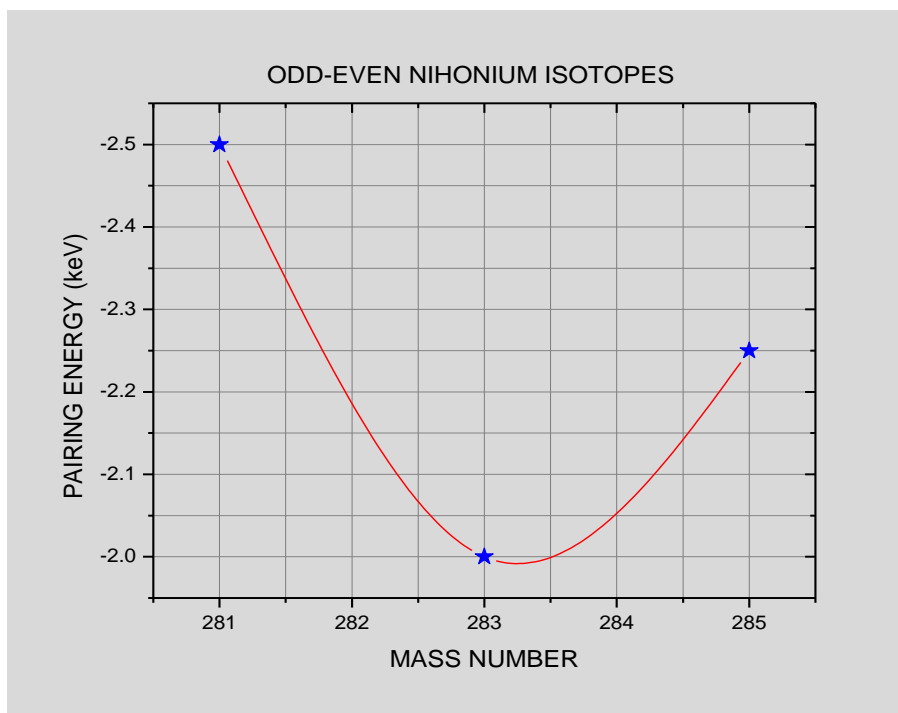
Figure 4.17: The graphical illustration of Odd-Even Nihonium isotopes using the calculations in Table 4.13
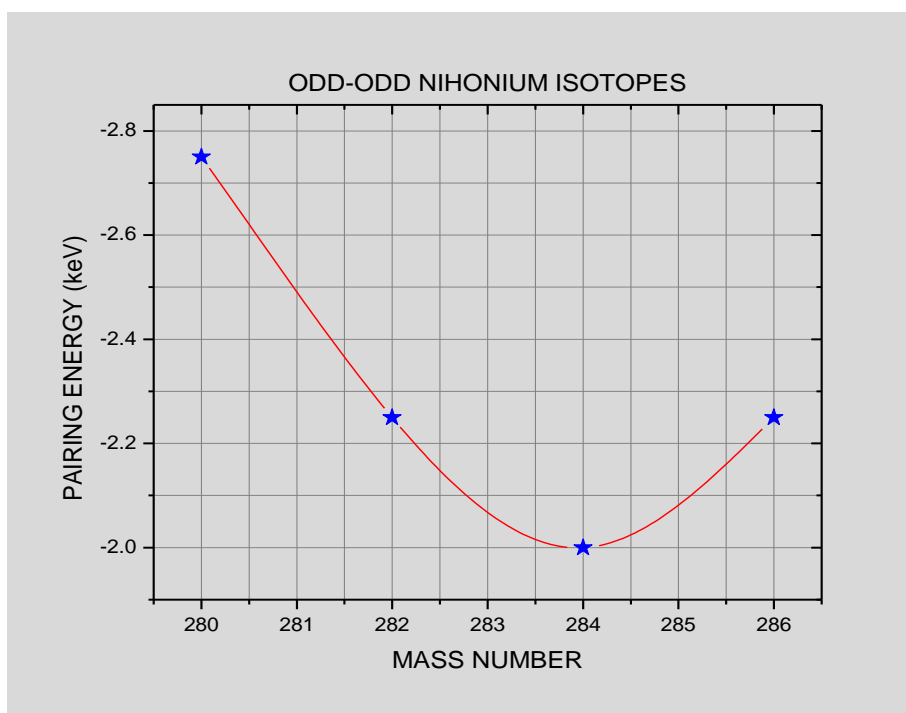
Figure 4.18: The graphical illustration of Odd-Odd Nihonium isotopes using the calculations in Table 4.13

Generally, the pairing energy-mass number graphs shown in Figure 4.11 to Figure 4.18 provide crucial information on the stability of the longest-lived isotopes among the super heavy elements. It was found that, the isotopes having the highest value of half-lives reside within the troughs and the peaks of the pairing energy curves. Some of the isotopes that satisfied this criterion include ^{277}Ds, ^{279}Rg, ^{280}Rg, ^{283}Nh and ^{284}Nh. These isotopes are among the long-lived radioactive isotopes, however, some of the longest-lived isotopes such as ^{281}Ds, ^{282}Rg, ^{285}Cn and ^{286}Nh were not identified using the criterion. It is surmised that such isotopes were not identified due to unavailability of sufficient experimental data on the binding energies.

Therefore, the pairing energy-mass number graphs for isotopes can provide a criterion for ascertaining the existence of stable and abundant isotopes of light and intermediate mass nuclei. In addition, the criterion can be applied in ascertaining the existence of the longest-lived radioactive isotopes among the super heavy elements. This theory is referred to as the peak-trough theory and it states that, the occurrence of the peaks and troughs in the pairing energy-mass number graphs corresponds to the regions where the most stable nuclei or the longest-lived isotopes having greater half-lives exist.

CHAPTER FIVE

CONCLUSIONS AND RECOMMENDATIONS

5.1 Introduction

This research has focused mainly on two significant areas in nuclear theory and quantum physics. These are the Coulomb potential and the Pairing interactions between nucleons in a nuclear system. The Coulomb energy is an essential component in the study of the binding energies of nuclei, which derives many applications in the synthesis of super heavy nuclei in particle accelerators and fusion or fission phenomena. On the other hand, the pairing interaction between nucleons, which are fermions, forms the basis behind the Bose-Einstein condensation, superfluidity and superconductivity. Collectively, these two pertinent areas at the basic atomic levels describe the mechanism behind the stability of the nucleus of an atom.

Various research groups have proposed several nuclear models that describe the binding energy of the nucleus of an atom (Ghoshal, 2008). However, the calculations of the binding energies are not accurate since they are based on the rough estimates of the large number of nucleons that are in collective motion. Therefore, the energy terms in the binding energy equation have to be modified in order to describe the contributions of nucleon interaction in nuclear systems. In this research, two energy terms were modified in the binding energy equation, namely, the Coulomb energy and the pairing energy terms. This was carried out in order to investigate the effects of Coulomb interactions and pairing interactions between nucleons in determining the stability of finite nuclei.

5.2 Conclusions

The results obtained in this research have shown that, the Coulomb's energy and the pairing interaction of nucleons are the major contributors on determining the nuclear stability of finite nuclei. The Coulomb energy is brought about by the repulsion between the protons in the nuclear core whose radius is denoted as R_0. The electrostatic proton-proton repulsion in the core of the nucleus is felt at the nuclear surface due to its long-range effect. As the effective nuclear radius (R) increases due to increase in the mass number (A) among the nuclei, the proton-proton repulsion also increases leading to an increase in the Coulomb energy. Therefore, the proton-proton repulsion within the nucleus yields some multiplying effect that forces the Coulomb energy to permeate throughout the entire volume of the nucleus, hence, contributing most of the Coulomb energy that is experienced at the nuclear surface.

Since the Coulomb potential in free space is a long-range potential, whereas the protons inside the nucleus are packed in a very small volume, the Coulomb potential was modified by introducing a multiplier exponential correction term. Consequently, a modified Coulomb potential model was obtained. It was found that the modified Coulomb energy model provides the necessary condition that accounts for most of the Coulomb's energy of all the finite nuclei with neutron number greater than the proton number (N > Z).

As the values of n increase uniformly from $n = 1$ to $n > 21$ in the modified Coulomb model, it was found that the nuclei undergo some nuclear transformations, which include beta decay in order to gain stability. As the powers of n in the correction term tend towards $n > 21$, the exponential correction term goes to unity. This idea was applied in determining the limits of Coulomb potential which was found to vary in the

range $2.718^{\frac{R_0}{R}} \beta \le E_c(Mod) \le \beta$. This range defines the limits of Coulomb stability among the finite nuclei and the super heavy elements in the "island of stability".

In order to calculate the values of stable atomic numbers (Z_{STABLE}) for the stability of isobars, the modified Coulomb energy model was substituted in the binding energy equation and the modified binding energy equation was obtained. The modified binding energy equation was used to calculate the values of Z_{STABLE} for a fixed mass number and the results obtained were compared with the results of the mass parabolas shown in appendices (X) and (XI). The two models that were derived to calculate the values of Z_{STABLE} are $Z_{STABLE-NMDF}$ and $Z_{STABLE-SEMF}$. From these models, two stable isobars which differ by a unit of the order of Z=1 in the super heavy nuclei were predicted to exist. It was found that, the difference in the values of the stable isobars obtained from the two methods was caused by the term $0.646695A$, which came from the difference in the masses of protons and neutrons, since, $M_p < M_n$. Consequently, the values of stable isobars obtained from the equation involving $Z_{STABLE-NMDF}$, were considered more accurate than that of $Z_{STABLE-SEMF}$ in the heavy nuclei. Therefore, it is concluded that the modified Coulomb potential energy model enriches the mass parabolas in calculating the most stable isobars among the super heavy and hyperheavy nuclei.

In the context of the pairing energies, the pairing energy calculations have shown that, the shell model can explain the pairing interaction of O–O (odd–odd), O–E (odd–even), E–E (even–even) and E–O (even–odd) nuclei in the shell structure. This was achieved through the analysis of the pairing energy-mass number graphs. It was found that, the absolute values of the pairing energies decrease with increase in the mass

numbers, with the occurrence of undulating peaks and troughs. These peaks and troughs were attributed to the effects of the shell closures or sub shell closures resulting from the proton or neutron magic numbers. Therefore, the isotopes that are stable and abundant in nature or long-lived radioisotopes were found either in the troughs or on the peaks of the pairing energy-mass number graphs. In addition, some stable and radioactive isotopes were found within the vicinity of the troughs and the peaks (crests) of the pairing energy-mass number graphs. Among the phosphorus isotopes, it was found that ^{31}P which is 100% abundant and ^{33}P which is the longest lived radioactive isotope were found in the troughs. Similarly, ^{53}Mn, which is the most stable and ^{55}Mn, which is 100% abundant were also found on the peaks of Manganese pairing energy-mass number graphs.

A Comparison of the pairing energy results with the experimental data of Zirconium and Neodymium natural abundance was carried out. From this comparison, it was noted that all Zirconium isotopes and Neodymium isotopes that are naturally occurring and abundant in nature were located either on the peaks or in the troughs of the pairing energy-mass number graphs.

In the super heavy nuclei, it was found that, the absolute values of pairing energies obtained from the calculations drop significantly when compared with the light or intermediate mass nuclei. This was attributed to the radioactive nature of the super heavy elements. Nonetheless, a relationship exists between the half-lives and the pairing energies of these nuclei in the sense that, the longest-lived isotope among the super heavy elements, despite having small values of probability decays, lies either in the troughs or at the peaks of the pairing energy-mass number graphs. Some of the isotopes that satisfied this criterion include ^{277}Ds, ^{279}Rg, ^{280}Rg, ^{283}Nh and ^{284}Nh. These

isotopes are among the long-lived radioactive isotopes, however, some of the longest-lived isotopes such as ^{281}Ds, ^{282}Rg, ^{285}Cn and ^{286}Nh were not identified using the criterion due to unavailability of sufficient experimental data on the binding energies.

On the contrary, some isotopes were predicted to be stable yet they do not exist in nature. These isotopes include, ^{82}Zr, ^{99}Zr, ^{93}Zr, ^{106}Zr, ^{131}Nd, ^{156}Nd, ^{143}Nd, ^{272}Ds, ^{276}Ds, ^{276}Rg, ^{280}Cn etc. Arguably, these nuclei could be stable in neutron stars or other interstellar bodies. It is surmised that, other forms of interactions such as electron-phonon pairing are predicted to occur in the high-mass nuclei and this problem can be solved by application of the BCS model.

Therefore, the pairing energy-mass number graphs of isotopes can provide a criterion for ascertaining the existence of stable and abundant isotopes. Such isotopes are found in the light and intermediate mass nuclei and the longest-lived radioactive isotopes among the super heavy elements in the island of stability, neutron stars and other interstellar bodies. The criterion that was developed to ascertain the existence of the most stable nuclei and the longest lived radioactive isotopes is referred as the peak-trough theory. This theory states that, the occurrence of the peaks and troughs in the pairing energy-mass number graphs corresponds to the regions where the most stable nuclei or the longest-lived isotopes having greater half-lives than their neighbouring isotopes exist.

5.3 Recommendations

This research work is of great importance in nuclear theory, especially, in defining the limits of the long-range Coulomb potential within the nucleus, and describing the stability and nuclear abundance of elements on earth and other interstellar bodies. According to this study, it is now possible to define the limits of Coulomb stability of

both finite and exotic nuclei. However, as the nuclear masses increase from the light nuclei to the super heavy nuclei, the Coulomb energy increases rapidly while the absolute values of the pairing energies decrease significantly. Therefore, it will be of great importance to derive a unifying model, which can link up the two forms of energies, such that, the stability of the elements and the nuclear abundance or rarity can be described simultaneously.

Calculations in this thesis have shown that, there could exist stable nuclei with Z=126, Z=132, Z=133, Z=134, Z=141, Z=148, Z=152, Z=162, Z=164 and Z=193. Thus, they will be stable against spontaneous fission (SF). New experiments using heavier targets with Z>80 and projectiles with Z>60 may have to be used to produce such nuclei. Thus, very high-energy accelerators may have to be designed to accelerate the nuclei with Z>60.

REFERENCES

Afanasjev, A. V., Agbemava, S. E., & Gyawali, A. (2018). Hyperheavy nuclei: Existence and stability. *Physics Letters B*, *782*, 533-540.

Afanasjev, A. V., & Frauendorf, S. (2005). Central depression in nuclear density and its consequences for the shell structure of superheavy nuclei. *Physical Review C*, *71*(2), 024308.

Agbemava, S. E., Afanasjev, A. V., Ray, D., & Ring, P. (2014). Global performance of covariant energy density functionals: Ground state observables of even-even nuclei and the estimate of theoretical uncertainties. *Physical Review C*, *89*(5), 054320.

Antia, A. D., Ituen, E. E., Obong, H. P., & Isonguyo, C. N. (2015). Analytical solution of the modified Coulomb potential using the factorisation method. *Int. J. Rec. Adv. Phys*, *4*, 55.

Bailey, D. (2011). Semi-empirical nuclear mass formula. *PHY357: Strings & Binding Energy. University of Toronto,* 03-31.

Barrett, B. R. (1999). Basic Ideas and Concepts in Nuclear Physics: An Introductory Approach, by Kris Heyde. *Physics Today*, *52*, 60-62.

Belyaev, S. T. (1959). Kgl. *Danske Videnskab. Selskab. Mat.-Fys. Medd*, *31*.

Bender, M., Nazarewicz, W., & Reinhard, P. G. (2001). Shell stabilization of super- and hyperheavy nuclei without magic gaps. *Physics Letters B*, *515*(1-2), 42-48.

Bender, M., Rutz, K., Reinhard, P. G., Maruhn, J. A., & Greiner, W. (1999). Shell structure of superheavy nuclei in self-consistent mean-field models. *Physical Review C*, *60*(3), 034304.

Bethe, H. A., & Bacher, R. F. (1936). Nuclear physics A. Stationary states of nuclei. *Reviews of Modern Physics*, *8*(2), 82.

Bjørnholm, S. & Lynn, J. E. (1980). The double-humped fission barrier. *Reviews of Modern Physics*, *52*(4), 725.

Bohr, A., Mottelson, B. R., & Pines, D. (1958). Possible analogy between the excitation spectra of nuclei and those of the superconducting metallic state. *Physical Review*, *110*(4), 936.

Bohr, A., & Mottelson, B. R. (1969). *Nuclear Structure (Vol. 2).* New York: WA Benjamin. *Inc.*

Bohr, A., & Mottelson, B. R. (1998). *Nuclear structure* (Vol. 1). Singapore: World Scientific publishing.

Bohr, N., & Wheeler, J. A. (1939). The mechanism of nuclear fission. *Physical Review*, *56*(5), 426.

Bolsterli, M., Fiset, E. Nix, J. R & Norton, J. L. (1972). New calculations of fission barriers for heavy and super heavy nuclei. *Physical Review C*, 5(3), 1050.

Brand, W. A., & Coplen, T. B. (2012). Stable isotope deltas: tiny, yet robust signatures in nature. *Isotopes in environmental and health studies*, *48*(3), 393-409.

Brinkman, W. F. (1986). *An overview: Physics through the 1990's*. Washington DC: The national Academies Press. Retrieved from: https:/doi.org/10.17226/626

Brynjolfsson, A., & Wang, C. P. (2018). Atomic structure. In *Preservation of Food by Ionizing Radiation,* (pp.79-108)*, CRC Press*,.

Campbell, D. (2016). Aristotle's On the Heavens. *Ancient History Encyclopedia*. Retrieved from https://www.ancient.eu/article/959/

Casten, R. F. (2000). *Nuclear structure from a simple perspective* (Vol. 23). Oxford University Press on Demand.

Chadwick, J. (1932). The existence of a neutron. *Proceedings of the Royal Society of London. Series A, Containing Papers of a Mathematical and Physical Character*, *136*(830), 692-708.

Changizi, S. A. (2017). *Pairing correlation in atomic nuclei under extreme conditions* (Doctoral dissertation, KTH Royal Institute of Technology): https:/www.diva-portal.org/smash/get/diva2.1156741/FULLTEST01.pdf

Chemogos, P. K., Muguro, K. M., & Khanna, K. M. (2019). Modified Phenomenological Formula for the Ground State Energy of Light Nuclei. *World Scientific News*, *136*, 148-158.

Cherop, H. K., Muguro, K. M., & Khanna, K. M. (2019a). The Role of the Modified Coulomb Energy in the Binding Energy Equation for Finite Nuclei. *Scientific Israel-Technological Advantages*, *21*(5-6), 82-89.

Cherop, H., Muguro, K., & Khanna, K. (2019b). The Role of Shell Model in Determining Pairing Interaction in Nuclei. *International Journal of Recent Research Aspects*, 6(4), 10-15.

Choppin, G., Liljenzin, J. O., & Rydberg, J. (2002). *Radiochemistry and nuclear chemistry*. Butterworth-Heinemann.

Collard, H. R., Elton, L. R. B., Hofstadter, R., & Schopper, H. F. (1967). *Nuclear radii*. Springer.

Dai, H., Wang, R., Huang, Y., & Chen, X. (2017). A novel nuclear dependence of nucleon–nucleon short-range correlations. *Physics Letters B*, *769*, 446-450.

Davies, P. C. W., & Brown, J. R. (1993). *The ghost in the atom: a discussion of the mysteries of quantum physics*. Cambridge University Press.

Dean, D. J., & Hjorth-Jensen, M. (2003). Pairing in nuclear systems: from neutron stars to finite nuclei. *Reviews of Modern Physics*, *75*(2), 607.

Del Bene, J. E., Perera, S. A., & Bartlett, R. J. (1999). Hydrogen bond types, binding energies, and 1H NMR chemical shifts. *The Journal of Physical Chemistry A*, *103*(40), 8121-8124.

Dolgov, A. D. (2002). Big bang nucleosynthesis. *Nuclear Physics B-Proceedings Supplements*, *110*, 137-143.

Draayer J. P., Gueorguiev V. G., Sviratcheva K. D., Bahri C., Pan F., and Georgieva A. I. (2005). Exactly solvable pairing models. In *Key topics of nuclear structure*, (pp .483-494).

Dumitrescu, O., & Horoi, M. (1990). An enlarged superfluid model of atomic nucleus. *II Nuovo Cimento A (1965-1970)*, *103*(5), 653-668.

Elliott, J. P. (1958). Collective motion in the nuclear shell model. I. Classification schemes for states of mixed configurations. *Proceedings of the Royal Society of London. Series A. Mathematical and Physical Sciences*, *245*(1240), 128-145.

En'yo, H. (2019). History of nihonium. *Pure and Applied Chemistry*, *91*(12), 1949-1958.

Erler, J., Birge, N., Kortelainen, M., Nazarewicz, W., Olsen, E., Perhac, A. M., & Stoitsov, M. (2012). The limits of the nuclear landscape. *Nature*, *486*(7404), 509-512.

Etkin, V. A. (2017). Modified Coulomb law. *World Scientific News*, *87*, 163-174.

Fan, T. S., Hu, J. M., & Bao, S. L. (1995). Study of multichannel theory for the neutron induced fissions of actinide nuclei. *Nuclear Physics A*, *591*(2), 161-181.

Fricke, B., Greiner, W., & Waber, J. T. (1971). The continuation of the periodic table up to Z= 172. The chemistry of superheavy elements. *Theoretica chimica acta*, *21*(3), 235-260.

Gandolfi, S., Carlson, J., Reddy, S., Steiner, A. W., & Wiringa, R. B. (2014). The equation of state of neutron matter, symmetry energy and neutron star structure. *The European Physical Journal A*, *50*(2), 10.

Gandolfi, S., Gezerlis, A., & Carlson, J. (2015). Neutron matter from low to high density. *Annual Review of Nuclear and Particle Science*, *65*, 303-328.

Ghahramany, N., Ghanaatian, M., & Hooshmand, M. (2007). Quark-Gluon Plasma Model and Origin of Magic Numbers. *Journal of theoretical and applied Physics (Iranian Physical Journal), 1(2),* 35-38.

Ghoshal, S. N. (2008). *Nuclear physics*. New Delhi: S. Chand Publishing.

Greiner, W. & Maruhn, J. A. (1996). *Nuclear models.* Berlin: Springer-Verlag, p.77.

Gross, J. H. (2017). Isotopic composition and accurate mass. In *Mass Spectrometry* (pp. 85-150). Springer, Cham.

Grzywacz, R., Béraud, R., Borcea, C., Emsallem, A., Glogowski, M., Grawe, H., & Mueller, A. C. (1998). New Island of μs Isomers in Neutron-Rich Nuclei around the Z= 28 and N= 40 Shell Closures. *Physical review letters*, *81*(4), 766.

Harvey, M. (1968). The Nuclear SU 3 Model. In *Advances in nuclear physics* (pp. 67-182). Springer, Boston, MA.

Haxel, O., Jensen, J. H. D., & Suess, H. E. (1949). On the" magic numbers" in nuclear structure. *Physical Review*, *75*(11), 1766.

Heisenberg, W. (1932). On the structure of atomic nuclei. *Z. Phys.*, *77*, 1-11.

Hentschel, K. (2009). Atomic Models, JJ Thomson's "Plum Pudding" Model. In *Compendium of Quantum Physics* (pp.18-21). Springer, Berlin, Heidelberg.

Heyde, K. (2004). *Basic ideas and concepts in nuclear physics: an introductory approach*. CRC Press.

Hjorth-Jensen, M., Lombardo, M. P., & Van Kolck, U. (2017). An advanced course in computational nuclear physics. *Springer Lecture Notes in Physics*, *936*.

Hofmann, S., Dmitriev, S. N., Fahlander, C., Gates, J. M., Roberto, J. B., & Sakai, H. (2018). On the discovery of new elements (IUPAC/IUPAP Provisional Report). *Pure and Applied Chemistry*, *90*(11), 1773-1832.

Hofmann, S., Münzenberg, G., & SCHÄDEL, M. (2004). On the discovery of superheavy elements. *Nuclear Physics News*, *14*(4), 5-13.

Indelicato, P., Bieroń, J., & Jönsson, P. (2011). Are MCDF calculations 101% correct in the super-heavy elements range?. *Theoretical Chemistry Accounts*, *129*(3-5), 495-505.

Ishkhanov, B. S., Stepanov, M. E., & Tretyakova, T. Y. (2014). Moscow University Phys. *Bull*, *69*(1), 1-20.

Itin Y., Lämmerzahl, C., & Perlick, V. (2014). Finsler-type modification of the Coulomb law. *Physical Review D*, *90*(12), 124057.

Jackson, J. D. (1999). Classical Electrodynamics 3rd ed John Wiley & Sons. *Inc., NewYork, NY*.

Jänecke, J. (1972). Coulomb energies of spherical nuclei. *Nuclear Physics A*, *181*(1), 49-75.

Johnson, K. E. (2004). From natural history to the nuclear shell model: Chemical thinking in the work of Mayer, Haxel, Jensen, and Suess. *Physics in Perspective*, *6*(3), 295-309.

Karpov, A. V., Zagrebaev, V. I., Martinez Palenzuela, Y., Felipe Ruiz, L., & Greiner, W. (2012). Decay properties and stability of heaviest elements. *International Journal of Modern Physics E*, *21*(02), 1250013.

Khugaev, A. V., Koblik, Y. N., Ioannou, P. D., & Flitsiyan, E. S. (2007). The determination of the Coulomb energy of a nuclear system at the scission point upon fission. *Bulletin of the Russian Academy of Sciences: Physics*, *71*(3), 401-404.

Kragh, H. (2017). The search for superheavy elements: Historical and philosophical perspectives. *arXiv preprint arXiv:1708.04064*.

Kragh, H. (2018). *From transuranic to superheavy elements: A story of dispute and creation*. Cham, Switzerland: Springer.

Kuzmina, A. N., Adamian, G. G., Antonenko, N. V., & Scheid, W. (2012). Influence of proton shell closure on production and identification of new superheavy nuclei. *Physical Review C*, *85*(1), 014319.

Lowrie, W. (2007). *Fundamentals of geophysics*. Cambridge university press.

Mackintosh, R., Jonsen, B., Al-Khalili, J., & Peña, T. (2002). Nucleus: A trip into the Heart of Matter.

Malov, L. A., & Solov'ev, V. G. (1980). Quasiparticle-phonon nuclear model. *Fizika Ehlementarnykh Chastits i Atomnogo Yadra*, *11*(2), 301-341.

Manjunatha, H. C., & Sridhar, K. N. (2017). Survival and compound nucleus probability of super heavy element Z= 117. *The European Physical Journal A*, *53*(5), 97.

Mayer, M. G. (1949). On closed shells in nuclei. II. *Physical Review*, *75*(12), 1969.

Michimasa, S., Kobayashi, M., Kiyokawa, Y., Ota, S., Ahn, D. S., Baba, H., & Ideguchi, E. (2018). Magic Nature of Neutrons in Ca 54: First Mass Measurements of Ca 55–57. *Physical review letters*, *121*(2), 022506.

Mishra, A., Gupta, T., & Sahu, B. (2016). Estimation of Nuclear Separation Energy and its Relation with Q Value. *International Journal of Applied Physics and Mathematics*, *6*(1), 17.

Mohammadi, S., & Bakhshabadi, F. (2015). Calculation of the energy levels of Phosphorus isotopes (A= 31 to 35) by using OXBASH code. *American Journal of Modern Physics. Special Issue: Many Particle Simulations*, *4*(3-1), 15-22.

Möller, P., & Nix, J. R. (1981a). Atomic masses and nuclear ground-state deformations calculated with a new macroscopic-microscopic model. *Atomic Data and Nuclear Data Tables*, *26*(2), 165-196.

Möller, P., & Nix, J. R. (1981b). Nuclear mass formula with a Yukawa-plus-exponential macroscopic model and a folded-Yukawa single-particle potential. *Nuclear Physics A*, *361*(1), 117-146.

Murthy, M. S. S. (2017). New Members of the Periodic Table, Feature article. Retrieved from: http://nopr.niscair.res.in/handle/123456789/42522

Nakada, H., & Sugiura, K. (2014). Predicting magic numbers of nuclei with semi-realistic nucleon–nucleon interactions. *Progress of Theoretical and Experimental Physics*, *2014*(3).

National Research Council. (1986). *Nuclear physics*. National Academy Press.

National Research Council. (2013). *Nuclear physics: exploring the heart of matter*. National Academies Press.

Naturali, F., De Rosi, G., & Noccioli, O. B. (2013). Superfluidity in neutron star matter (Doctoral dissertation, Sapienza Universita Di Roma). Retrieved from: http://chimera.roma1.infn.it/OMAR/dottorato/tesi_de_rosi.pdf

Négréa, D. (2013). *Proton-neutron pairing correlations in atomic nuclei* (Doctoral dissertation, Paris 11). Retrieved from: https://tel.archives-ouvertes.fr/tel-00870588/document

Neufcourt, L., Cao, Y., Nazarewicz, W., Olsen, E., & Viens, F. (2019). Neutron drip line in the Ca region from bayesian model averaging. *Physical review letters*, *122*(6), 062502.

Nilsson, S. G., & Prior, O. (1961). Kgl. Danske Videnskab. Selskab, Mat. Fys. Medd, 32. 16.

Nilsson, S. G., Tsang, C. F., Sobiczewski, A., Szymanski, Z. Wycech, S. Gustafson, C, Lamm, I.L, Moller, P. & Nilsson, B. (1969). On The nuclear structure and stability of heavy and super heavy elements. *Nuclear Physics A*, 131(1), 1-66.

Nolen, J. A., & Schiffer, J. P. (1969). Coulomb energies. *Annual Review of Nuclear Science*, *19*(1), 471-526.

Oganessian, Y. (2012). Nuclei in the" Island of Stability" of Superheavy Elements. *Journal of Physics, Conference Series* , 337 (1), p. 012005, IOP Publishing.

Oganessian, Y. T., & Rykaczewski, K. P. (2015). A beachhead on the island of stability. *Physics Today*, *68*(8).

Oganessian, Y. T., & Utyonkov, V. K. (2015). Super-heavy element research. *Reports on Progress in Physics*, *78*(3), 036301.

Ogle, W., Wahlborn, S., Piepenbring, R., & Fredriksson, S. (1971). Single-Particle Levels of Nonspherical Nuclei in the Region 150< A< 190. *Reviews of Modern Physics*, *43*(3), 424.

Ozawa, A., Suzuki, T., & Tanihata, I. (2001). Nuclear size and related topics. *Nucl. Phys. A*, *693*(RIKEN-AF-NP-384), 32-62.

Pedram, P. (2010). Modification of Coulomb's law in closed spaces. *American Journal of Physics*, *78*(4), 403-406.

Peter R. & Schuck, P. (1980). *The nuclear many-body problem*. Springer-Verlag.

Pritychenko, B., Sonzogni, A. A., Winchell, D. F., Zerkin, V. V., Arcilla, R., Burrows, T. W. & Sanborn, Y. (2006). Nuclear reaction and structure data services of the National Nuclear Data Center. *Annals of Nuclear Energy*, *33*(4), 390-399.

Prout, W., & Thomson, T. (1815). *On the relation between the specific gravities of bodies in their gaseous state and the weights of their atoms.*

Pyykkö, P. (2011). A suggested periodic table up to Z≤ 172, based on Dirac–Fock calculations on atoms and ions. *Physical Chemistry Chemical Physics*, *13*(1), 161-168.

Rabinowitz, M. (2015). General derivation of mass-energy relation without electrodynamics or Einstein's postulates. *Journal of Modern Physics*, *6*(09), 1243.

Reid, J. M. (1984). *The atomic nucleus*. Manchester University Press.

Ring, P., & Schuck, P. (2004). *The nuclear many-body problem*. Springer Science & Business Media.

Roberto, J. B., Alexander, C. W., Boll, R. A., Burns, J. D., Ezold, J. G., Felker, L. K. & Rykaczewski, K. P. (2015). Actinide targets for the synthesis of super-heavy elements. *Nuclear Physics A*, *944*, 99-116.

Rocke, A. J. (2005). In search of El Dorado: John Dalton and the origins of the atomic theory. *Social research*, 125-158.

Rosman, K. J. R., & Taylor, P. D. P. (1999). Table of isotopic masses and natural abundances. *Pure and Applied Chemistry*, *71*, 1593-1607.

Rowe, D. J., & Wood, J. L. (2010). *Fundamentals of nuclear models: foundational models*. World Scientific Publishing Company.

Rutherford, E. (1911). LXXIX. The scattering of α and β particles by matter and the structure of the atom. *The London, Edinburgh, and Dublin Philosophical Magazine and Journal of Science*, *21*(125), 669-688.

Rutherford, E. (1920). Bakerian lecture: nuclear constitution of atoms. *Proceedings of the Royal Society of London. Series A, Containing Papers of a Mathematical and Physical Character*, *97*(686), 374-400.

Sakaguchi, H., & Zenihiro, J. (2017). Proton elastic scattering from stable and unstable nuclei-Extraction of nuclear densities. *Progress in Particle and Nuclear Physics*, *97*, 1-52.

Sakho, I., (2018). Electrodynamics Calculations of the unit Nuclear Radius in agreement with the constant Density Model. *American Association for Science and Technology, 4*(2), 26-44.

Scerri, E. (2013). Moseley Centennial Lecture: The Works of Henry Moseley, 1887-1915. *Bulletin of the American Physical Society*, *58*.

Schwarzschild, B. (2010). Testing the doubly magic character of tin-132. *Physics Today*, *63*(8), 16-18.

Sivulka, G. (2017). Experimental Evidence for the Structure of the Atom. Retrieved from: http://large.stanford.edu/courses/2017/ph241/sivulka2/

Shreepad H.R. (2011), "Lecture notes," Government College (Autonomous), Mandya.

Staszczak, A., & Wong, C. Y. (2008). Toroidal Super-Heavy Nuclei in Skyrme-Hartree-Fock Approach. *arXiv preprint arXiv:0811.1052*.

Talmi, I. (2005). Nuclear magnetic moments—50 years of the Arima–Horie paper. In *Journal of Physics: Conference Series*, (Vol. 20, no.1, p. 28.) IOP Publishing.

Tarasov, O. B., Ahn, D. S., Bazin, D., Fukuda, N., Gade, A., Hausmann, M., & Komatsubara, T. (2018). Discovery of Ca 60 and Implications For the Stability of Ca 70. *Physical review letters*, *121*(2), 022501.

Thoennessen, M. (2016). *The Discovery of Isotopes.* Switzerland: Springer Int. Publ.

Thoennessen, M. (2017). Fusion and the Discovery of Isotopes. In *EPJ Web of Conferences*, (Vol.163, p. 00060). EDP Sciences.

Thomas, J. M. (2006). JJ Thomson: winner of the Nobel Prize for Physics 1906. *Angewandte Chemie International Edition*, *45*(41), 6797-6800.

Thompson, J. J., & Thomson, J. J. (1913). *Rays of positive electricity and their application to chemical analyses*. Longmans, Green.

Tilton, H. B. (1996). The hydrogen atom: The Rutherford model. In *Models and modelers of hydrogen*, 33-47.

Van Melsen, A. G. (2004). *From atomos to atom: The history of the concept atom*. Courier Corporation.

Van Roosbroeck, J. (2002). *Systematic Nuclear-Structure Study of Even-Mass Zn and Cu Isotopes between N= 40 and 50* (Doctoral dissertation, PhD thesis, Katholieke Universiteit Leuven). Retrieved from: https://fys.kuleuven.be/iks/ns/files/thesis/thesis-jvr.pdf

Villeneuve, D. M. (2005). Toward creating a Rutherford atom. *Science*, *307*(5716), 1730-1731.

Wang, M., Audi, G., Kondev, F. G., Huang, W. J., Naimi, S., & Xu, X. (2017). The AME2016 atomic mass evaluation (II). Tables, graphs and references. *Chinese Physics C*, *41*(3), 030003.

Wang, X., Wang, Z., Wang, X., & Zhang, X. (2012). Spin-Orbit Interaction of Nuclear Shell Structure. *arXiv preprint arXiv:1202.6619*.

Warda, M. (2007). Toroidal structure of super-heavy nuclei in the HFB theory. *International Journal of Modern Physics E*, *16*(02), 452-458.

Webber, B. R., & Davis, E. A. (2012). Commentary on 'The scattering of α and β particles by matter and the structure of the atom' by E. Rutherford (Philosophical Magazine 21 (1911) 669–688). *Philosophical Magazine*, *92*(4), 399-405.

Weizsäcker, C. F. V. (1935). On the theory of nuclear masses. *Journal of Physics*, *96*, 431-458.

Whittaker, E. T. (1910). *A History of the Theories of Aether and Electricity from the Age of Descartes to the Close of the Nineteenth Century*. Longmans, Green and Company.

Wigner, E. (1937). On the Consequences of the Symmetry of the Nuclear Hamiltonian on the Spectroscopy of Nuclei. *Physical Review*, *51*(2), 106.

Wikipedia contributors. (2020, August 18). Even and odd atomic nuclei. In *Wikipedia, The Free Encyclopedia*. Retrieved 10:37, August 31, 2020, from https://en.wikipedia.org/w/index.php?title=Even_and_odd_atomic_nuclei&oldid=973689582

Williams, M. (2016). What is binding energy? *Universe Today: Space and Astronomy News*. Retrieved from: https://www.universetoday.com/81869/binding-energy/

William, T. (2018). "Notes on Subatomic Particles (nuclear models) PHY 357," University of Toronto. Retrieved from: https://www.physics.utoronto.ca/~william/courses/phy357/

Wilson, D. (1983). *Rutherford-simple genius*, United Kingdom, Hodder and Stoughton.

Zagrebaev, V. I., Itkis, M. G., & Oganessian, Y. T. (2003). Fusion-Fission dynamics and perspectives of future experiments. *Physics of Atomic Nuclei*, *66*(6), 1033-1041.

Zinner, E. (2002). Using Aluminum-26 as a Clock for early solar system events. *Planetary Science Research Discoveries Report*, 1-9.

APPENDICES

APPENDIX I

Correction term for $^{238}_{92}\text{U}$ calculated using Eq. (3.9) and the nuclear radius parameter $r_0 = 1.135\,\text{fm}$.

n	R_o^n	R^n	$\dfrac{R_0^n}{e^{nR^n}}$
1	6.4556E-15	7.03E-15	2.50377
2	4.16748E-29	4.95E-29	1.64872
3	2.69036E-43	3.48E-43	1.39561
4	1.73679E-57	2.45E-57	1.28403
5	1.1212E-71	1.72E-71	1.22140
6	7.23802E-86	1.21E-85	1.18136
7	4.6726E-100	8.5E-100	1.15356
8	3.0164E-114	6E-114	1.13315
9	1.9473E-128	4.2E-128	1.11752
10	1.2571E-142	3E-142	1.10517
11	8.1153E-157	2.1E-156	1.09517
12	5.2389E-171	1.5E-170	1.08690
13	3.382E-185	1E-184	1.07996
14	2.1833E-199	7.3E-199	1.07404
15	1.4094E-213	5.1E-213	1.06894
16	9.0988E-228	3.6E-227	1.06449
17	5.8738E-242	2.5E-241	1.06059
18	3.7919E-256	1.8E-255	1.05713
19	2.4479E-270	1.2E-269	1.05404
20	1.5803E-284	8.8E-284	1.05127
21	1.0202E-298	6.2E-298	1.04877
n>21	R_o^n < 1.0202E-298	R^n < 6.2E-298	1.00000

APPENDIX II

Correction terms of finite nuclei with Z=113, Z=118, Z=138, Z=156, and Z= 174 calculated using Eq. (3.9) and the nuclear radius parameter $r_0 = 1.22\,\text{fm}$.

n	CORRECTION TERMS				
	Z=113 (A=282)	Z=118 (A=294)	Z=138 (A=368)	Z=156 (A=466)	Z=174 (A=584)
1	2.5317	2.5329	2.4807	2.3985	2.3199
2	1.5395	1.5401	1.5110	1.4662	1.4248
3	1.3063	1.3068	1.2840	1.2500	1.2197
4	1.2046	1.2050	1.1857	1.1577	1.1336
5	1.1483	1.1487	1.1318	1.1079	1.0881
6	1.1130	1.1134	1.0983	1.0776	1.0610
7	1.0890	1.0893	1.0757	1.0576	1.0436
8	1.0718	1.0720	1.0598	1.0438	1.0319
9	1.0589	1.0592	1.0480	1.0339	1.0238
10	1.0490	1.0492	1.0391	1.0266	1.0180
11	1.0412	1.0414	1.0322	1.0211	1.0137
12	1.0350	1.0352	1.0267	1.0169	1.0106
13	1.0299	1.0301	1.0224	1.0136	1.0082
14	1.0258	1.0259	1.0188	1.0110	1.0064
15	1.0223	1.0225	1.0159	1.0090	1.0050
16	1.0194	1.0195	1.0136	1.0074	1.0040
17	1.0169	1.0171	1.0116	1.0061	1.0031
18	1.0148	1.0150	1.0099	1.0050	1.0025
19	1.0130	1.0132	1.0085	1.0042	1.0020
20	1.0115	1.0116	1.0074	1.0035	1.0016
21	1.0102	1.0103	1.0064	1.0029	1.0013
n>21	1.0000	1.0000	1.0000	1.0000	1.0000

APPENDIX III

Coulomb energies of finite nuclei with Z=92, Z=113, Z=118, Z=138, Z=156 and Z=174 calculated using Eq. 3.8 and the nuclear radius parameter of $r_0 = 1.22\,\text{fm}$.

n	Coulomb Energies (MeV)					
	Z=92	Z=113	Z=118	Z=138	Z=156	Z=174
1	2606	3720	4002	5095	6048	7021
2	1716	2262	2433	3103	3697	4312
3	1453	1920	2065	2637	3152	3692
4	1337	1770	1904	2435	2919	3431
5	1271	1687	1815	2324	2794	3293
6	1230	1636	1759	2255	2717	3211
7	1201	1600	1721	2209	2667	3159
8	1180	1575	1694	2176	2632	3123
9	1163	1556	1673	2152	2607	3099
10	1150	1541	1658	2134	2588	3081
11	1140	1530	1645	2120	2575	3068
12	1131	1521	1636	2109	2564	3059
13	1124	1513	1628	2100	2556	3051
14	1118	1507	1621	2092	2549	3046
15	1113	1502	1616	2086	2544	3042
16	1108	1498	1611	2082	2540	3039
17	1104	1494	1607	2077	2537	3036
18	1100	1491	1604	2074	2534	3034
19	1097	1489	1601	2071	2532	3033
20	1094	1486	1598	2069	2530	3031
21	1092	1484	1596	2067	2529	3031
n>21	1041	1469	1580	2054	2521	3027

APPENDIX IV

Coulomb energies calculated using Eq. (3.8) and the nuclear radius parameter, $r_0 = 1.135\,\text{fm}$.

n	Coulomb Energies (MeV)											
	Z=15	Z=24	Z=25	Z=32	Z=40	Z=60	Z=92	Z=113	Z=118	K* (A=368)	L* (A=466)	M* (A=584)
1	137	300	314	493	696	1348	2802	3999	4302	5476	6501	7547
2	83	182	191	299	423	822	1845	2431	2616	3335	3974	4636
3	70	154	162	254	359	698	1562	2063	2219	2834	3388	3968
4	65	142	149	233	331	645	1437	1903	2047	2617	3138	3688
5	61	135	142	222	316	616	1367	1814	1951	2498	3003	3540
6	59	131	138	215	306	598	1322	1758	1891	2424	2920	3452
7	58	128	135	210	300	586	1291	1720	1850	2375	2866	3395
8	57	126	133	207	295	577	1268	1693	1821	2339	2829	3357
9	56	124	131	204	291	571	1250	1672	1799	2313	2802	3331
10	56	123	130	202	289	566	1237	1657	1782	2294	2782	3312
11	55	122	129	200	286	562	1225	1645	1769	2278	2767	3298

12	55	121	128	199	285	559	1216	1635	1758	2266	2756	3288
13	54	120	128	197	283	557	1208	1627	1750	2257	2747	3280
14	54	120	127	196	282	555	1202	1620	1742	2249	2740	3274
15	54	119	127	196	281	554	1196	1615	1736	2243	2735	3270
16	54	119	126	195	281	553	1191	1610	1732	2237	2730	3266
17	54	119	126	194	280	552	1187	1606	1727	2233	2727	3264
18	53	118	126	194	279	551	1183	1603	1724	2229	2724	3262
19	53	118	125	193	279	550	1179	1600	1721	2226	2721	3260
20	53	118	125	193	278	549	1176	1598	1718	2224	2720	3259
21	53	118	125	193	278	549	1174	1596	1716	2221	2718	3258
n>21	51	115	124	189	275	546	1119	1580	1698	2207	2710	3254

APPENDIX V

The graphical comparison of the Coulomb energy per nucleon in the super heavy nuclei calculated using Eq. (3.8) and the nuclear parameter $r_0 = 1.135\,\text{fm}$ and $r_0 = 1.22\,\text{fm}$.
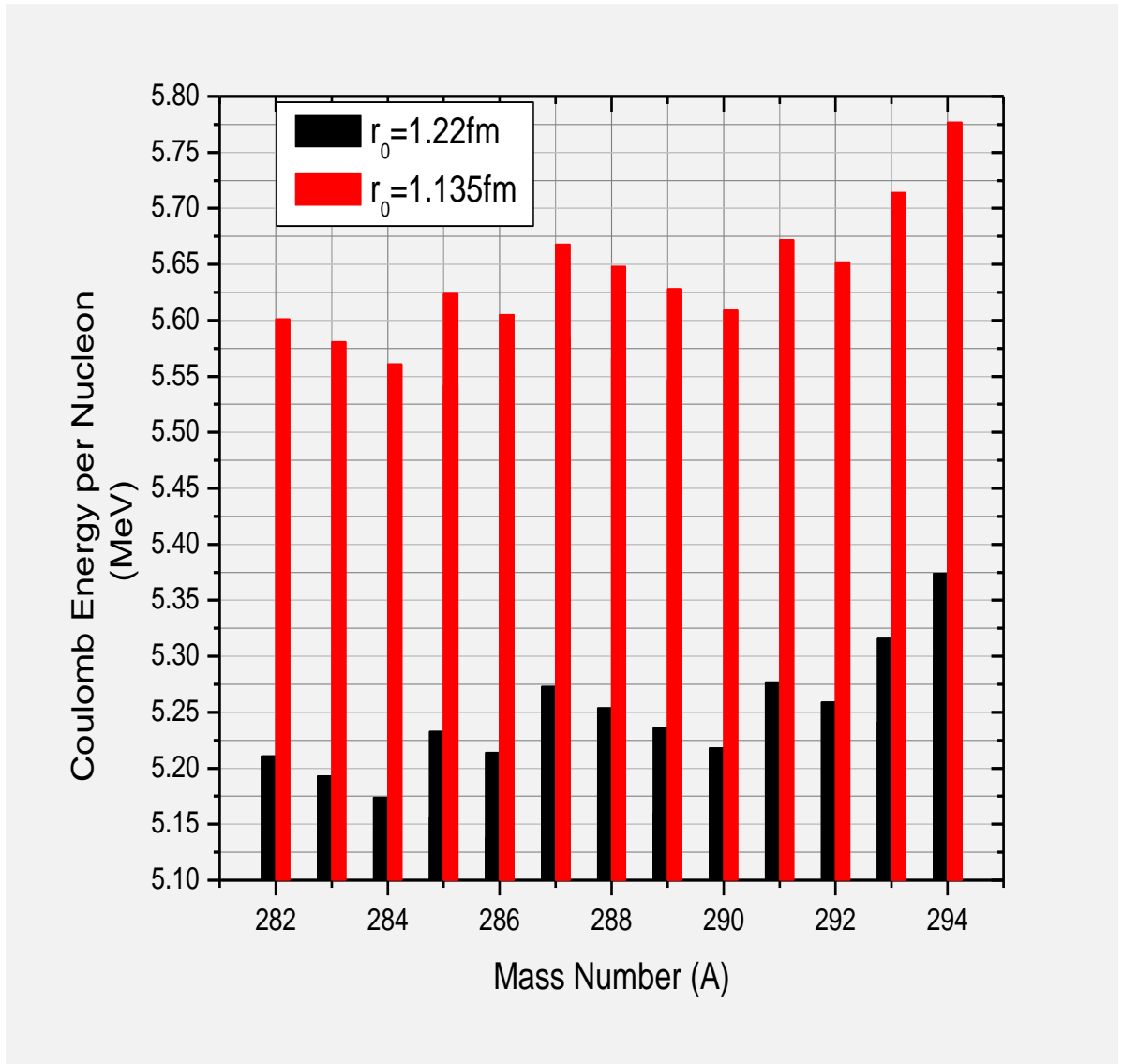
APPENDIX VI

(a) Calculated Coulomb energies per nucleon of some elements with $Z \leq 92$ using Eq. (2.4), Eq. (2.5) and Eq. (3.8).

ELEMENTS	A	Z1	Z2	E_C(SEMFE)	E_C(Dir)	E_C(Mod) r_0=1.135fm	E_C(Mod) r_0=1.22fm
Li	7	3	2	0.32	0.34	0.36	0.33
B	11	5	4	0.58	0.62	0.64	0.60
C	14	6	5	0.63	0.68	0.71	0.66
O	18	8	7	0.84	0.90	0.94	0.87
F	19	9	8	1.01	1.08	1.10	1.02
P	32	15	14	1.47	1.57	1.61	1.49
Ca	46	20	19	1.64	1.76	1.84	1.71
Cr	55	24	23	1.87	2.01	2.10	1.95
Kr	78	36	35	2.68	2.87	2.95	2.75
Zr	100	40	39	2.39	2.57	2.75	2.56
In	124	49	48	2.70	2.91	3.13	2.91
Ba	140	56	55	3.01	3.24	3.47	3.23
Gd	156	64	63	3.41	3.66	3.90	3.63
Po	218	84	83	3.77	4.07	4.41	4.10
U	238	92	91	4.03	4.34	4.70	4.37

(b) Calculated Coulomb energies per nucleon of some elements with $Z \leq 174*$ using Eq. (2.4), Eq. (2.5) and Eq. (3.8).

ELEMENTS	Z	E_C(SEMFE)	E_C(Dir)	E_C(Mod) r_0=1.135fm	E_C(Mod) r_0=1.22fm
P	15	1.47	1.59	1.61	1.49
Cr	24	1.87	2.03	2.10	1.95
Mn	25	1.74	1.88	2.00	1.86
Ge	32	2.35	2.54	2.62	2.44
Zr	40	2.39	2.57	2.75	2.56
Nd	60	2.85	3.06	3.37	3.13
U	92	4.03	4.33	4.70	4.37
Nh	113	4.86	5.22	5.60	5.21
Og	118	5.01	5.39	5.78	5.37
K*	138	5.09	5.46	6.00	5.58
L*	156	4.75	5.10	5.82	5.41
M*	174	4.38	4.70	5.57	5.18

APPENDIX VII

Calculations for Z_{STABLE} values for Even A nuclei using Eq. (3.14) and Eq. (3.22).

n	A=72		A=172		A=368*		A=466*		A=584*	
	$Z_{STABLE-SEMF}$	$Z_{STABLE-NMDF}$	$Z_{STABLE-SEMF}$	$Z_{STABLE-NMDF}$	$Z_{STABLE-SEMF}$	$Z_{STABLE-NMDF}$	$Z_{STABLE-SEMF}$	$Z_{STABLE-NMDF}$	$Z_{STABLE-SEMF}$	$Z_{STABLE-NMDF}$
1	27	27	54	54	93	95	111	112	130	132
2	30	30	63	64	116	117	139	141	166	168
3	31	31	66	66	122	124	148	150	177	179
4	31	31	67	68	126	127	152	154	182	184
5	31	32	68	68	127	129	154	157	185	187
6	31	32	68	69	129	130	156	158	186	189
7	31	32	68	69	129	131	157	159	188	190
8	31	32	69	69	130	132	158	160	188	191
9	31	32	69	70	130	132	158	160	189	191
10	32	32	69	70	131	133	158	161	189	192
11	32	32	69	70	131	133	159	161	190	192
12	32	32	69	70	131	133	159	161	190	192
13	32	32	69	70	131	133	159	161	190	193
14	32	32	69	70	131	133	159	161	190	193
15	32	32	69	70	132	133	159	161	190	193
16	32	32	69	70	132	133	159	162	190	193
17	32	32	69	70	132	134	159	162	190	193
18	32	32	69	70	132	134	159	162	190	193
19	32	32	69	70	132	134	159	162	190	193
20	32	32	69	70	132	134	160	162	190	193
21	32	32	69	70	132	134	160	162	190	193
n>21	32	32	70	71	132	134	160	162	190	193

APPENDIX VIII

Calculations for Z_{STABLE} values for Odd A nuclei using Eq. (3.14) and Eq. (3.22)

n	A=27		A=277	
	$Z_{STABLE-SEMF}$	$Z_{STABLE-NMDF}$	$Z_{STABLE-SEMF}$	$Z_{STABLE-NMDF}$
1	11	12	76	77
2	12	12	92	94
3	12	13	97	99
4	12	13	100	101
5	12	13	101	102
6	13	13	102	103
7	13	13	102	104
8	13	13	103	104
9	13	13	103	104
10	13	13	103	105
11	13	13	103	105
12	13	13	104	105
13	13	13	104	105
14	13	13	104	105
15	13	13	104	105
16	13	13	104	105
17	13	13	104	106
18	13	13	104	106
19	13	13	104	106
20	13	13	104	106
21	13	13	104	106
n>21	13	13	105	106

APPENDIX IX

Calculations for Z_{STABLE} for Super heavy nuclei using Eq. (3.22)

| n	Z_{STABLE} for A=292	Z_{STABLE} for A=340	Z_{STABLE} for A=360	Z_{STABLE} for A=364	Z_{STABLE} for A=392	Z_{STABLE} for A=416	Z_{STABLE} for A=432	Z_{STABLE} for A=476
1	80	90	94	94	100	102	108	111
2	97	111	116	116	124	128	134	141
3	103	117	122	123	131	136	142	151
4	105	120	125	126	135	140	146	155
5	107	122	127	128	137	142	148	158
6	108	123	128	129	138	143	149	159
7	108	123	129	130	139	144	150	160
8	109	124	130	131	139	145	151	161
9	109	124	130	131	140	145	151	162
10	109	124	130	131	140	146	151	162
11	110	125	131	132	140	146	152	163
12	110	125	131	132	140	146	152	163
13	110	125	131	132	140	147	152	163
14	110	125	131	132	140	147	152	163
15	110	125	131	132	141	147	152	164
16	110	125	131	132	141	147	152	164
17	110	125	131	132	141	147	152	164
18	110	125	131	132	141	147	152	164
19	110	125	131	132	141	147	152	164
20	110	125	131	132	141	147	152	164
21	110	125	131	133	141	147	152	164
$n>21$	111	126	132	133	141	148	152	164

APPENDIX X

Graphical representation of even A mass parabola (A=72) using the values of the mass excess obtained from AME2016 (Wang *et al*., 2017)
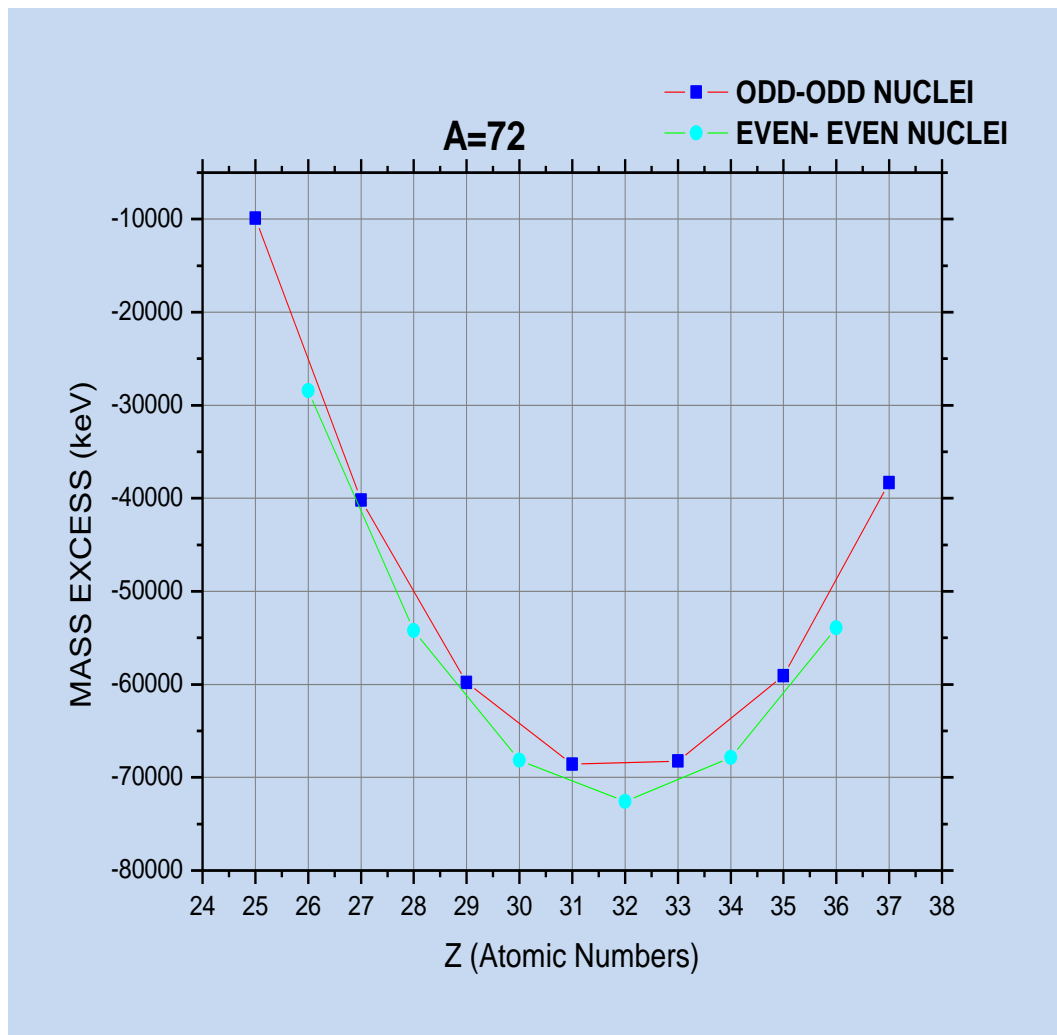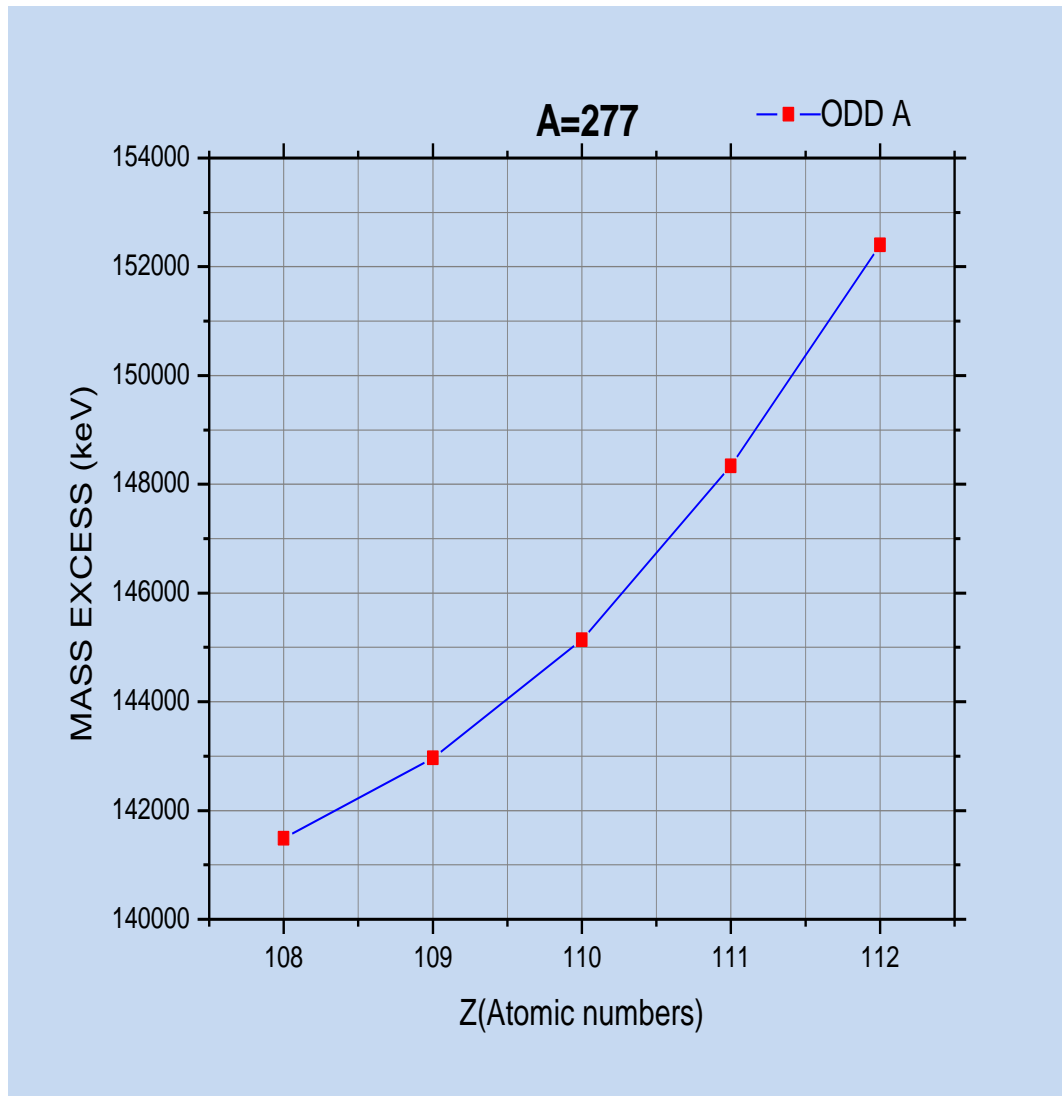
APPENDIX XI

Graphical representation of odd A mass parabola (A=113) using the values of the mass excess obtained from AME2016 (Wang *et al*., 2017)
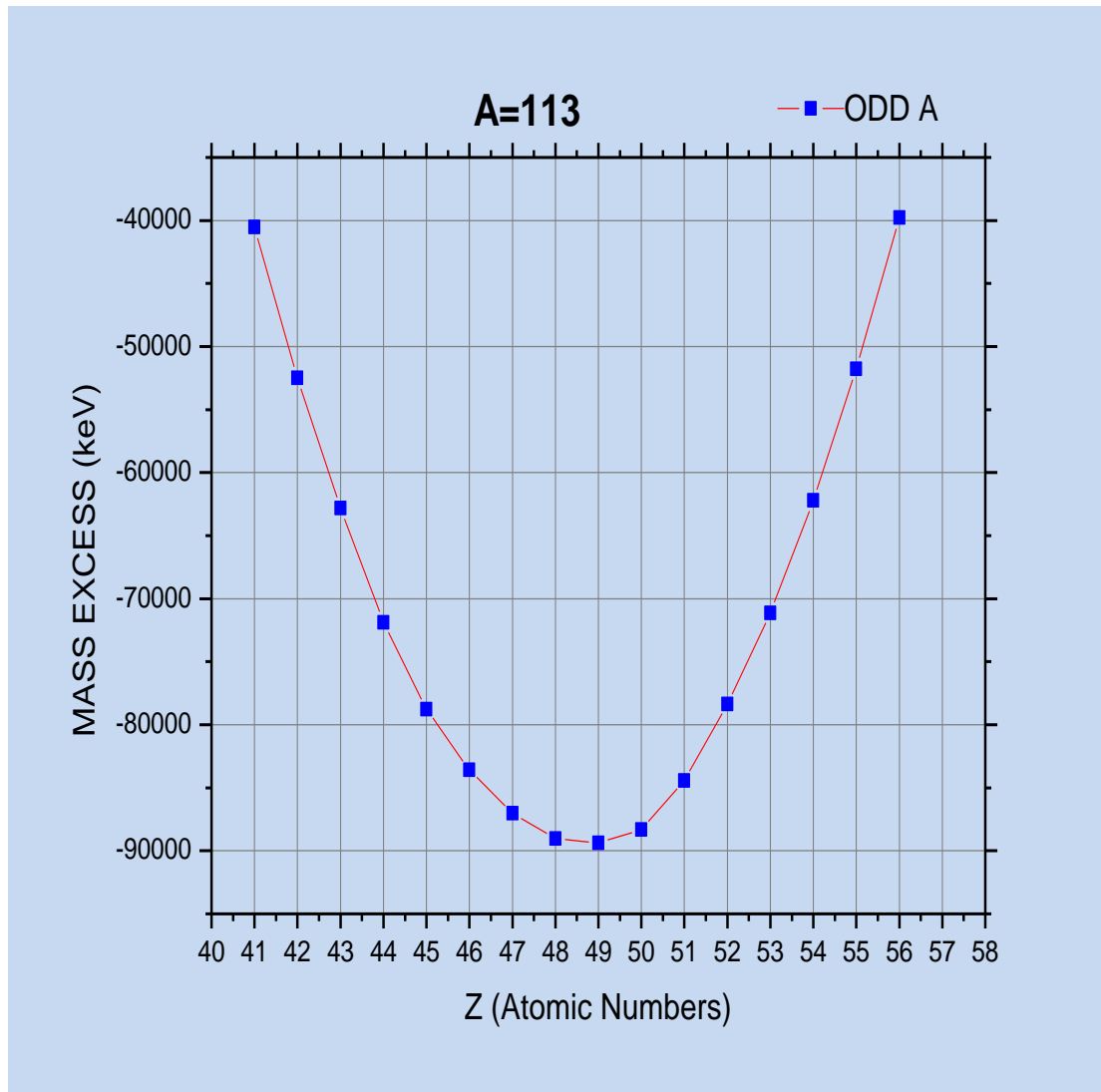
APPENDIX XII

Graphical representation of odd A mass parabola for the heavy nuclei (A=277) using the values of the mass excess obtained from AME2016 (Wang *et al*., 2017)

APPENDIX XIII: Similarity Index/Anti-Plagiarism Report

Document Viewer

Turnitin Originality Report

Processed on: 15-Feb-2021 12:40 EAT
ID: 1509933443
Word Count: 27976
Submitted: 1

SSCI/PHY/P/004/17 By
Hezekiah Cherop Komen

Similarity Index	Similarity by Source		
11%	Internet Sources:	7%	
	Publications:	5%	
	Student Papers:	2%	

Include quoted   Include bibliography   excluding matches < 5 words   mode:

quickview (classic) report   Change mode   print   refresh   download

<1% match (Internet from 31-May-2020)
https://ooku.pub/documents/reservoir-fluids-properties-heinemann-7l5rqrdpxmqk

<1% match (student papers from 13-Feb-2018)
Submitted to University of Kapianga on 2018-02-13

<1% match (publications)
Handbook of Nuclear Chemistry, 2011.

<1% match (publications)
Michael F. L'Annunziata. "The atomic nucleus, nuclear radiation, and the interaction of radiation with matter", Elsevier BV, 2020

<1% match (publications)
Moller, P.. "Nuclear pairing models", Nuclear Physics, Section A, 19920106

<1% match (publications)
Ervin B. Podgorsak. "Radiation Physics for Medical Physicists", Springer Science and Business Media LLC, 2016

<1% match (Internet from 01-Nov-2019)
http://www.radiation-shielding.co.za

<1% match (Internet from 09-Aug-2020)
https://mafiadoc.com/effectiveness-of-integrating-information_5cb2e8bc097c47665e8b4645.html

<1% match (Internet from 13-Jan-2021)
http://www.redhuntington.com